CUKUROVA UNIVERSITY
INSTITUTE OF NATURAL AND APPLIED SCIENCES

MSc THESIS

Design of A Hybrid MPPT Method for PV Systems Under Partial Shading Conditions

Bayram Kaan UZUNDAĞ

Electrical and Electronics Engineering Department

December, 2024

CUKUROVA UNIVERSITY
INSTITUTE OF NATURAL AND APPLIED SCIENCES

MSc THESIS APPROVAL

Design of A Hybrid MPPT Method for PV Systems Under Partial Shading Conditions

---

Bayram Kaan UZUNDAĞ

Electrical and Electronics Engineering Department

This Master's Thesis was evaluated by the following Jury Members on 04/12/2024 and was approved by unanimity / majority of votes.

Jury : Asst. Prof. Dr. Oğuzhan TİMUR (Advisor) ………………………

: Prof. Dr. Ahmet TEKE ………………………

: Asst. Prof. Dr. Kasım ZOR ………………………

This Thesis was written in the Department of Electrical and Electronics Engineering, Institute of Natural and Applied Sciences.

Thesis Number:

Prof. Dr. Sadık DİNÇER
Director
Institute of Natural and Applied Sciences

CONTENTS

CUKUROVA UNIVERSITY
INSTITUTE OF NATURAL AND APPLIED SCIENCES

MSc THESIS

Design of A Hybrid MPPT Method for PV Systems Under Partial Shading Conditions

Bayram Kaan UZUNDAĞ

Advisor: Asst. Prof. Dr. Oğuzhan TİMUR

Department of Electrical and Electronics Engineering

ABSTRACT

Nowadays where the world population is increasing rapidly, it is important to discuss the importance of limited resources along with the advancement of industry and technology. In recent years, the energy demand has been at an unprecedented level, leading humanity to seek new and inexhaustible resources. The fact that solar electricity production depends on factors such as solar radiation, temperature, and shading has led researchers to seek maximum utilization of this energy. Partial shading conditions on solar panels in particular have been one of the important factors that reduce the efficiency of photovoltaic systems. Various Maximum Power Point Tracking (MPPT) algorithms have been developed to prevent power losses due to weather conditions and partial shading. These algorithms aim to keep the system at the maximum power point by monitoring the current and voltage irregularities that occur in solar energy production. The aim of this thesis is to examine the MPPT methods, to compare various features and to develop a new hybrid method based on Perturb and Observe and Particle Swarm Optimization. In the study, a hybrid MPPT method is developed by using MATLAB/Simulink environment. The proposed method was tested under different irradiation level irradiance values of 1000 W/m^2, 500 W/m^2, 600 W/m^2, 900 W/m^2 and 800 W/m^2, respectively. In addition, the developed algorithm was compared with various MPPT methods and the obtained results were examined in detail. It was concluded that the applied method was an efficient method in terms of convergence speed, tracking accuracy, and fluctuations for partial shading situations.

Keywords: Partial Shading Situations, MPPT Methods, Maximum Power Point Tracking (MPPT), Comparison of MPPT Algorithms, MATLAB Simulink.

ÇUKUROVA ÜNİVERSİTESİ
FEN BİLİMLERİ ENSTİTÜSÜ

YÜKSEK LİSANS TEZİ

Kısmi Gölgeleme Koşulları Altında FV Sistemler İçin Hibrit MPPT Yönteminin Tasarımı

Bayram Kaan UZUNDAĞ

Danışman: Dr. Öğr. Üyesi Oğuzhan TİMUR

Elektrik ve Elektronik Mühendisliği Anabilim Dalı

ÖZ

Günümüzde dünya nüfusu hızla artarken, endüstri ve teknolojinin ilerlemesiyle birlikte sınırlı kaynakların önemini tartışmak önem arz etmektedir. Son yıllarda enerji ihtiyacının hiç olmadığı kadar yüksek seviyede olması, insanoğlunun yeni ve tükenmez kaynakları arayışına yönlendirmiştir. Güneşten elektrik üretiminin güneş ışınımı, sıcaklık, gölgelenme gibi faktörlere bağlı olması, araştırmacıları bu enerjiden maksimum şekilde yararlanma arayışlarına itmiştir. Özellikle güneş panelleri üzerindeki kısmi gölgelenme durumları, fotovoltaik sistemlerin verimlerini düşüren önemli olgulardan birisi olmuştur. Hava şartları ve kısmi gölgelenme durumları sonucu oluşan güç kayıplarını önlemek amacıyla çeşitli Maksimum Güç Noktası İzleyicisi (MGNİ) algoritmaları geliştirilmiştir. Bu algoritmalar güneş enerjisi üretiminde meydana gelen akım ve voltaj düzensizliklerini izleyerek sistemi maksimum güç noktasında tutmayı hedeflerler. Bu tezin amacı, MPPT yöntemlerini incelemek, çeşitli özelliklerini karşılaştırmak ve Perturb ve Observe ile Parçacık Sürüsü Optimizasyonuna dayalı yeni bir hibrit yöntem geliştirmektir. Çalışmada, MATLAB/Simulink ortamı kullanılarak hibrit bir MPPT yöntemi geliştirilmiştir. Önerilen yöntem sırasıyla 1000 W/m^2, 500 W/m^2, 600 W/m^2, 900 W/m^2 ve 800 W/m^{2}' lik farklı ışınlama seviyesi ışınım değerlerinde test edildi. Ayrıca geliştirilen algoritma, çeşitli MPPT yöntemleri ile karşılaştırılmış ve elde edilen sonuçlar detaylı olarak incelenmiştir. Uygulanan yöntemin kısmi gölgelenme durumları için yakınsama hızı, izleme doğruluğu ve dalgalanmalar açısından etkili bir yöntem olduğu sonucuna varılmıştır.

Anahtar Kelimeler: Kısmi Gölgeleme Durumları, MPPT Yöntemleri, Maksimum Güç Noktası İzleyicisi (MGNİ), MPPT Algoritmalarının Karşılaştırılması, MATLAB Simulink.

GENİŞLETİLMİŞ ÖZET

Günümüzde insanlığın elektrik enerjisine olan ihtiyacı, son yüzyıllarda yaşanan savaşlar, kıtlıklar ve hızlı nüfus artışı gibi sebepler ile sürekli olarak artmaktadır. Devletler, enerjinin önemli olduğunu, yaşanan felaketler ve sonrası zamanlarda içinde bulundukları durumlar sayesinde öğrenmişlerdir. Özellikle son yüzyılda enerji ihtiyacı görülmemiş bir biçimde artmıştır.

Devletlerin enerji üretiminde dış devletlere bağımlı olması, gelişimleri önündeki önemli engellerden birisidir. Devletlerin enerji ihtiyaçlarını ne oranda kendi iç kaynaklarından karşıladıkları incelenirse, kendi kaynaklarından enerji üreten devletlerin gelişmiş ülkeler olduğu görülebilmektedir. Kendi iç kaynağı (özellikle fosil yakıtlar gibi) hiç olmayan veya yeterli düzeyde olmayan ülkeler dışa bağımlı ülkeler haline gelmektedir. Bu durumdaki devletler, enerjilerini kendi ülkelerinde bulunan yenilenebilir enerji kaynaklarından sağlayarak gelişmekte yol katebilmektedir. Bunun örnekleri dünyada mevcuttur. Bir çok devlet yenilenebilir enerji kaynaklarına yönelerek dışa bağımlılıklarını azaltmışlardır.

Yenilenebilir enerji kaynakları, kaynağını güneşten alan, tükenmeyen, temiz ve çevre dostu enerji kaynaklarıdır. Fosil yakıtlar olarak bilinen petrol, kömür, doğalgaz vb. kaynaklar elektrik üretimi için yakılmaktadırlar. Bu yanma sonucu açığa karbondioksit gazı gibi zararlı bir sürü kimyasal atmosfere yayılmaktadır. Bu şekilde enerji üretimin dünyada fazla olması düşünüldüğünde çok yüksek miktardaki zararlı gaz havayı, çevreyi, doğayı ve en genel anlamda dünyamızı kirletmektedir. Sadece görsel kirlilik bir yana atmosferdeki yüksek zararlı gazların olması, sera etkisi olarak bilinen olguya yol açır. Zararlı gazlar atmosfer tabakalarını inceltmekte ve özellikle ozon tabakasına zarar vermektedir. Sera gazlarının atmosferdeki miktarı, son yıllarda sürekli artmakta, iklim değişiklikleri görülmekte ve bunun sonucunda küresel ısınmaya sebep olmaktadır.

Fosil yakıtların günden güne tükenmekte olduğu araştırmalar sonucunda ortaya çıkmış bir gerçektir. Bu kaynakların tükenmekte olması sebebiyle devletler son yıllarda yeni arayışlar içerisine girmişlerdir. Yenilenemeyen enerji kaynaklarında vazgeçmeye ve temiz bir enerji kullanımına geçmeye başlamışlardır. Bir çok devlet yenilenebilir enerji kullanımını arttırmak için yasa ve yönetmelikler hazırlamış, verilen teşvik ve indirimlerle bu temiz enerji kaynaklarına yönelme çalışmalarına başlamıştır. Son zamanlarda dünyada enerji üretiminde yenilenebilir enerji kaynaklarının kullanımının ivmesel olarak arttığı bilinmektedir.

Yenilenebilir enerji kaynağı çeşitlerine bakıldığında hidroelektrik enerjisi, rüzgar enerjisi, güneş enerjisi, jeotermal enerji ve biyokütle enerjisi, gelgit enerjisi ve daha bir çok diğer temiz enerji kaynağı bulunabilir. Çeşitlerin fazla olması alternatif bir çok seçenek sunmaktadır. Ülkeler kendi coğrafik konumlarına göre araştırma ve incelemeler yaparak hangi yenilenebilir enerji kaynağının kendi ülkelerinde potansiyelinin olduğunu görebilmektedirler.

Yapım aşamasının hızlı olması, kaynağını direkt olarak güneşten alması, ekonomik kurulum maliyetleri, teşvikler, indirimler ve artan teknolojisi ile birlikte güneş enerjisi kullanımı son on yıllarda insanlığın tercih ettiği bir yenilenebilir enerji kaynağı olmuştur. Özellikle gelişmiş bir çok ülke GW ları geçen büyük üretim santralleri kurmuştur. Özellikle güneş enerjisi santrallerinin büyük oranda yatırım alması ancak planlı analizler, öngörüler ve iyi araştırmalar ile mümkündür. Yapılan araştırmalar ve yatırımlar incelendiğinde bu yönde büyük bir yönelim söz konusudur. Trendi yakalamak amacıyla bir çok yatırımcı bu alanda yatımlarına devam etmektedir.

Güneş enerjisi santrallerinden üretilen elektrik her zaman yeterli düzeyde olmamaktadır. Gölge etmenleri, sıcaklık, kirlilik, güneş ışınımı seviyeleri ve diğer çevresel faktörler üretimi büyük oranda etkilemektedir. Özellikle güneş ışınımı ve sıcaklık fotovoltaik panellerden elde edilen elektrik miktarını ciddi anlamda etkileyen iki etmendir. Bu etmenler kaynağını güneşten aldıkları için miktarları her zaman istenen düzeyde olmamaktadır. Bu etmenleri istenen düzeyde tutmak zordur ve ekonomik anlamda maliyet problemlerini getirmektedir. Ayrıca voltaj ve akım dengesizliğine sebep olan bu sorunlar ile üretimde güç kayıpları oluşmaktadır. Bu kayıpları en az seviyeye indirmek ve üretimi en üst seviyeye çıkarmak amacıyla Maksimum Güç Noktası İzleyicisi (MGNİ) algoritmaları geliştirilmiştir.

Güneş enerjisinden elektrik üretiminde en temel bileşenler olarak güneş panelleri, doğru akım - doğru akım (DA-DA) dönüştürücüler, eviriciler, filtre elemanları ve diğer ekipmanlar sıralanabilir. En basit işleyiş açıklanırsa, güneş panellerinden üretilen doğru akım, DA-DA dönüştürücüler ile istenilen doğru akım seviyesine getirilir. Daha sonraki aşamada eviriciler ile doğru akım, alternatif akıma (AA) çevirilir. Ardından elektrik enerjisi filtre ve çeşitli diğer ekipmanlardan geçerek kullanıma hazır hale getirilir.

MGNİ algoritmaları bu temel güneş enerjisi bileşenlerinden DA-DA dönüştürücülerin anahtarlama sinyallerini yönetmek amacıyla kullanılır. Güneş enerjisinden elektrik üretiminde değişen koşullarda her zaman aynı güç değerini sağlamak için panel çıkışlarında sıcaklık, ışınım, voltaj, akım vb. gibi elde edilebilen ölçümler alınır ve MGNİ algoritmaları bu bilgileri işler, ardından diğer anahtarlama elemanları için en uygun anahtarlama sinyali oluşturulur. Bu uygun sinyallerle birlikte anahtarlama elamanı güç seviyesini maksimum tutacak şekilde çalıştırılmış olur.

Litaratürde çeşitli MGNİ algoritmaları oluşturulmuş ve araştırmacılar tarafından incelenmiştir. MGNİ algoritmaları temelde aynı görevi yapsa da işleyiş bakımından farklılıklara sahiptirler. Bu algoritmalar maksimum güç noktası takip hızı, verimlilik seviyesi, ekonomik maliyeti, pratikliği, esnekliği, hassasiyeti vb gibi bir çok başlık bakımından incelenmiş ve birbirleriyle karşılaştırılmıştır.

Bu tez çalışmasında başlangıç olarak literatürde bulunan çeşitli MGNİ algoritmalarının detaylı incelenmesi yapılmıştır. Literatürdeki MGNİ algoritmalarının avantaj, dezavantaj ve işleyiş özellikleri gibi konular hakkında bilgiler verilmiş ve karşılaştırmalar yapılmıştır. Daha sonra MATLAB/Simulink benzetim programı kullanılarak bir 11.76 kW gücünde bir PV sistem modellenmiştir. PV dizi, DA-DA yükselten dönüştürücü, MGNİ algoritma bloğu ve DA-DA yükselten dönüştürücü kontrol devresi oluşturulan PV sistemin bölümleridir. PV panel olarak Helios

Energy Europe 96M420 modeli kullanılmıştır. PV panel gücü 420 W olarak seçilmiştir. Her bir dizide seri bağlı 7 PV panelin olduğu, bu dizilerin 4 adedinin paralel olarak bağlandığı ve toplamda 28 adet PV panelin olduğu bir PV sistem oluşturulmuştur. Tüm sistem için ışınım değeri başlangıç için 1000 W/m^2 ve sıcaklık değeri 25 °C seçilmiştir. Sistemi test etmek amacıyla 4 farklı simülasyon çalışması hazırlanmıştır. Oluşturulan simülasyonlarda sadece MGNİ algoritmalarını içeren MATLAB/Simulink fonksiyon blokları birbirlerinden farklıdır. Sistemin genel çalışma yapısı özetlenirse, öncelikle PV diziden alınan voltaj ve akım ölçümleri, MGNİ algoritma blokları içindeki algoritmalara giriş olarak alınır. Algoritmalarda MGN takibi yapılır ve çıkışta uygun referans voltajı üretilir. Çıkışta üretilen referans voltajı PI denetleyicide kullanılır. PI denetleyicinin çıkışındaki sinyal oluşturulan tepe değeri 0.6 ve frekansı 20 kHz olan üçgen taşıyıcı sinyal ile karşılaştırılır ve darbe genlik modülasyonu sinyali oluşturulur. Oluşturulan bu sinyal DA-DA yükselten dönüştürücünün anahtarlanması için kullanılır. DA-DA yükselten dönüştürücü bu sayede çalıştırılarak çıkışta PV diziden üretilmiş olan voltaj seviyesi arttırılmış olur. Oluşturulan sistem için DA-DA yükselten dönüştürücü giriş voltajı 346.71 V ve çıkış voltajı 540 V olarak seçilmiştir. Dönüştürücü anahtarlama frekansı 20 kHz olacak şekilde ayarlanmış ve diğer devre elemanları uygun hesaplamalar yapılarak seçilmiştir.

Bu tez çalışmasında Dürt ve Gözlemle ile Parçacık Sürü Optimizasyonu tabanlı yeni bir hibrit MGNİ algoritması geliştirilmiştir. Oluşturulan yapıda her iki algoritmanın avantajlı yönleri kullanılmıştır. Parçacık Sürü Optimizasyonu algoritması doğadaki canlıların sürü davranışlarını örnek alarak oluşturulmuş bir algoritmadır. Bu algoritmada öncelikle bir parçaçık kümesi oluşturulur. Bu parçacıklar bir çözüm uzayında sürekli hareket ederler. Hareket halindeki parçacıklar sürekli olarak en iyi çözüm noktasına ulaşmaya çalışırlar. Her parçacık bir hız ve bir konum bilgisine sahiptir. Bu algoritmada her parçacık başlangıç olarak rastgele konumlarla başlarlar. Her konum, bir çözümü temsil etmektedir. Algoritmada hareket eden parçacıklar bir sonraki hareketleri kendi konumlarına ve diğer parçacıkların konumlarına göre yaparlar. Sürekli olarak her parçacık hareketi sonrası parçacıkların konum ve hız bilgisi güncellenmektedir. Algoritma çeşitli paremetrelere sahiptir ve bu parametreler uygun değerlerde ayarlanması gereklidir. Sonuç olarak algoritmada parçacıklar en iyi çözümü bulana kadar hareketlerine devam ederler. Önerilen algoritmada öncelikli olarak PV diziden voltaj ve akım ölçümleri alınır. Bu ölçümler ile güç değeri hesaplanır. İlk olarak Dürt ve Gözlemle algoritması devreye girer. Bu yöntem güç ve voltaj ölçümlerinin bir önceki değerleri ile güncel değerleri sürekli olarak karşılaştırır. Sonuç olarak bir referans voltajı üretir. Dürt ve Gözlemle algoritmasında üretilen referans voltajı, Parçacık Sürü Optimizasyonu algoritmasına giriş olarak alınır. Bu voltaj, Parçacık Sürü Optimizasyonu algoritmasında başlangıçta rastgele parçacık konumu oluşturulması aşamasında kullanılır. Parçacık Sürü Algoritması en iyi çözümü bulmayı tekrar deneyerek çıkış olarak tekrardan bir referans voltajı üretir. Bu hibrit yapı MPP takibi yapabilmek amacıyla art arda sürekli olarak çalıştırılır. Üretilen referans voltajı PI denetleyiciden geçer. DA-DA yükselten dönüştürücü kontrol devresinde Darbe Genişlik Modülasyonu sinyali üretilerek dönüştürücü anahtarlanmış olur.

Önerilen metot, MATLAB/Simulink programında fonksiyon jenaratörü bloğu kullanılarak sırasıyla 1000 W/m^2, 500 W/m^2, 600 W/m^2, 900 W/m^2 ve 800 W/m^2 ışınım değerleriyle simülasyon ortamında test edilmiştir. Ek olarak karşılaştırma amacıyla 3 farklı simülasyon çalışması hazırlanmıştır. MGNİ algoritması olmayan PV sistem, Dürt ve Gözlemle MGNİ Algoritmalı PV sistem ve Dürt ve Gözlemle ve Kalman Filtresi Hibrit MGNİ Algoritmalı PV sistem olmak üzere 3 farklı simülasyon çalışması hazırlanmıştır. Toplamda 4 farklı simülasyon çalışması çalıştırılarak MGNİ metotları karşılaştırılmış ve elde edilen sonuçlar detaylı olarak incelenmiştir. Sonuçlar incelendiğinde önerilen Dürt ve Gözlemle ve Parçacık Sürü Optimizasyonu tabanlı yeni bir hibrit MGNİ algoritmasının kısmi gölgelenme durumlarında referans voltajı üretimi, maksimum güç noktası takip doğruluğu ve maksimum güç noktası takip hızı kategorilerinde verimli bir yöntem olarak öne çıktığı sonucuna ulaşılmıştır.

Gelecekteki çalışmalarla birlikte yapay zeka destekli yeni MGNİ algoritmaları geliştirilebilir. Akıllı algoritmaların verimliliği düşünüldüğünde bu konuda yeni araştırmalar yapılabilir. Bilgisayar ve teknoloji alanındaki gelişmeler ile birlikte tasarlanabilecek yeni MGNİ algoritmalarınının maliyetleri azaltılabilir. DA-DA dönüştürücü teknolojisi geliştirilerek güç kayıpları azaltılarak MGNİ algoritmalarının verimliliğine katkı sağlanabilir. Sonuç olarak yapılan bu çalışmalar ile birlikte literatürdeki MGNİ metotlarını araştırmak ve geliştirmek, fotovoltaik teknolojiyi ilerletmek ve daha temiz bir dünyaya katkıda bulunmak istenmiştir.

ACKNOWLEDGEMENTS

First of all, I would like to thank my valuable thesis advisor Asst. Prof. Dr. Oğuzhan TİMUR for the experience and knowledge he has given me during this thesis project, for the continuous support he has provided, and for his understanding and patience.

I would also like to thank Asst. Prof. Dr. Özgür ÇELİK for the ideas, knowledge and support he has given me during my thesis work.

I would also like to express my sincere thanks to Prof. Dr. Ahmet TEKE and Asst. Prof. Dr. Kasım ZOR for accepting to be a member of the jury for my thesis and for their advises and support.

Finally, I would like to thank my wife Hürü Gül UZUNDAĞ, my mother Ayşe UZUNDAĞ, my father Tekin UZUNDAĞ and my brother Hakan UZUNDAĞ, who have always been with me and whose support I have always felt throughout this process.

LIST OF TABLES

LIST OF FIGURES

SYMBOLS AND ABBREVIATIONS

AC : Alternating Current
ANN : Artificial Neural Network
BST : Bisection Search Theorem
CC : Constant Current
CS : Cuckoo Search
CSI : Current Source Inverter
CV : Constant Voltage
D : Duty Cycle
DC : Direct Current
F_{grid} : Grid Frequency
F_s : Switching Frequency
GMPP : Global Maximum Power Point
GW : Gigawatt
GWO : Graf Wolf Optimization
HC : Hill Climbing
HPF : High Pass Filter
IEEE : Institute of Electrical and Electronics Engineers
IGBT : Insulated Gate Bipolar Transistor
INC : Incremental Conductance
I_{out} : Output current
KW : kilowatt
LCC : Linear Current Control
MAPE : Mean Absolute Percentage Error
MPC : Maximum Power Control
MPP : Maximum Power Point
MPPT : Maximum Power Point Tracker
MSE : Mean Squared Error
NRMSE : Normalized Root Mean Squared Error
OCC : One Cycle Control
OCV : Open Circuit Voltage
P&O : Perturb and Observe
PI : Proportional-Integra
PID : Proportional Integral Derivative
PLL : Phase Locked Loop
Ppv : PV Power

PSC : Partial Shading Circumstances

PSO : Particle Swarm Optimization

PV : Photovoltaic

PVM : PV Modules

PWM : Pulse With Modulation

RES : Renewable Energy Sources

R_L : Load Impedance

R_s : Series Resistance

R_{sh} : Shunt Resistance

SCC : Short Circuit Current

SDM : Single Diode Model

STC : Standard Test Conditions

THD : Total Harmonic Distortion

TWH : Terawatt hours

TWy : Terawatt years

V_{dc} : DC Link Voltage

V_{out} : Output voltage

VSI : Voltage Source Inverter

VSS-INR : Variable Step Size - Incremental Resistance

1. INTRODUCTION

1.1. Background and Research Motivation

For a variety of factors, including the dwindling of traditional energy sources, environmental concerns, and the fluctuating price of fossil fuels, the usage of renewable energy sources has significantly increased during the past ten years (El-Helw et al., 2017). One of the most effective and dependable renewable energy sources now in use is photovoltaic (PV) technology that is incorporated into power Networks (Joisher et al., 2020). PV sources are clean, renewable, and need less maintenance, which is just one of their many benefits (El-Dein et al., 2013). Photovoltaic (PV) arrays have made significant advancements all around the world as a practical method of utilizing solar energy (Zhang et al., 2019). Although the total installed capacity was just 72 GW in 2011 in the world, it increased to approximately 708 GW by the end of 2020 (Renewable Capacity Statistics 2021, 2021). This expansion has been fuelled in recent years by technological advancements, mostly linked to an increase in efficiency and a decrease in prices, and it is anticipated that this trend will persist (Victoria et al., 2021).

PV systems have a robust modular capability that allows for significant design flexibility and enables their usage in a wide variety of applications, from a few hundred watts to a few gigawatts (Bishop, 1998). When compared to conventional energy sources, PV systems still have significant obstacles to overcome and PV arrays are nonlinear systems. The properties of a PV array at constant irradiation levels are shown in Figure 2.1. (Elobaid, et al., 2022).

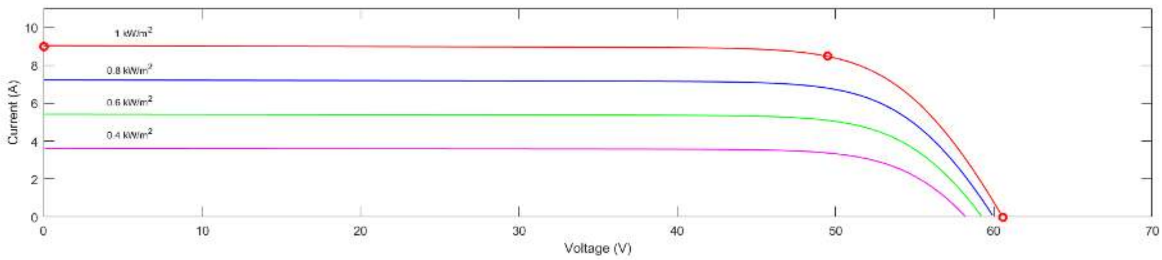

(a)

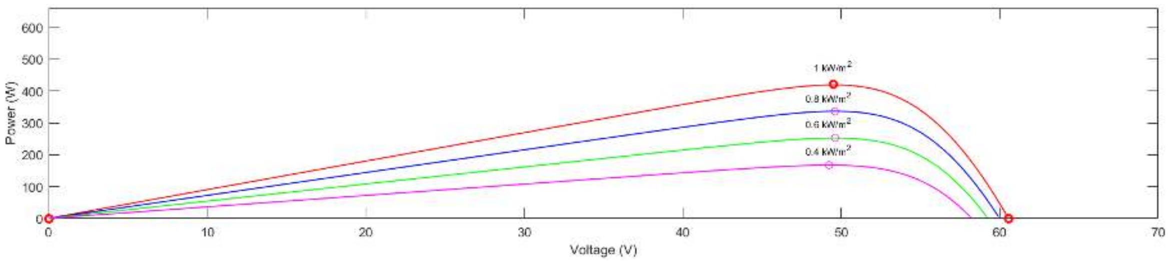

(b)

Figure 2.1. Characteristics of photovoltaic arrays: (a) Current-Voltage curve, (b) Power-Voltage curve

The ambient PV cell temperature, solar irradiation, and load that the PV array is under determine the output power of the PV array. The output power of a PV array depends on its terminal voltage under uniform irradiance and in the same weather. Consequently, there is only one working voltage that yields the most power. Maximum power point tracking is the technique used to find this ideal voltage (Elobaid, et al., 2022; Ji et al., 2009; Chekired et al., 2012; Jiang et al., 2015; El-Helw et al., 2016).

When linked components have different qualities or operate under different operating circumstances, output power losses result. Because PV cells connected in a series must function at the same current level, enforced by the most restricted cell (Filho et al., 2021). However, a major difficulty continues to be the poor efficiency of PV systems, which is frequently caused by their nonlinear electrical characteristics and fluctuating atmospheric conditions. Local atmospheric factors, including as moving clouds, dust, nearby buildings, and trees, have a significant impact on the efficiency of PV systems. These obstacles cause PV systems to produce less power. Therefore, a PV system must function at its “Maximum Power Point (MPP)” in order to overcome this primary disadvantage (El-Dein et al., 2013).

A PV system typically consists of the PV array, power electronics interface circuit, and load and Figure 2.2. (Patcharaprakiti et al., 2005; Ngan et al., 2011) shows this system.

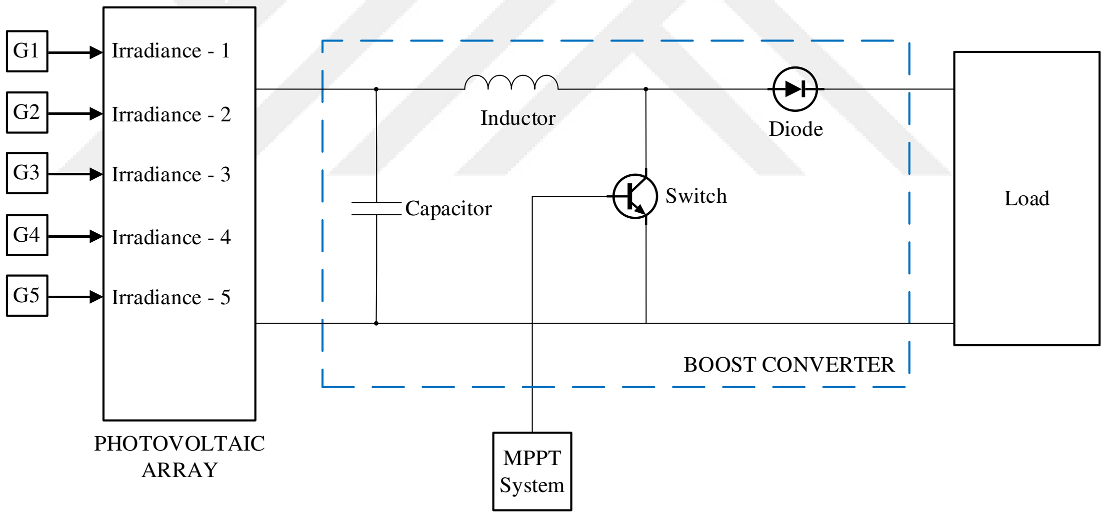

Figure 2.2. The photovoltaic system’s structure

A boost converter is available to connect a PV array with four modules that have various irradiance levels. The primary purpose of the power electronics circuit is to utilize the MPPT technology to extract the most power possible from the PV array and send it to the load or electrical grid (Patcharaprakiti et al., 2005; Ngan et al., 2011). With an open circuit voltage of 0.5 - 0.6 V, PV Modules (PVM) comprises of solar cells connected in series. Usually, solar cells are wired together in series to create submodules (also known as cell strings), and several submodules are wired together to create PVMs. The size and electrical characteristics of the solar cells have a restricted range of uses. As a result, a PVM may be defined as the smallest PV component in solar power systems. The

PVMs are supplies with logarithmic current-voltage (*I-V*) properties that can provide the most power for a single current and voltage value. Additionally, it generates changeable DC power based on temperature and sun radiation levels (Reisi et al., 2013). As a result, MPPT is a crucial necessity for PV systems (Esram et al., 2007).

An increasing amount of emphasis is placed on integrated solar energy applications (Klasen et al., 2022). To provide the most power from the PV array, a number of maximum power point tracking (MPPT) systems in conjunction with power electronic devices have been presented recently (Joisher et al., 2020). These methods differ in some fundamental ways, including complexity, exactness, price, and speed. Due to their simplicity and ease of implementation, the "Hill Climbing (HC) and Perturb and Observe (P&O)" algorithms are the most often utilized among them (Zhu et al., 2018; Abdelsalam et al., 2011). These two methods demonstrate a similar core strategy for obtaining the MPP. The HC algorithm works by irregularly changing a power converter's duty cycle. The P&O algorithm operates with a change in the PV system's operating voltage (Kollimalla et al., 2014; Petrone et al., 2011).

When a solar device is shaded, it ceases to produce electricity; even little shading can result in considerable reductions in the anticipated energy harvest (Jahn et al., 2004). Frequently, trees, poles, chimneys, and antennas provide shade (Eke et al., 2015; Schuss et al., 2014; Deutsche Gesellschaft Für Sonnenenergie, 2013; Gotz et al., 2019; Brecl et al., 2021). The PV module is forced to work in conditions of partial shade due to the impact of shadows created by nearby objects (Bi et al., 2019).

In PV systems deployed in urban locations, partial shading is a frequent loss factor that should be taken into account when estimating electrical output (Trzmiel et al, 2020). The partial shading phenomena in some PV array modules restrict the total current of the series modules and decreases the overall output power (Torkian and Ghandehari, 2022). Although a full shadow on the PV array may be tolerated, the amount of energy that can be harvested is greatly reduced by a partial shade that covers a portion of the array. The photovoltaic modules in an array are often connected in series, and since the shaded modules impose their own lower current on the other modules, the output power of the PV array is decreased (Bidram at al., 2012). This situation is represented in Figure 2.3. (El-Dein et al., 2012).

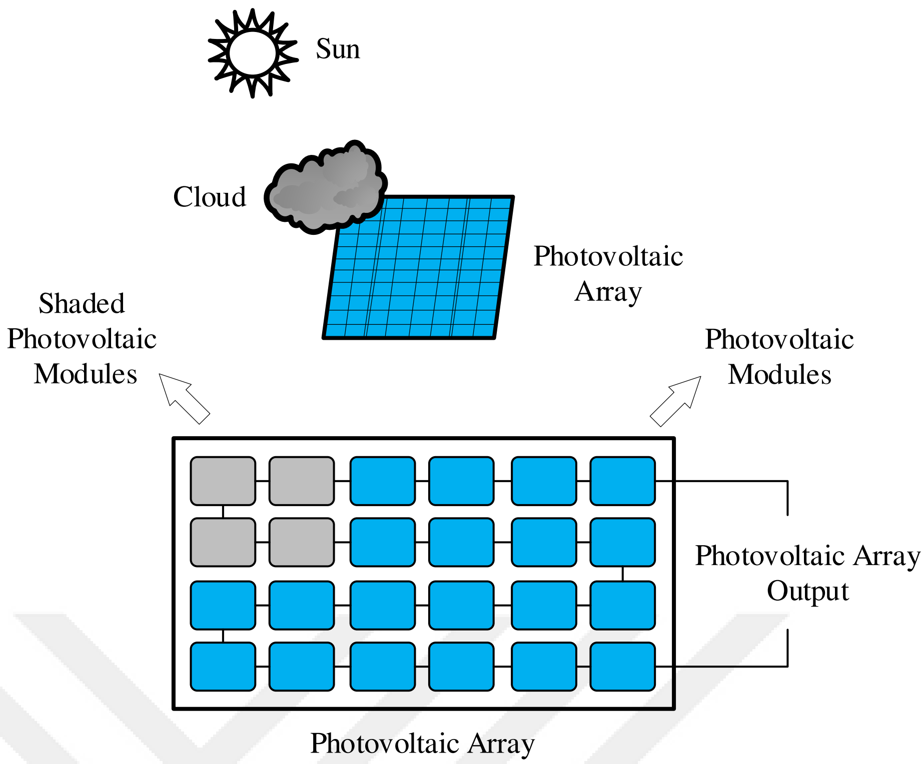

Figure 2.3. A PV array's series connection has a current restriction because of the shaded modules

As seen in Figure 2.4. (El-Helw et al., 2017), the shaded PV cells use a portion of the energy produced by the non-shaded PV cells if any of these panels are shaded by passing clouds, nearby trees, or other buildings (El-Helw et al., 2017).

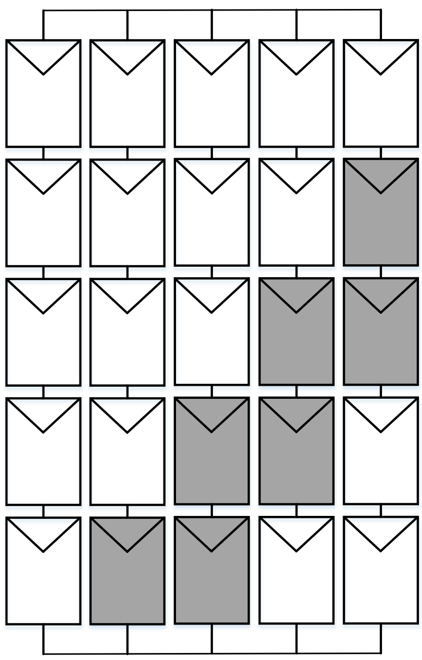

Figure 2.4. Partial shading condition as representative

This used energy is converted to heat, creating a hotspot that might hurt. By adding bypass diodes, the hotspot problem may be removed. On the other hand, the PV arrays properties are altered by the bypass diodes that are utilized to prevent the hotspot issue (Bidram et al., 2012).

The characteristics of photovoltaic (PV) systems can vary and have several power peaks, under partial shading circumstances (PSCs) (Joisher et al., 2020). This situation can be seen in Figure 2.5. (El-Helw at al., 2017).

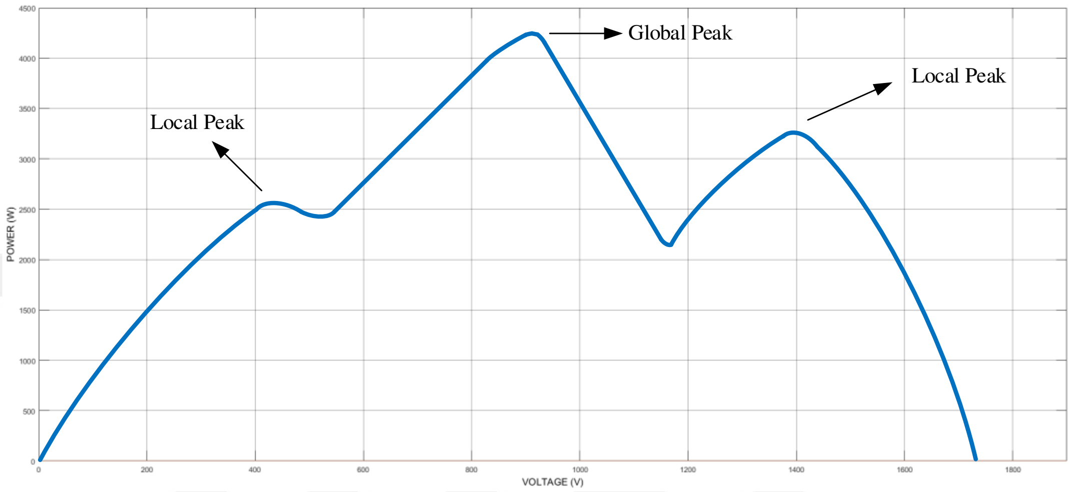

Figure 2.5. Characteristics of photovoltaic arrays while partially shaded

There are several research studies that address the issue of partial shading in PV arrays (Horoufiany and Ghanderehari, 2017). The global peak cannot be tracked using conventional Maximum Power Point Tracking (MPPT) methods. Furthermore, it takes a long time to reach the Maximum Power Point (MPP) (Joisher et al., 2020).

1.2. Outline of the Thesis

The main objectives of this thesis are to investigate the MPPT methods used under partial shading conditions in the literature, to compare the algorithms in the literature, to design a new MPPT algorithm that can be used for partial shading conditions, to test the proposed MPPT algorithm in the MATLAB/Simulink simulation program, to examine the simulation results and to compare it with other algorithms. In order to test the proposed algorithm in the study, a PV system with a PV array, a DC-to-DC boost converter, an MPPT algorithm block, a PI controller and a converter control circuit was designed. After the first section, where the purpose of the study is explained, the researched topics are explained and a brief summary of the study is made, the structure of the thesis continues as follows.

In Section 2, general information about renewable energy and solar energy is explained. Topics such as PV cells, PV modules, PV arrays, mathematical modelling of PV cells, characteristics of PV cells, and application areas of PV systems are explained. In addition, various MPPT algorithms used for changing radiation conditions in the literature are explained in detail. The effect of MPPT algorithms on efficiency is discussed.

In Section 3, a PV system with a new hybrid MPPT algorithm based on Perturb and Observe and Particle Swarm Optimization was designed in the MATLAB/Simulink simulation program. In addition, three different simulations were prepared for comparison while testing the proposed algorithm. The working logic and other information of the proposed algorithm and the algorithms in the other test simulations were explained.

In Section 4, the proposed MPPT method and other different algorithms were tested under different irradiation conditions in the MATLAB/Simulink simulation program. In this section, the test conditions and simulation information were explained. The simulation results were shown with graphics and interpreted.

In Section 5, the simulation results performed in the study were interpreted and summarized. The importance of the study was explained and the general aspects of the proposed MPPT algorithm were explained.

1.3. Contributions of the Thesis

The innovations that this thesis adds to the literature and the importance of the study can be explained as follows:

i. A literature review explaining the status of renewable energy in the world and Turkey has been prepared. A detailed literature review of many MPPT methods developed for partial shading conditions has been conducted and these methods have been compared.

ii. A new hybrid MPPT method based on Perturb & Observe and Particle Swarm Optimization algorithms has been developed to solve the problems of partial shading conditions in PV systems.

iii. The proposed MPPT algorithm has been tested in different irradiation scenarios with different MPPT algorithms in the MATLAB/Simulink simulation program by preparing a PV system simulation. The graphs of the simulation results have been prepared and the results have been interpreted.

iv. (iv) According to the study results, it has been understood that the developed method is good at tracking MPP, the MPP tracking speed is better and the efficiency of the system is increased.

2. PRELIMINARY WORK

2.1. Renewable Energy

Global Warming is a phenomenon in the last decades that impair to humanity and entire world (Elavasrasan et al., 2020). Nowadays, climate change menace is raised and bad effects are started on humanity. Because of these circumstances, clean energy usage considerably has been the centre of attraction of investigators (Gao and Chen, 2023). Fossil fuels have become a main source of dependency and it is owing to extraordinary production requirements and rising energy usage (Hashim, 2021). Consequently, Fossil fuels caused to begin increasing carbon dioxide emission in the air (Halicioglu and Ketenci, 2018). Nearly three out of four percentage carbon dioxide emissions is accounted for the energy generation area. Global warming is formed because of this major rating (Elavasrasan et al., 2020).

Recently, non-renewable energy usage becomes major problem and fear in world (Khalili and Breyer, 2022). Protecting the world from climate change and global warming have become increasingly popular in latest days (Xiong et al., 2021). Main energy source being fossil fuels started with the technological revolution (Hangun et al., 2022). To achieve a clean future, a shift to renewable energy is necessary. Sustainability should be examined because meeting needs leads to a decrease in sources (Elavarasan et al., 2020). It is climate change that causes financial damages (Husak et al., 2020). Renewable energy use should be increased due to energy cost (Khalili and Breyer, 2022).

The United Nations advises using renewable energy sources in order to decelerate the consequences of climate change (Elavarasan et al., 2020). We can equate the word renewable energy with the word green power. Being eco-friendly puts this green power at a very important point (Qazi et al., 2019). Renewable Energy does not consume sources. No detrimental gases are released into our world (Gao and Chen, 2023). One of the finest options to win our future is renewable energy (Ghute et al., 2021). In the use of renewable energy, no CO_2 is released into nature. To refrain from global warming problems, non-renewable resources are not used (Husak et al., 2020). Renewable energy is more beneficial than fossil fuels in protecting the world. Financial gains and safety are possible with renewable energy (Qazi et al., 2019). Renewable energy sources are not only used to keep away from polluting the atmosphere. Moreover, it is one of the main purposes of states to preserve our world. Before achieving these goals, it is necessary to create knowingness and devotion (Harrauz et al., 2020).

Exhaustion of non-renewable energy sources may be imminent (Hangun et al., 2022). Renewable energy is the main way for countries to development. This is mainly important for all countries contingent upon non-renewable energy sources (Hua et al., 2016). Energy generation worldwide is achieved by nuclear energy sources, renewable energy sources and fossil fuels (Hangun et al., 2022). Today, importance is given to energy generation with renewable energy sources such as wind energy and solar energy (Wang et al., 2021). Many major states have turned to using renewable energy for a long-lasting and greener world (Hangun et al., 2022). The use of renewable energy in energy systems has increased significantly in lately (Sadiq et al., 2021). Utilizing sustainable energy sources is attracting more and more attention not only from authorities but also from the broader audience (Qazi et al., 2019). Renewable energy sources include, wind energy, hydroelectric energy, geothermal energy, biomass energy and solar energy. These types of resources are very useful to deal with energy problems (Asfaq and Ianakiev, 2018; Raheem et al., 2016). Local energy needs can be met from renewable energy sources (Qazi et al., 2019). There are many benefits to turning to renewable energy. Contributes to reducing tomorrow costs of energy. It helps financial growth. Increases occupation job in the long run. It reduces the need for non-renewable energy sources (Gaon and Chen, 2023). Energy generation depends on renewable energy for both today and tomorrow.

The sun is an inexhaustible source of energy and is the main element in renewable energy sources (Qazi et al., 2019). Photovoltaic energy is obtained by generating electrical energy from the energy received from the sun. In the photovoltaic sector, prices have decreased and efficiency has risen last days. For this reason, the use of PV energy has become widespread and is supposed to progress (Chepp et al., 2021). This widespread use has been achieved due to its rapid construction and modularity (Victoria et al., 2021). Supply of energy produced by photovoltaic panels is variable. The energy produced is affected by variables such as panel type, seasonality, shading, weather, temperature, and amount of irradiation (Yavuz and Botsalı, 2022). PV technologies will become more prevalent in our lives in later (Xiong et al., 2021).

Thanks to technological, financial, industrial and wellbeing developments, issues such as energy production and energy demand have become issues that need to be addressed in the world (Kılıç and Kekeoğlu, 2021). The world has the potential to benefit from 23 thousand TWy of solar energy per year by using solar energy. The total energy consumed in the world for 100 years corresponds to approximately 1,600 TWy of power. This situation is seen in Figure 2.6. (Rao et al., 2021) below. The amount of non-renewable energy resources in the world has been determined as 1,655 TWy. With an optimistic estimate, the amount of renewable resources that are not directly solar-based is determined as 94 TWy (Rao et al., 2021).

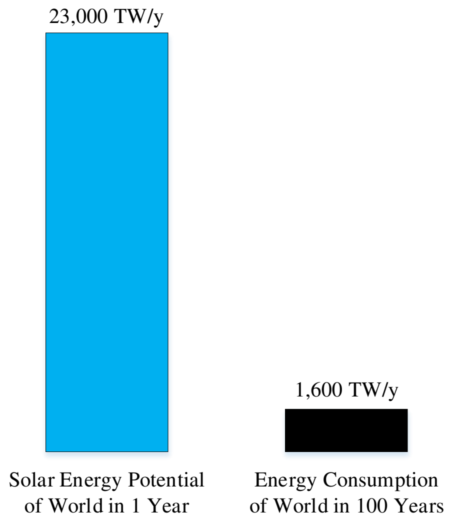

Figure 2.6. The world potential to benefit from solar energy and energy use in the world

Energy demand continues to increase in the world due to the increase in population and industry. The world's need for power grew by 627 TWh in 2023. This rate corresponds to percentage 2.2. Total annual demand has been about 30,000 TWh. This is the highest demand value to date (Rao et al., 2021).

The amount of electrical energy used in the world has been increasing continuously over the years. In recent years, especially in 2020, it is thought that the decrease was due to the global coronavirus pandemic. This increase continued after the pandemic. This situation is seen in Figure 2.7. (Statista, 2024).

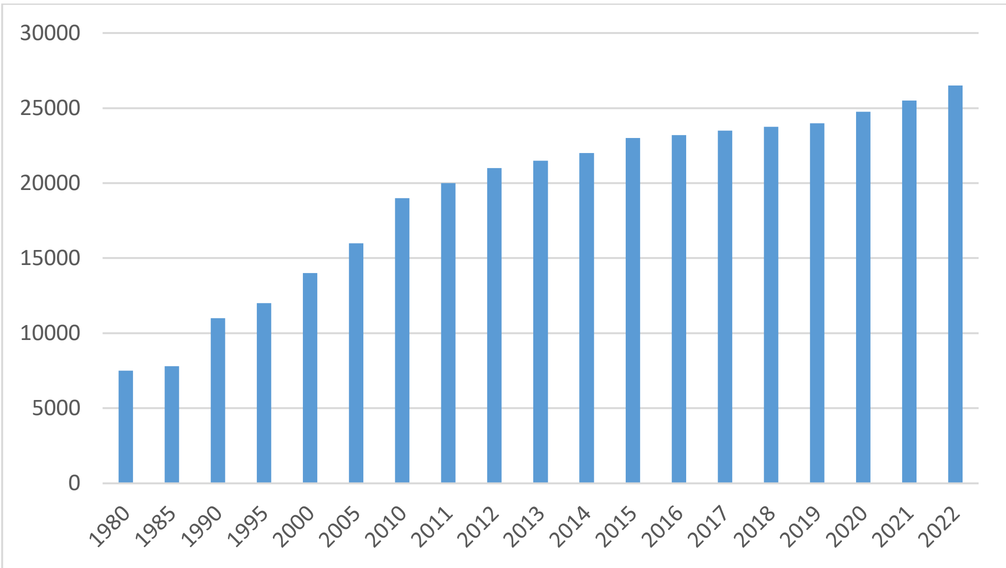

Figure 2.7. Global electricity consumption (TW/h)

Energy production has been increasing globally. In 2020, energy production decreased again due to the coronavirus pandemic. After the pandemic, energy production has started to increase again. Figure 2.8. (Statista, 2024) below shows this global electrical energy production.

Many resources are used in global electricity production. With the new electricity production plants, distributions are constantly changing over the years. This trend in renewable energy is heading towards a positive shape. As in every year, various data on global electrical energy production have been published in 2023.

By the end of 2023, the share of electricity produced in the world using gas and coal was 61 percent. Thirty five percent of the production was realized using coal. This production share, which is approximately 10,434 Terawatt/hours, is at the highest level. The share of electricity production using gas is 23 percent. This corresponds to a production of 6,634 Terawatt/hours. The 2.7% rate shows electricity production using other fossil fuels. This production amount is 786 Terawatt/hours. The share of hydroelectric energy was 14%. 4,210 Terawatt/hours of production was realized (EMBER, 2024).

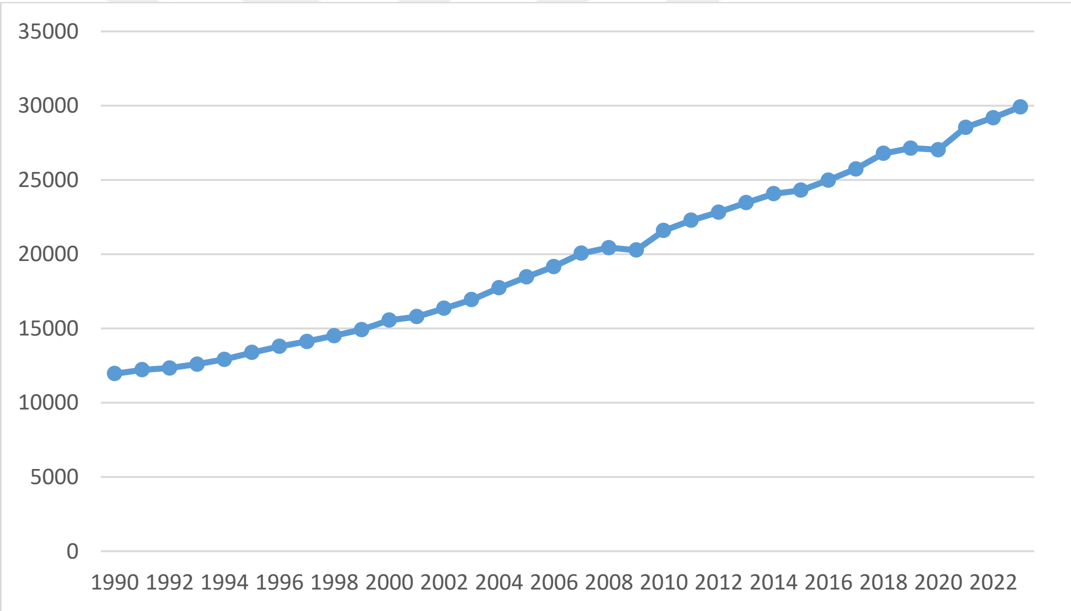

Figure 2.8. Global electrical energy production (TW/h)

Nuclear Power Plants provided nine-point one percent of global energy. The generation amount of this source appears to be 2,686 Terawatt/hours. The share of wind energy was 7.8 percent. The amount of wind energy generation was calculated as 2,304 Terawatt/hours. Solar electricity generation was recorded with a share of five-point five percent. An annual production amount of 1,631 Terawatt/hours was calculated for solar energy. Energy generated using bioenergy has a share of 2.4 percent. Globally, this type of resource generates 697 Terawatt/hours. In addition, the share of other renewable energies was 0.3 percent. A total of ninety Terawatt/hours of energy was produced from these sources in one year (EMBER, 2024). The distribution graph of this global energy production is as in Figure 2.9. (EMBER, 2024).

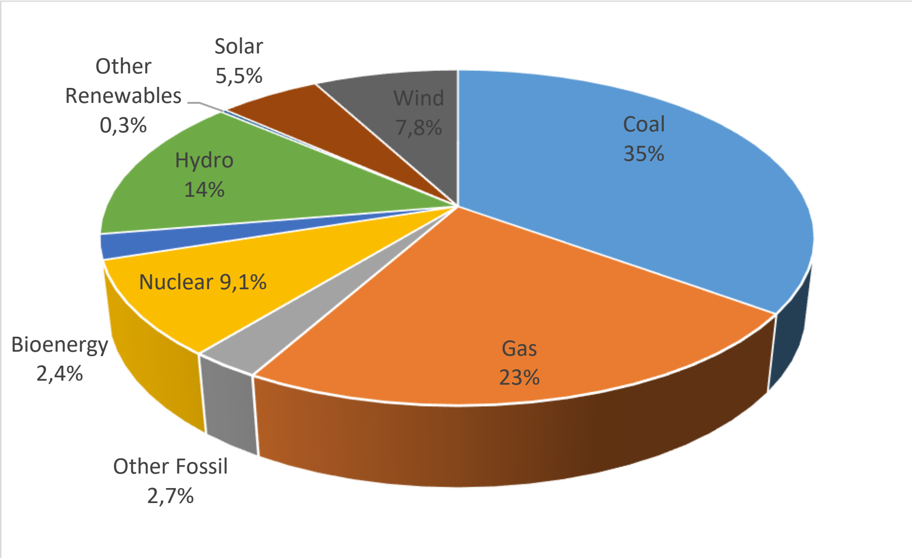

Figure 2.9. Share distribution in global electricity production by resources (%)

The number of power plants using renewable energy in the world has increased significantly in recent years. The total renewable energy installed capacity in the world has reached 3,869.7 GW with 2023 data. When compared to the 1,223.5 GW installed capacity in 2010, it is seen in Figure 2.10. (Statista, 2024) that there has been an increase of approximately 2,700 GW in power in 13 years.

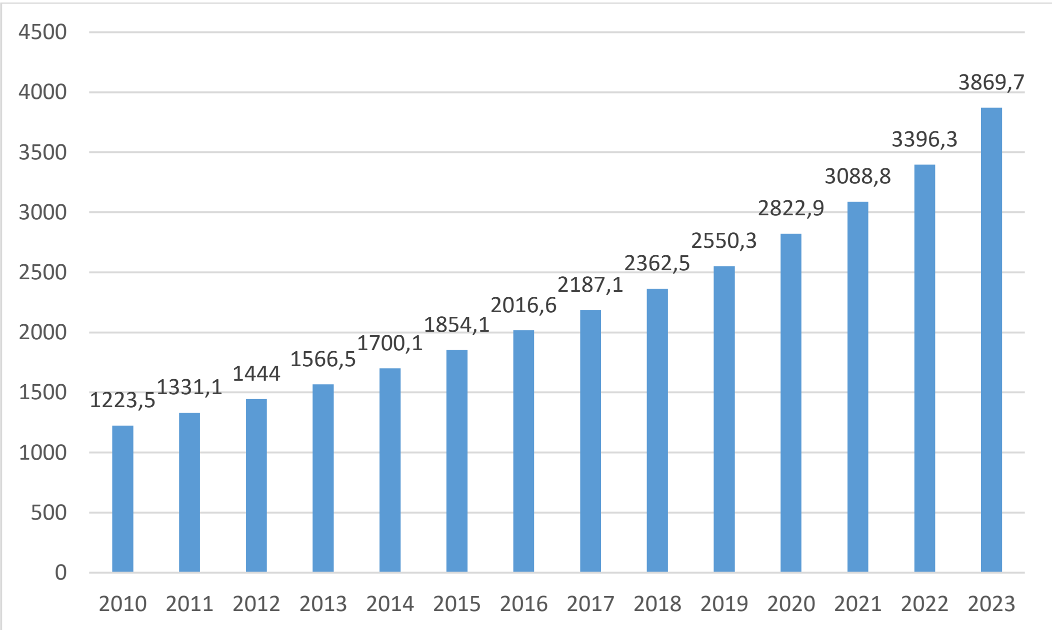

Figure 2.10. Global renewable energy total installed capacity (GW)

When the global renewable energy total installed capacity by sources used in Figure 2.11. (Statista, 2024) is examined, it is seen that solar energy has reached 1,412.1 GW installed power. Hydroelectric power installed power follows it from the second place. Moreover, wind energy has taken its place in the third place. As can be understood from the graph, solar energy has become a type of energy where investments are increased as the new trend of today.

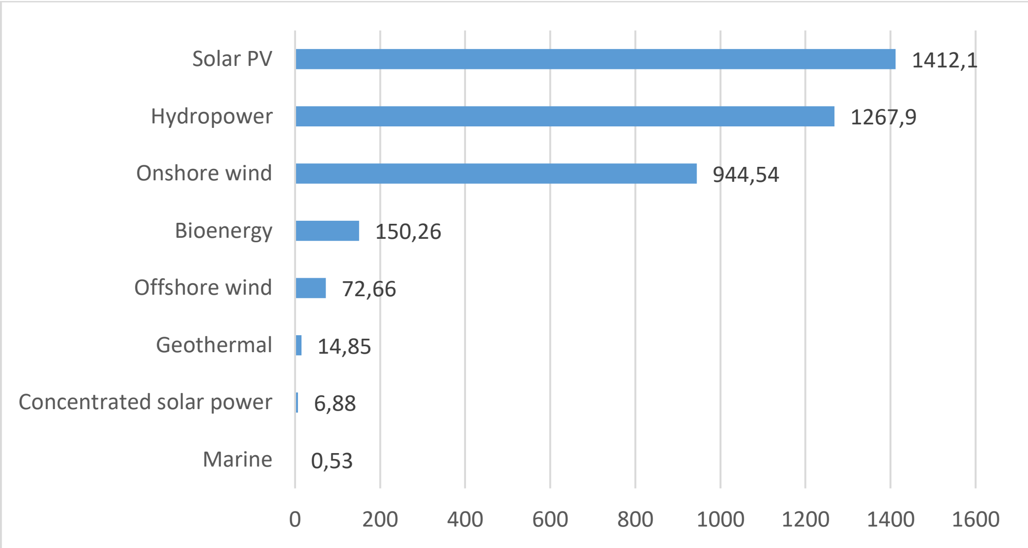

Figure 2.11. Global Renewable Energy Total Installed Capacity by Sources Used (GW)

With the use of renewable energy sources in recent years, thirty percent of the world electricity generated now comes from renewable sources. Thus, the highest share of renewable energy in world energy production was achieved to date. Low-emission resources account for approximately 40% of the world's electricity generation, thanks to the use of nuclear energy (EMBER, 2024).

When examining the renewable energy issue, it is necessary to draw attention to Türkiye, a country with high solar energy potential in Europe. Türkiye is a peninsula country in the northern hemisphere, close to the European continent, where four seasons are seen and surrounded by sea on three sides.

The 26° - 45° east meridian and 36° - 42° north parallel are where Türkiye is located on Earth. Türkiye's area of surface is calculated as 783,562 km^2 (Emikönel and Bilhan, 2022). This country's solar energy potential surpasses many European regions. This solar potential cannot be used at the desired and high level (Kılıç and Adalı, 2022). Many regulations and discounts have been put into effect by the Turkish Government to increase renewable energy (Yavuz and Botsalı, 2022). Progress is expected with many beneficial developments like this in the country (Kılıç and Adalı, 2022). Solar radiation map of Türkiye's is as shown in Figure 2.12. (General Directorate of Renewable Energy (YEGM), 2024) and shows Türkiye's solar energy potential (Emikönel and Bilhan, 2022).

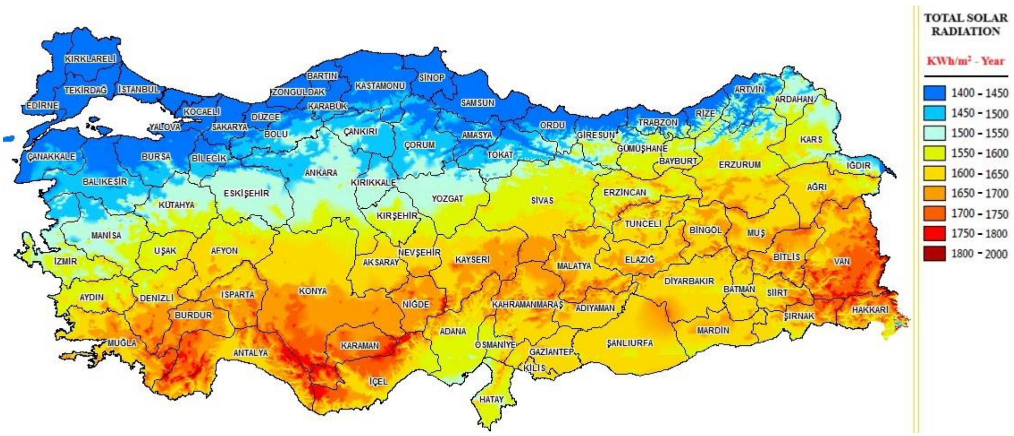

Figure 2.12. Türkiye solar energy potential map

When the map is examined, the areas with high solar radiation are in the areas with dark redness. The areas with low solar radiation are represented by light blue (Emikönel and Bilhan, 2022). The top solar radiation in Türkiye is in the Southeastern Anatolia Region (lower right border regions of the map). The least solar radiation is in the Black Sea Region (upper regions of the map). Türkiye sees an average of 7.49 hours of sunshine per day. The annual total is 2,736.89 hours (Emikönel and Bilhan, 2022).

Figure 2.13. (General Directorate of Renewable Energy (YEGM), 2024) shows the graph containing daily sunshine durations in Türkiye (Altınkök et al., 2022). As can be seen from the graph, the highest duration was reached in July with 11.31 hours of daily sunshine. The smallest situation is 3.75 hours per day in December month (Emikönel and Bilhan, 2022).

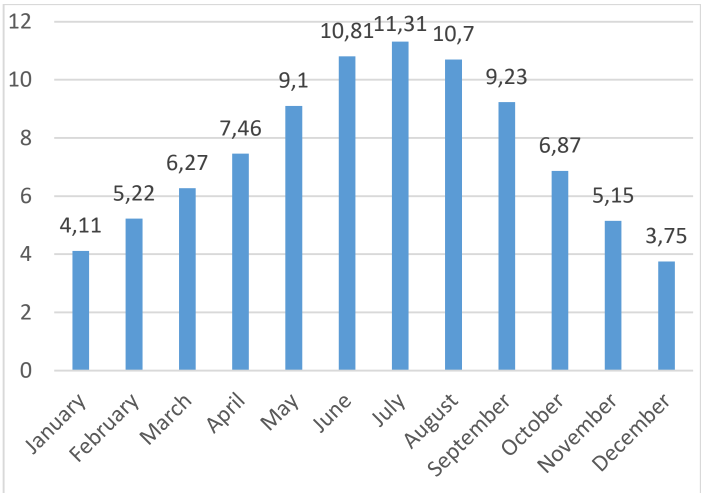

Figure 2.13. Average monthly sunshine duration in Türkiye (hours/day)

Türkiye's monthly solar radiation graph is as shown in Figure 2.14. (General Directorate of Renewable Energy (YEGM), 2024). Similar to the sunshine durations, the highest radiations are seen in June and July. The lowest radiations are in December and January.

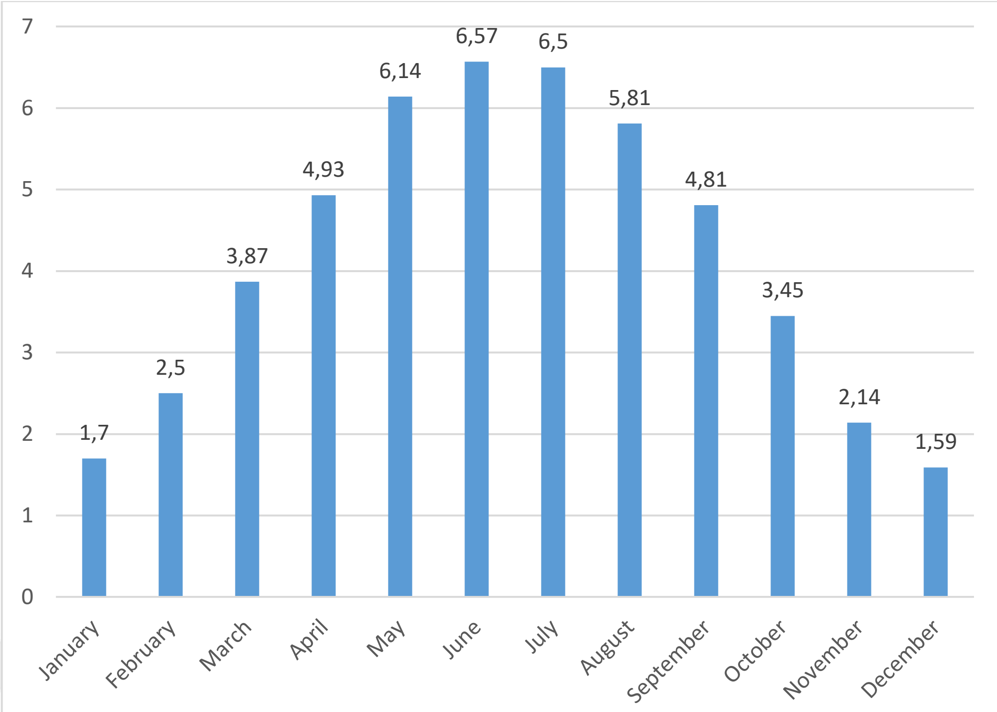

Figure 2.14. Global monthly solar radiation values in Türkiye (kWh/m^2 - day)

In light of these circumstances, when the latest situation in renewable energy in Türkiye is examined, it is obvious that there is a shift towards renewable energy.

2.2. Photovoltaic Systems

2.2.1. Photovoltaic Cells

Light from the sun reaches photovoltaic cells where light energy is used to produce electrical energy. Semiconductor materials are found in their internal structures (Çabuk, 2022). The performance of photovoltaic cells depends on the internal structure of the semiconductor material used in them. Naturally, the voltage and current features of these materials affect the efficiency of photovoltaic cells (Joshi and Vaishnav, 2021).

Inside photovoltaic cells, there is a n-p junction, just like a diode containing semiconductor materials. Among the n-p junctions found in photovoltaic cells, the n junction carries negative charges. The p junction is responsible for carrying positive charges (Çabuk, 2022). Figure 2.15. (Joshi and Vaishnav, 2021) shows the internal structure of the PV cell.

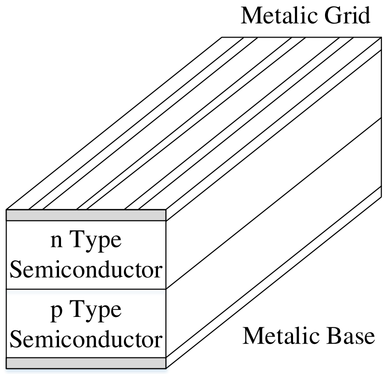

Figure 2.15. Basic internal structure of a PV cell

In a photovoltaic cell, electricity is produced as a result of the photoelectric event. (Joshi and Vaishnav, 2021). This phenomenon was put forward by scientist Alexandre Edmond Becquerel in 1839 (Mesquita et al., 2019).

The photoelectric effect can be explained as the electrons in a substance becoming free when exposed to radiation (Patel and Agarwal, 2008). As a result of this event, the free electrons flow from the n junction to the holes in the p junction and electric current occurs.

In a perfect photovoltaic cell, leakage currents and other losses do not occur, but in practice, these losses can occur (Keles et al., 2013). Various technologies are used in photovoltaic cells. If we talk about the first technology, it is thin solar cell technology. This technology has copper and Cadmium-Telluride. Another technology can be based on semi-conductor substances technology. Hybrid cells can be given as another cutting-edge technology (Joshi and Vaishnav, 2021).

Silicon is commonly found in traditional PV cells. Copper Indium Gallium Selenide and Gallium Arsenide are also used in some new technology products. Photovoltaic cells are generally produced in two different types: polycrystalline and monocrystalline cell types (Joshi and Vaishnav, 2021).

The monocrystalline cell type is seen in Figure 2.16.a. (Mesquita et al., 2019). The polycrystalline cell image can be found in Figure 2.16.b. (Mesquita et al., 2019). A PV cell made of monocrystalline material can usually be black to dark blue. PV cells made of polycrystalline material have an inhomogeneous appearance, as the name suggests. They are usually blue in appearance (Mesquita et al., 2019).

(a) (b)

Figure 2.16. (a) Image of a PV cell made of monocrystalline material, (b) Image of PV cell made of polycrystalline material

2.2.2. Photovoltaic Modules

A photovoltaic cell usually produces a voltage between 0.5V and 0.6V. A short circuit current of between 2A and 2.5A occurs in this PV cell. 1W and 1.5W output power can be observed in these PV cells. When these values are considered, the power value is sufficient for simple electronic devices. When general usage is considered, a single PV cell will be insufficient. When it is desired to store a battery, these values will be deficient. To eliminate this inadequacy, the voltage value is increased by connecting PV cells in series. Parallel connections are made to increase the current value (Sarıoğlu and Eke, 2012). In summary, photovoltaic modules are composed of many PV cells brought together with these connections.

Thirty-six or seventy-two PV cells are the number of PV cells used in common module types. Due to their front surface coating and reflection properties, their efficiency is lower compared to PV cells. Tempered Transparent Glass and iron structures are found in the front areas of PV modules (Joshi and Vaishnav, 2021). The PV module image, which is created by combining PV cells made of monocrystalline material, is shown in Figure 2.17.a. (Mesquita et al., 2019). Similarly, the polycrystalline PV module is as in Figure 2.17.b. (Mesquita et al., 2019).

(a) (b)

Figure 2.17. (a) Image of a PV module made of monocrystalline cells, (b) Image of a PV module made of polycrystalline cells

2.2.3. Photovoltaic Arrays

Photovoltaic arrays are formed by connecting many photovoltaic modules in parallel and series. If it is desired to generate electricity on an industrial basis, a single photovoltaic module will not meet the needs (Joshi and Vaishnav, 2021). A large number of solar cells are connected in series by mounting them together. Thus, series-connected photovoltaic cell arrays are created. These structures are reassembled in the next stage and a larger structure is obtained (Ma et al., 2014). As a result, the current values and voltage values produced from these parallel and series connections become higher (Joshi and Vaishnav, 2021). In order to have a high voltage value, a series connection is made. For current, it should be made in parallel (Ma et al., 2014). PV panels are generally structures formed by combining several PV modules. The visual images of PV cells, PV modules, PV panels and PV arrays are as shown in Figure 2.18. (Dulaimi, 2017).

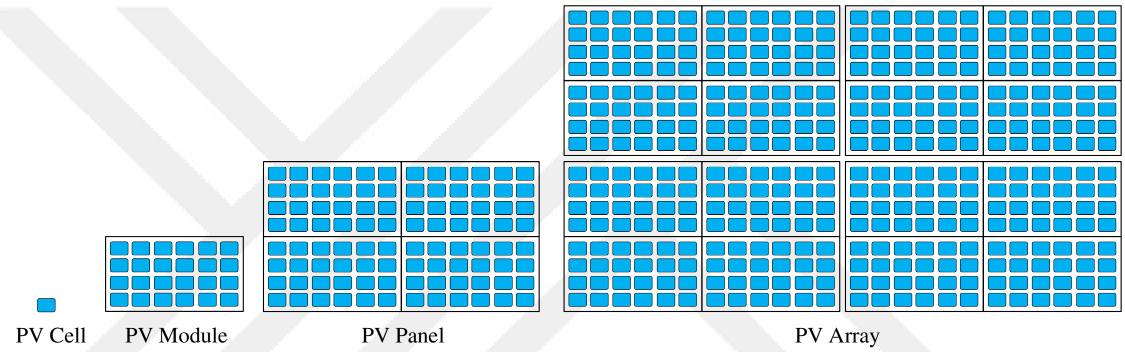

Figure 2.18. Images of PV cells, PV modules, PV panels and PV arrays

The clear representation of the arrays obtained by connecting photovoltaic arrays in parallel and connecting in series is as in Figure 2.19. (Ma et al., 2014).

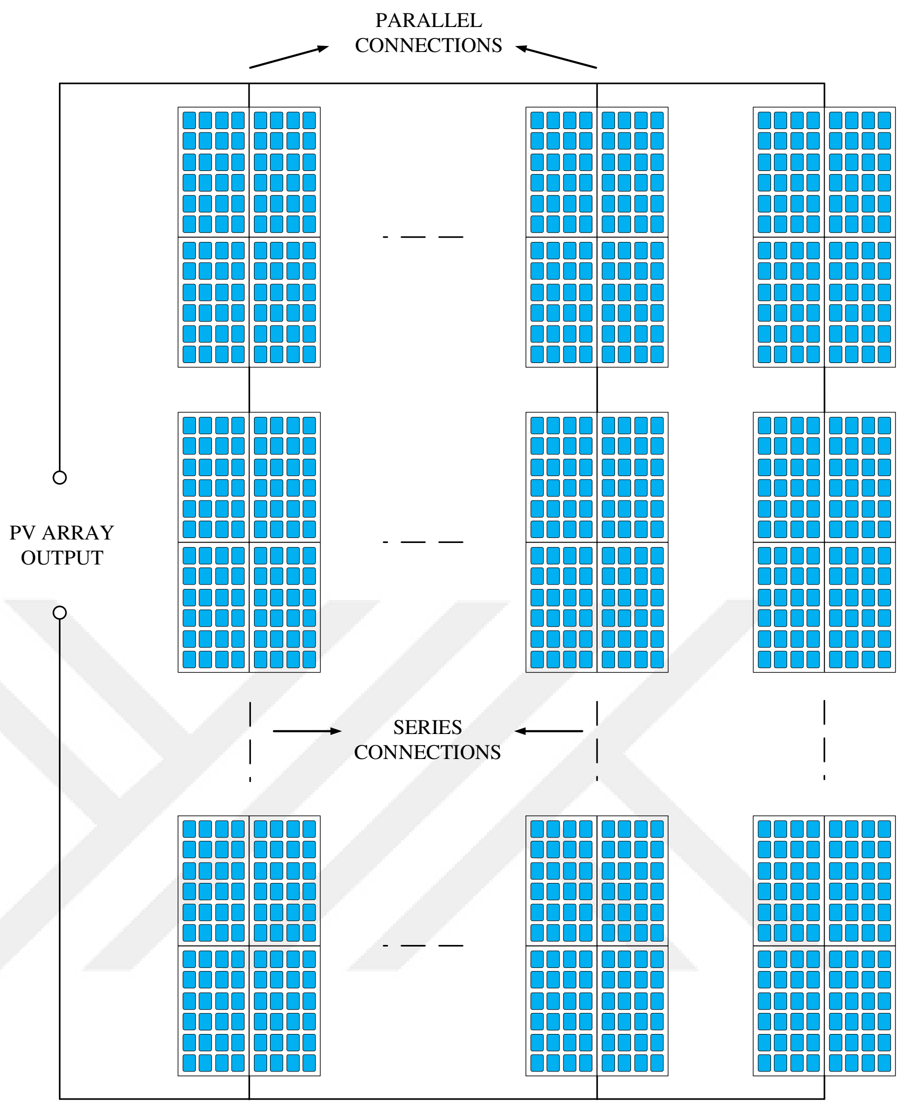

Figure 2.19. Representation of the photovoltaic arrays

Three types of connections are used in photovoltaic arrays. Firstly, photovoltaic arrays can be built with series panels. As a result of this structure, voltage can be incremented. All photovoltaic panels are connected with the identical current via a series panel connection. The connection is made by bringing the positive and negative connection ends of the panels together (Adak et al., 2019).

The current value is incremented in parallel panel connection. In parallel-connected arrays, the junction parts of the photovoltaic panels with the same polarity are connected to each other. Photovoltaic arrays can be constructed with both parallel and series (Adak et al., 2019). It can be said that this connection is a generally used structure depending on the needs. Additionally, both series and parallel PV array connections are shown in Figure 2.19. (Ma et al., 2014).

2.2.4. Equivalent Circuit and Modelling of Photovoltaic Cells

An equivalent model of solar panels is prepared to facilitate calculation work. To achieve this, the equivalent model is also made mathematically. Photovoltaic panels can be simply modelled as a circuit consisting of a single diode and resistors connected in series and parallel. This model also has a revised version that uses two diodes (Xiong et al., 2021). Here, modelling with a simple diode will be discussed.

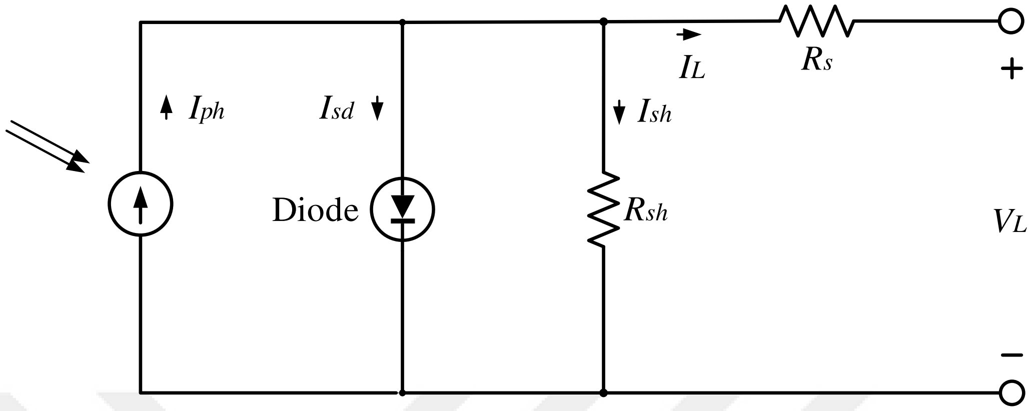

Figure 2.20. Modelling a photovoltaic panel represented single diode

Figure 2.20. (Xiong et al., 2021) shows the modelling of a photovoltaic panel. Five main equations can be mentioned in the mathematical modelling of photovoltaic cells. The following equations are valid for single diode modelling (Xiong et al., 2021).

$$I_{\mathrm{L}} = I_{\mathrm{ph}} - I_{\mathrm{d}} - I_{\mathrm{sh}} \tag{2.1.}$$

$$I_{\mathrm{d}} = I_{\mathrm{sd}}^{\left(\frac{V_L + I_L \times R_S}{n \times V_t}\right)-1} \tag{2.2.}$$

$$V_t = \frac{k \times T}{q} \tag{2.3.}$$

$$I_{sh} = \frac{V_L + I_L \times R_S}{R_{sh}} \tag{2.4.}$$

$$I_L = I_{ph} - I_{\mathrm{sd}}^{\left(\frac{V_L + I_L \times R_S}{n \times V_t}\right)-1} - \left(\frac{V_L + I_L \times R_S}{R_{sh}}\right) \tag{2.5.}$$

The value of the I_L current can be found as in Equation 2.1.

- The current coming out of the photovoltaic cell is I_{ph}.
- Current I_{d} passes through the diode.
- The I_{sh} current will pass through the resistor in the arm parallel to the diode (Xiong et al., 2021).

Shockley formula is given in Equation 2.2.

- Diode current can also be expressed with this equation.
- The voltage at the output end of the model is represented as V_L.
- The saturation current of the diode can be represented by I_{sd}.
- The ideal factor constant of the diode is expressed by n.
- The value of the resistance represented as a series connected resistor in the model is represented by R_s.
- The value of the resistance connected in parallel with the diode is expressed by R_{sh} (Xiong et al., 2021).

In the model, the junction thermal voltage is denoted by V_t. V_t can be calculated as in Equation 2.3.

- In physics, the value of the Boltzmann constant is 1.3806503 x 10^{-23} Joule/Kelvin. It is expressed with the letter k in the equation.
- The value of the charge of an electron in electricity is 1.60217646 × 10^{-19} Coulomb.
- In the model, the letter q represents the electron charge. Temperature in Kelvin is symbolized by the letter T in the model (Xiong et al., 2021).

The shunt resistance current can be shown mathematically as in Equation 2.4. (Xiong et al., 2021).

The output current can be converted to Equation 2.5. by using the above equations (Xiong et al., 2021).

2.2.5. Characteristics of Photovoltaic Cells

Photovoltaic array, boost converter, inverter, power control circuit are structures that are connected to each other in solar photovoltaic systems, respectively. Under Standard Test Conditions (STC), solar photovoltaic panels operate at normal operating voltage (Adak et al., 2019). External factors such as temperature, shading and radiation are factors that change the amount of energy produced in solar photovoltaic systems. Situations such as shadows falling on the panels particularly reduce production. Since they are interconnected, the reduction of production in the entire array occurs as a result of these shadings (Alqaisi and Mahmoud, 2019). As a result, the power value of the entire system is significantly affected (Adak et al., 2019). Two different systems can be described as non-homogeneous systems and homogeneous systems. In homogeneous systems, air temperature values and solar radiation values are equal for all photovoltaic cells. This is not the case in non-homogeneous systems. In homogeneous systems, a single Maximum Power Point (MPP) is observed in the power-voltage graph. More than one MPP is seen in non-homogeneous systems. These points can be called local maximum power points. One of them is a correct point and this is called global maximum power point. The occurrence of hot spot phenomenon in photovoltaic systems is due to the photovoltaic cells receiving different radiation like these situations. Malfunctions usually occur as a result of this event (Alqaisi and Mahmoud, 2019). As the cells heat up, the output current reaches high levels and the output potential comes to low levels. A low level of power is achieved as a result of these situations (Adak et al., 2019). In shading cases, if we consider the partial shading case, as the name suggests, only part of the photovoltaic cells is shaded. These situations occur as a result of shadow elements such as objects that can cast shadows, partial dust, tree branches, clouds, covering materials on the panel. These situations are the main problems that reduce productivity (Alqaisi and Mahmoud, 2019). In current technologies, panel power efficiencies have begun to exceed 20%. Panel powers are determined by experiments conducted at twenty-five degrees, one point five atmospheric pressure and thousand Watt/square meter radiation conditions in STC and information labels are prepared (Adak et al., 2019).

2.2.6. Classification of Photovoltaic Systems Based on Their Applications

Solar PV cells provide electricity generation from the sun. The electricity obtained from solar panels is direct current (DC) (Kılıç and Kekezoğlu, 2021). Figure 2.21. (Kılıç and Kekezoğlu, 2021) shows a representative form of a solar energy system with battery.

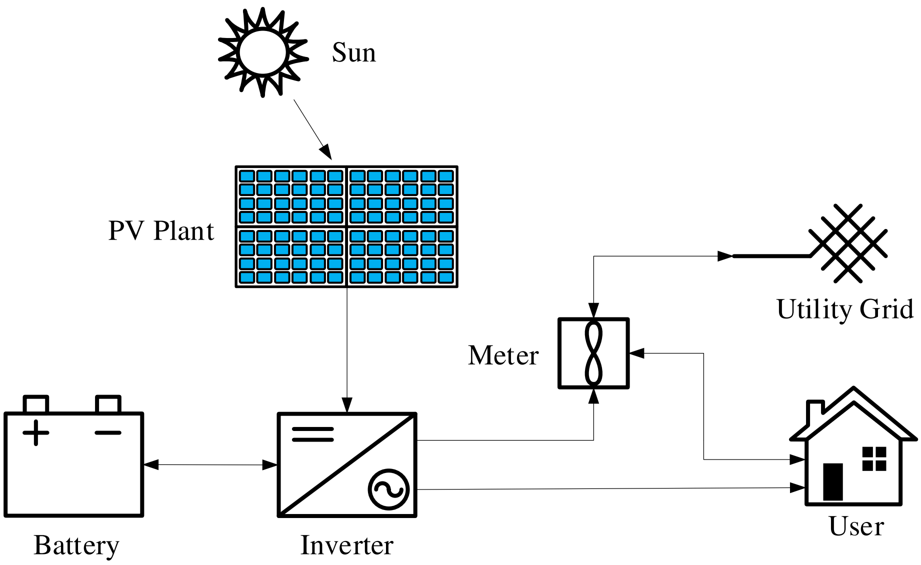

Figure 2.21. Representative image of the solar energy system with battery

Inverters are devices that convert direct current electricity produced by PV panels into alternating current. During the installation phase of solar energy systems, a selection and calculation process is first carried out. A number of issues such as the location of installation, distance to the grid, desired power, and compatibility with the grid are examined. The equipment is selected by taking into account the specified issues. There are two types of grid connection in solar energy systems. The first system is called grid-integrated system and is also called on-grid PV system. The other system is a system that is not connected to the grid and is called off-grid PV system. The features of delivering the produced energy to the grid and at the same time being able to use electricity from the grid are seen in systems that are connected to the grid. In on-grid PV systems, electricity can be sold to the grid. Off-grid PV systems used in places where electricity is not accessible are lifesavers. In this system, electricity cannot be sold to the grid (Kılıç and Kekezoğlu, 2021).

There are two types of solar power plant installations: solar power plants installed on land and solar power plants installed on roofs. In solar power plants installed on land, money is earned from electricity production. Rooftop production, which can be seen on the roofs of industrial facilities and workplaces, is widely used. When electricity production is not sufficient, electricity is taken from the grid. When it is excessive, electricity can be sold to the grid. However, meeting the electricity consumption of industrial facilities and workplaces is generally the main purpose of use. (Kılıç and Kekezoğlu, 2021).

2.3. Maximum Power Point Tracking (MPPT)

2.3.1. Definition of Maximum Power Tracking

There are numerous Maximum Power Point Tracking (MPPT) methods used to ensure that the PV system can operate in unfavourable conditions and reach the maximum power point (Dube et al., 2016). With MPPT methods, an optimum level of power is provided even in adverse conditions (Arhan and Bilgin, 2022). Due to the effects, current, voltage and voltage values become volatile (Aygül et al., 2019). The two most critical of these factors are the temperature value and the values of sunlight. Since these two factors are environmental factors and are constantly affected by environmental events, electricity generation is not stable. These factors change the production amount even with small fluctuations. Shading conditions and cloudiness affect these two factors (Aygül et al., 2019). Due to the rotation of the earth, solar radiation does not reach the photovoltaic cells at constant values (Hao et al., 2022). When there is constant solar irradiance, a single maximum power point is observed in the power-voltage graph. In case of volatile solar radiation, this number of points will increase (Dube et al., 2016). Especially when equal solar radiation does not fall on the photovoltaic cells due to atmospheric and environmental factors, the phenomenon of multiple power points is observed. Partial shading is the name given to situations where shadows form on some of the photovoltaic cells (Aygül et al., 2019). Partial shading is the main cause of these situations. The local power point and global power point are as in Figure 2.22. (Boonmee and Kumsuwan, 2013; Aygül et al., 2019).

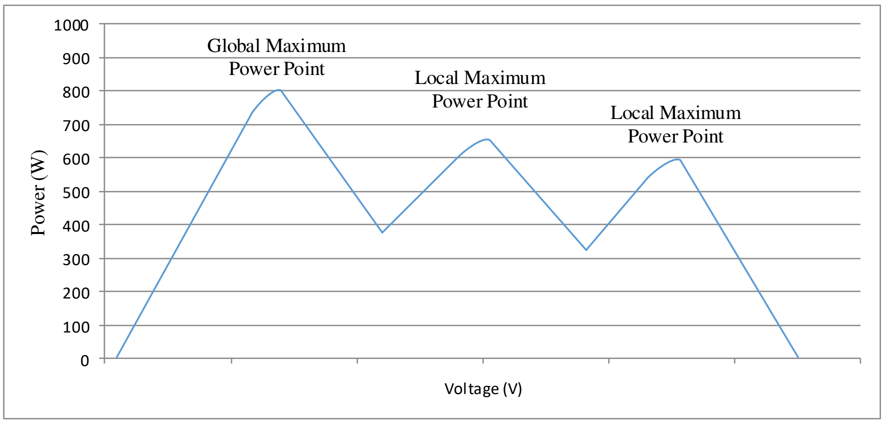

Figure 2.22. Local maximum power points (LMPP) and global power points (GMPP) appear on the power-voltage graph

The purpose of using MPPT here is to ensure that we reach a single correct power point (Dube et al., 2016). Power-voltage and current-voltage graphs from a sample photovoltaic cell output at a specific solar irradiation level and a specific temperature will look like Figure 2.23. (Omar et al., 2023). When the graph is examined, the features of photovoltaic cells are not linear (Omar et al., 2023).

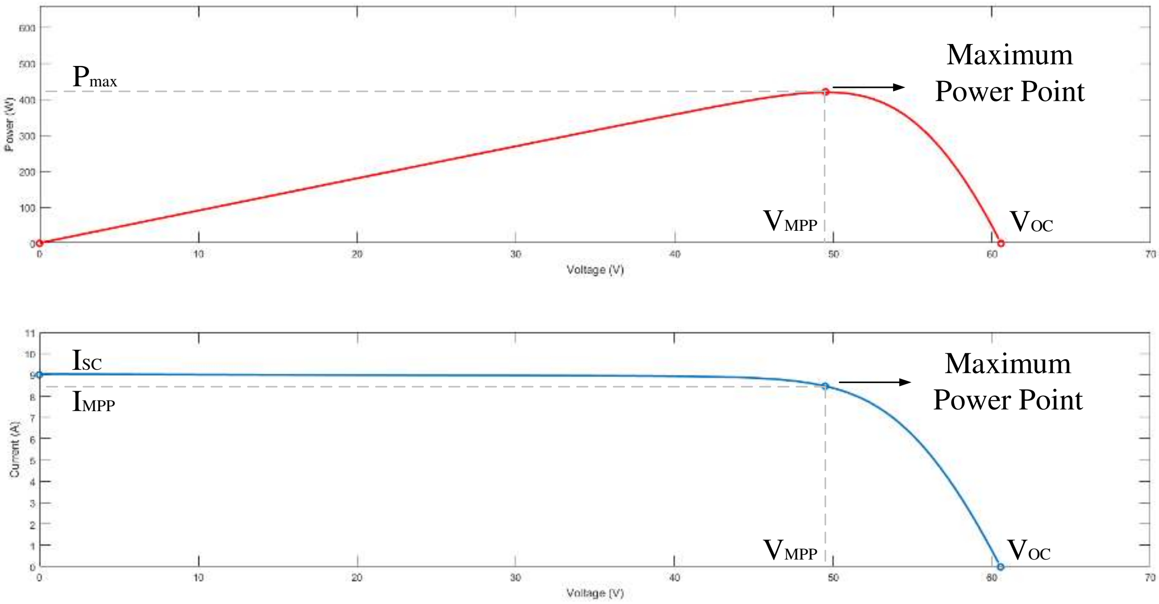

Figure 2.23. Power-voltage and current-voltage graphs from a sample photovoltaic cell output at a specific solar irradiation

When the figure is examined, V_{OC} shows the open circuit voltage of the photovoltaic panel. I_{SC} indicates the short circuit current of the photovoltaic panel. The current at the maximum power point is symbolized by I_{MPP}. The voltage at the maximum power point is shown by V_{MPP}. P_{max} represents the maximum power.

Power-voltage and current-voltage graphs taken from an example photovoltaic cell output obtained with different solar radiations can be seen in Figure 2.24. (Bi et al., 2020).

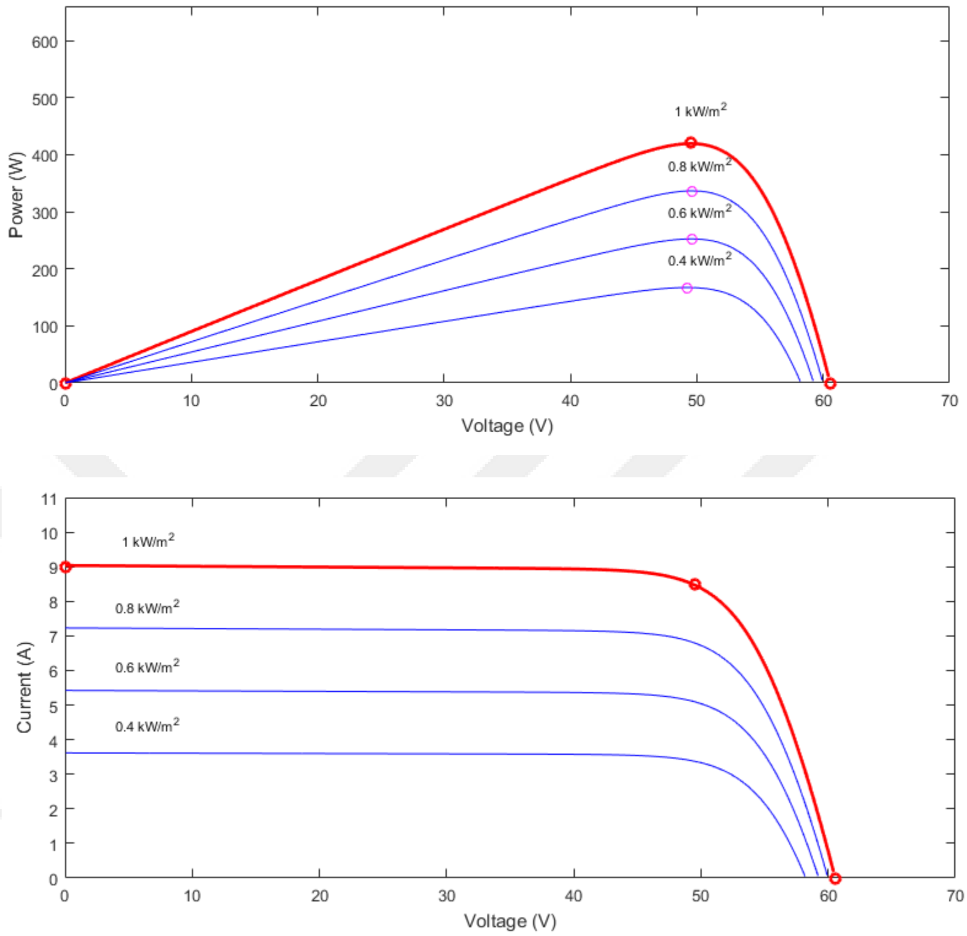

Figure 2.24. Power-voltage and current-voltage graphs from a sample photovoltaic cell output at different solar irradiation

In the graph in Figure 2.24. (Bi et al., 2020), the MPP sections are the sections where the fractures start and the slope is zero. They are shown in red in the graph (Bi et al., 2020).

In PV panels, the absence of short circuit current, hot spot phenomenon and power losses are the result of partial shading. Diodes are added in parallel to the PV cells for these situations. The current flowing through the diodes protects the PV panels. The occurrence of more than one MPP is also related to the use of these elements. The partial shading situation is represented in Figure 2.25. (Karanfil, 2021) below.

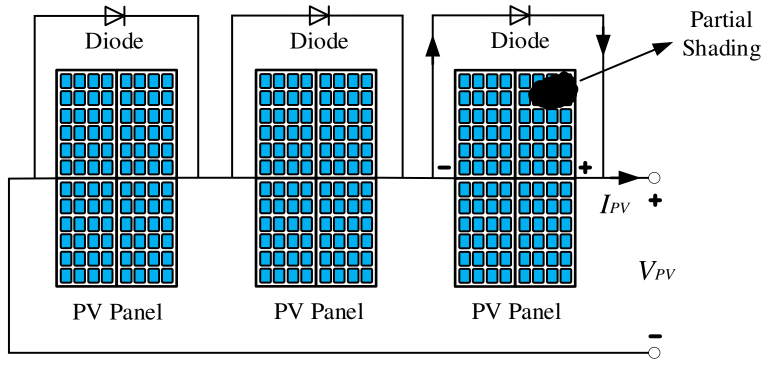

Figure 2.25. Partial shading phenomenon in photovoltaic systems

There are many structures in photovoltaic systems. Figure 2.26. (Bingöl and Özkaya, 2019) is a simple example of this that includes MPPT (Bingöl and Özkaya, 2019).

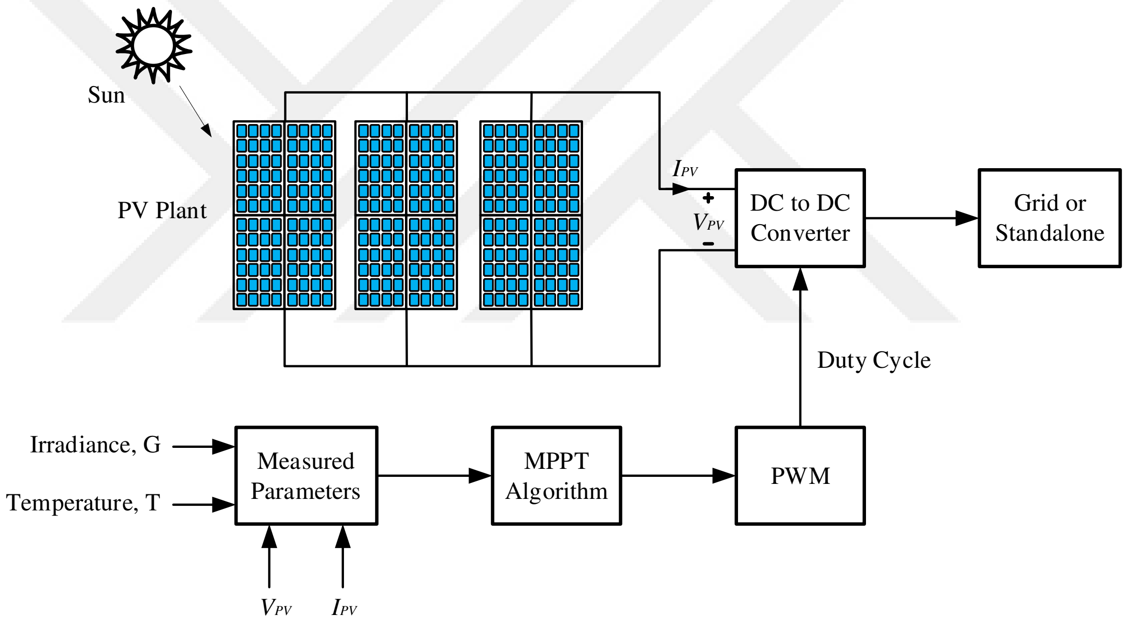

Figure 2.26. Illustration of a photovoltaic system containing a simple MPPT structure

In the structure shown, the MPPT's function is to provide the necessary information for the DC-to-DC converter's switching signal. The MPPT algorithm processes the information from measurements such as radiation, voltage, current, power, temperature and sets the duty cycle required for the switching signal (Bingöl and Özkaya, 2019). If the duty cycle can be adjusted well, successful power tracking can be achieved.

2.3.2. Impact of MPPT Technology on Efficiency

Efficiency in photovoltaic systems is provided by MPPT methods (Arhan and Bilgin, 2022). Since MPPT methods increase efficiency in solar power plant installations, fewer panels are required

(Badak and Yıldız, 2020). When MPPT methods are used in photovoltaic systems, a power increase of around forty-five percent can be achieved. The effect of MPPT methods on power is seen in Figure 2.27. (Arhan and Bilgin, 2022).

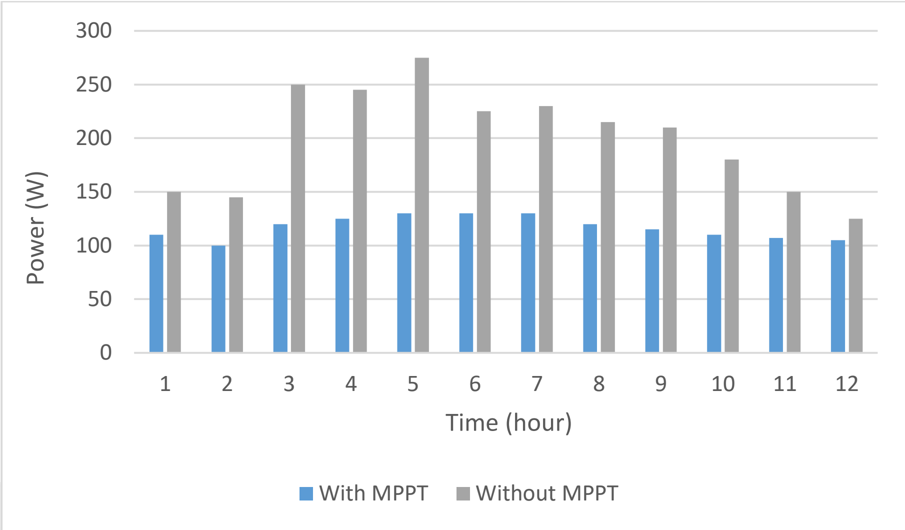

Figure 2.27. Power/time graph showing the effect of MPPT methods on efficiency

An example study (Badak and Yıldız, 2020) was conducted to examine the cases where the MPPT method was used and not used in a photovoltaic system. According to the research results, the current and voltage values at the output of the photovoltaic system are higher in the system using MPPT. Additionally, the power value was higher in the system using MPPT. In addition, the efficiency values of photovoltaic systems were examined by looking at whether the MPPT system was used or not. As a result of the study, it was observed that efficiency increased with MPPT. Using MPPT, the efficiency value of 72.6 percent was determined to be 92.95 percent. Thus, it was concluded that the efficiency value and power value were higher in the results using the MPPT method. In this method, where the power value and efficiency value are higher, maximum profits can be achieved with the minimum number of panels (Badak and Yıldız, 2020).

2.4. Maximum Power Tracking Algorithms in the Literature

2.4.1. MPPT Algorithms under Uniform Radiation

In cases where there is uniform solar radiation, some MPPT methods can work more stably and better. In this section, MPPT methods that can be used for cases where photovoltaic panels receive constant solar radiation are explained. Figure 2.28. (Ali et al., 2020) shows the MPPT methods that can be used under uniform solar radiation.

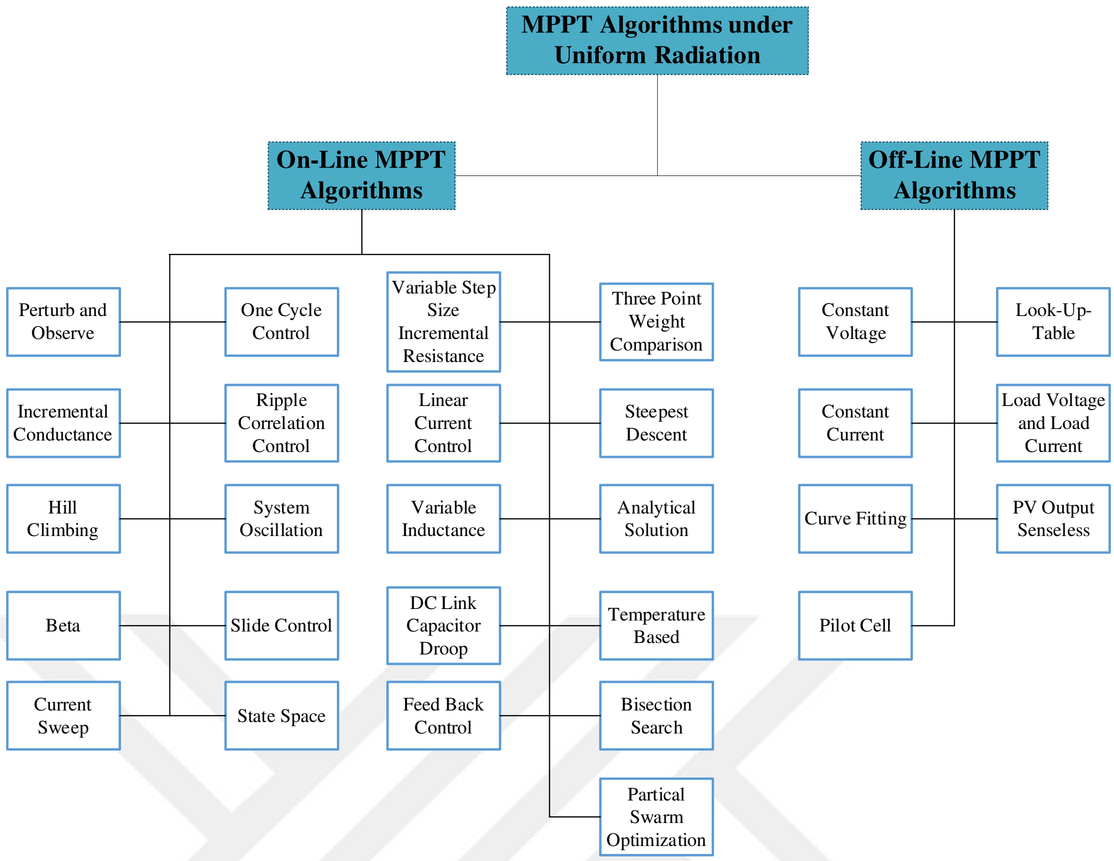

Figure 2.28. MPPT methods that can be used in conditions of uniform radiation

As can be seen from the figure, MPPT methods that can be used in uniform radiation conditions can be examined under two subheadings as online algorithms and offline algorithms, depending on the operating logic of the power tracking system.

Online MPPT Algorithms

In these control algorithms, the current and voltage values received from the photovoltaic panels are continuously measured. The MPPT algorithm processes the instant data obtained. In order to ensure that the switching signal of the DC-to-DC converter is generated the MPPT method helps to determine the value of the duty cycle. It calculates the most suitable value by looking at the rate of change in power, current and voltage. The duty cycle has its exact value with PI and PID controllers. Duty cycle is found to its exact value using PID or PI control (Ali et al., 2020).

Below, online methods of MPPT algorithms that can be used under uniform radiation conditions are explained.

Perturb & Observe (P&O) Algorithm

The Perturb and Observe (P&O) algorithm contains only a few parameters and has a simple feedback structure. It has low cost, ease of application and good performance. It is therefore a widely used MPPT method to track the maximum power point (Bidram et al., 2012; Horoufiany and

Ghandehari, 2017; Dhivya and Kumar, 2017). The P&O algorithm generates an output value based on the measured system parameters (Güler and Biricik, 2021). In the P&O algorithm, the operating voltage of the solar panel is increased or decreased, and then the amount of change in output power is measured. In this algorithm, during a cycle, the power value received in the previous cycle is compared with the power value received in the next cycle. If the power value received in the previous cycle is greater than the new power value, the direction of voltage rise or fall is changed. After this change, the cycle is completed by returning to the beginning (Badak and Yıldız, 2020). The flow chart of this algorithm is given in Figure 2.29. (Irmak and Güler, 2020).

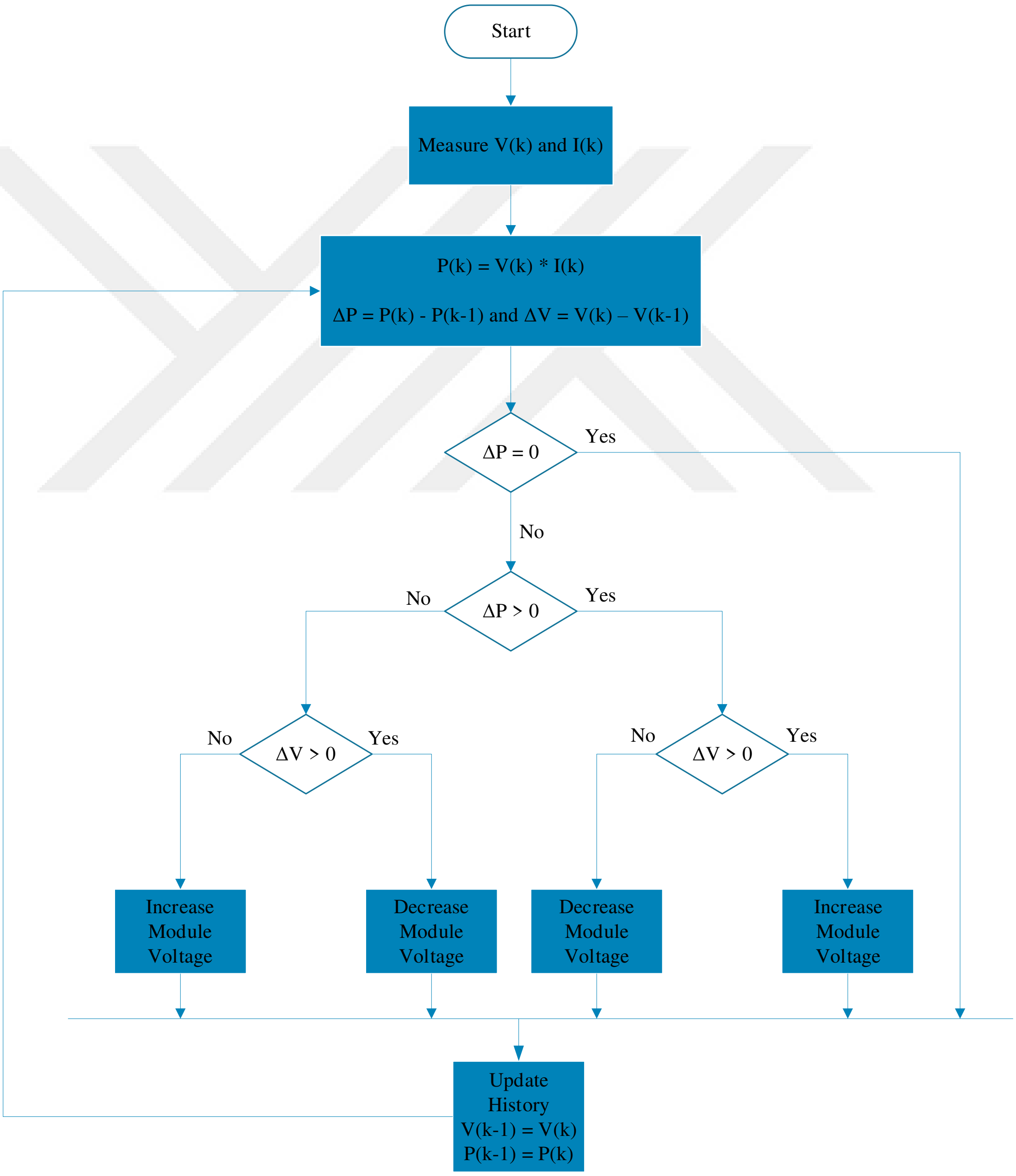

Figure 2.29. Flowchart of P&O algorithm

The algorithm starts with the measurement of the instantaneous parameters at the output of the solar panel group and calculates the power value. At the same time, it determines the direction of change by comparing the previous power value *P*(*k*-1) and voltage value *V*(*k*-1) with the current values. If the previous power value and the calculated power value are the same, then the reference current value is equalized to the old value since MPP has been detected. If there is a power change, it is decided whether to increase or decrease the reference current value in line with the explanations given above. As a result of this algorithm, the generated reference current value $I_{(REFPV)}$ is used in the MPC algorithm to provide maximum power control (Irmak and Güler, 2020). The behaviour of this widely used algorithm is given in the PV power-voltage graph in Figure 2.30. (Güler, 2021).

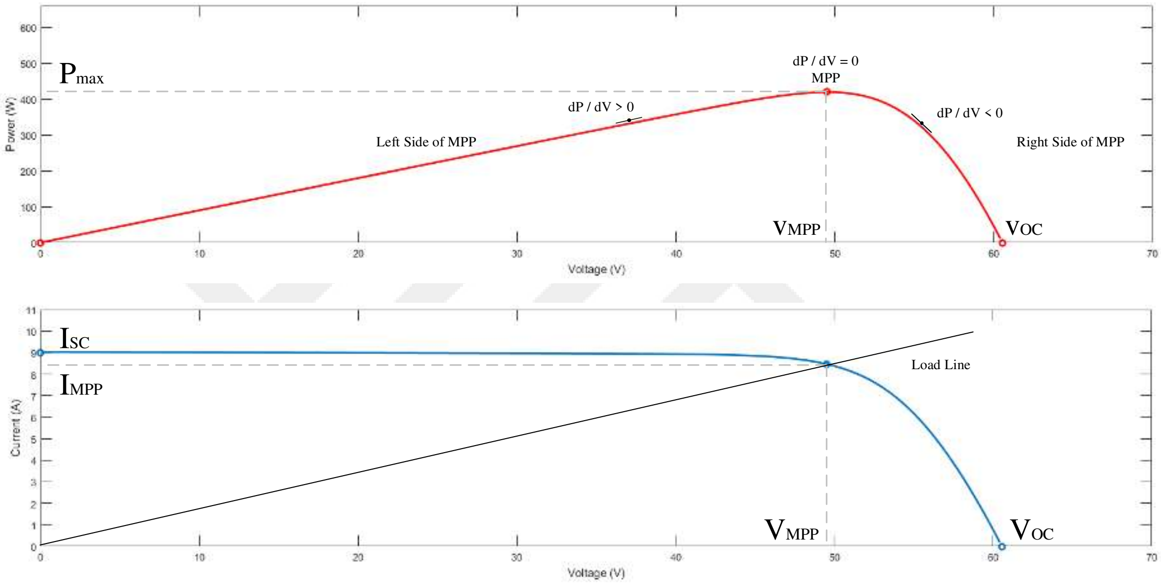

Figure 2.30. Maximum power curve

According to the representation in the graphs, the status of the Maximum power point (MPP) is as follows.

$$\frac{\Delta P}{\Delta V} < 0 \qquad P < MPP \tag{2.6.}$$

$$\frac{\Delta P}{\Delta V} = 0 \qquad P = MPP \tag{2.7.}$$

$$\frac{\Delta P}{\Delta V} > 0 \qquad P > MPP \tag{2.8.}$$

Incremental Conductance Algorithm

Using the PV array's incremental and instantaneous conductance as a basis, the incremental conductance (IC) method is a common tracking technique (Rajesh and Mabel, 2015). This approach is thought to be inexpensive and simple to use for (MPPT) (Jasim and Shepetov, 2017). Although it uses a different check for perturbation, it uses the same fundamental concept as the P&O approach (Awan, 2022). The fluctuation around MPP and the poor rate of adaptation to rapidly varying air conditions are the two key drawbacks of the P&O approach. In order to prevent these drawbacks, this approach has been devised (Wasynczuk, 1983).

The power and conductivity of solar panels are calculated by measuring their output voltage and current. The duty cycle needed to run the system at MPP is then calculated (Tey and Mekhilef, 2014). The incremental conductance (IC) approach is based on the assumption that the slope of the *P-V* curve is equal to zero, taking into account the convex feature of the *P-V* characteristic. ($\Delta P/\Delta V = 0$) (Bhatnagar and Nema, 2013). The following equations show the working system of this method (Arhan and Bilgin, 2022).

Slope	*Operating Voltage of System*	
$\frac{\Delta I}{\Delta V} = \frac{-I}{V}$	(At Maximum Power Point)	(2.9.)
$\frac{\Delta I}{\Delta V} > \frac{-I}{V}$	(To the Left of Maximum Power Point)	(2.10.)
$\frac{\Delta I}{\Delta V} < \frac{-I}{V}$	(To the Right of Maximum Power Point)	(2.11.)

Figure 2.31. (Jasim and Shepetov, 2017) shows the flow diagram of the Incremental Conductance Method.

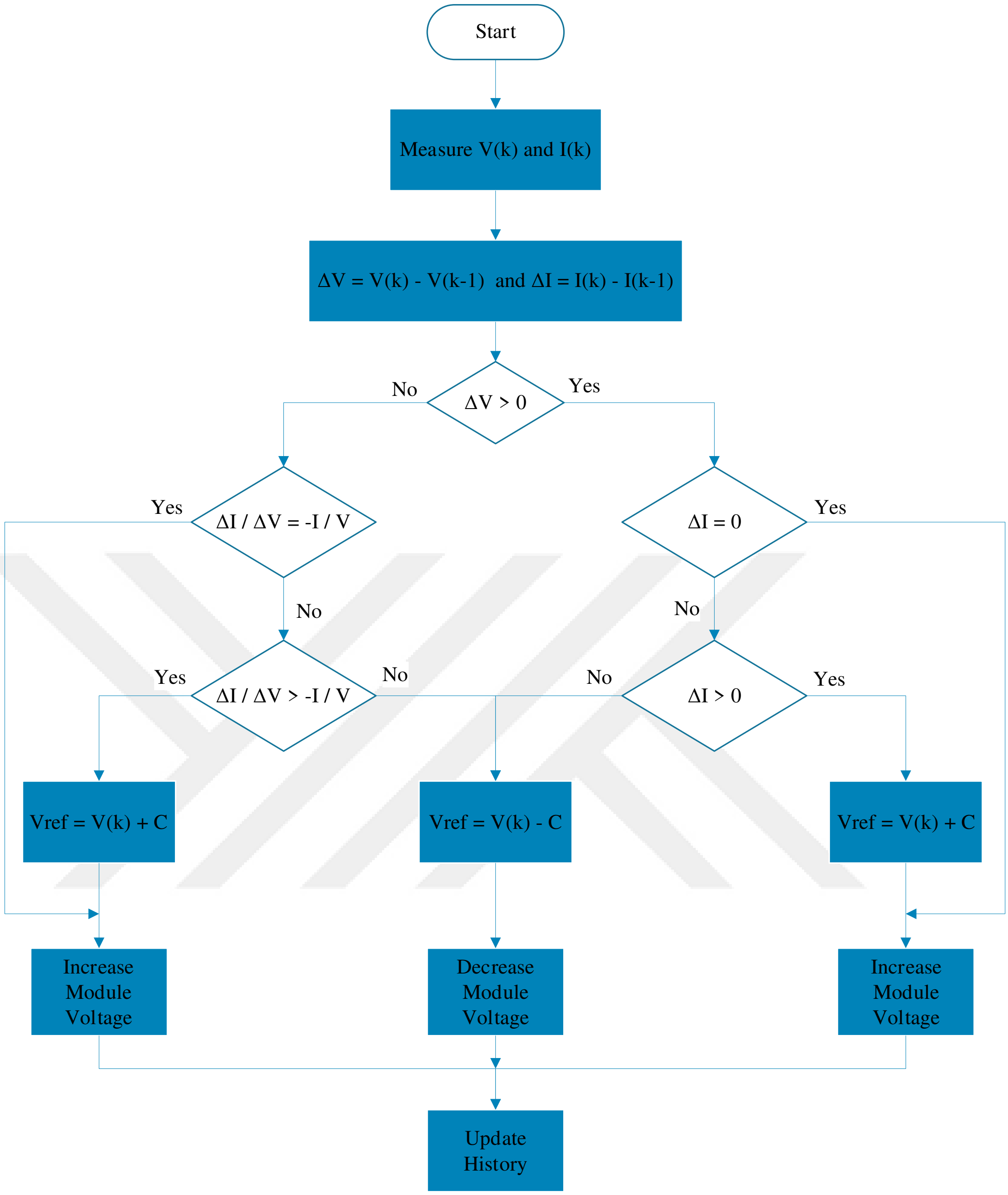

Figure 2.31. Schematic for the incremental conductance approach

Hill Climbing (HC) Algorithm

The Hill Climbing (HC) method is identical to the Perturb & Observe (P&O) method in terms of operating principle, but the difference is the parameter of the perturbation (Tuelings et al., 1993). The P and O sense and perturb the voltage or current for MPP tracking, whereas the HC perturbs the duty cycle (Xiao and Dunford, 2004). One common problem in both methods is the performance trade-off between steady-state and dynamic response error. For the Hill Climbing (HC) method, this problem is of a more significant worry because it controls Duty (δ) instead of voltage, as depicted in Figure 2.32. (Tan et al., 2015; Ons et al., 2015) while in the Perturb & Observe (P&O), voltage is controlled directly (Tan et al., 2015; Ons et al., 2015).

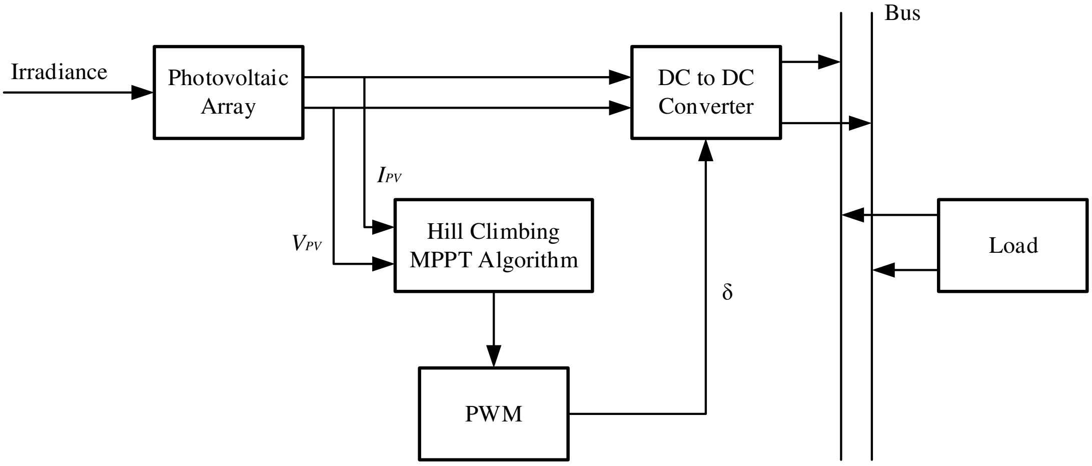

Figure 2.32. Hill climbing MPPT diagram

The Hill Climbing (HC) operational methodology is outlined in Table 2.1. (Tan et al., 2015; Ons et al., 2015), where the fixed Duty (δ) step size may be used, but this does not guarantee a fixed voltage change (Tan et al., 2015; Ons et al., 2015).

Table 2.1. Hill climbing method operation methodology

Present Perturbation	Change in Power	Next Perturbation Direction
Positive	Positive	Positive (Duty ratio increase)
Negative	Positive	Negative (Duty ratio decrease)
Positive	Negative	Negative (Duty ratio decrease)
Negative	Negative	Positive (Duty ratio increase)

Furthermore, the conventional Hill Climbing (HC) method fails to track the MPP effectively under intermittent weather conditions because of a steady duty cycle (Dash et al., 2015). Flow chart of the Hill Climbing algorithm is shown in Figure 2.33. (Dash et al., 2015).

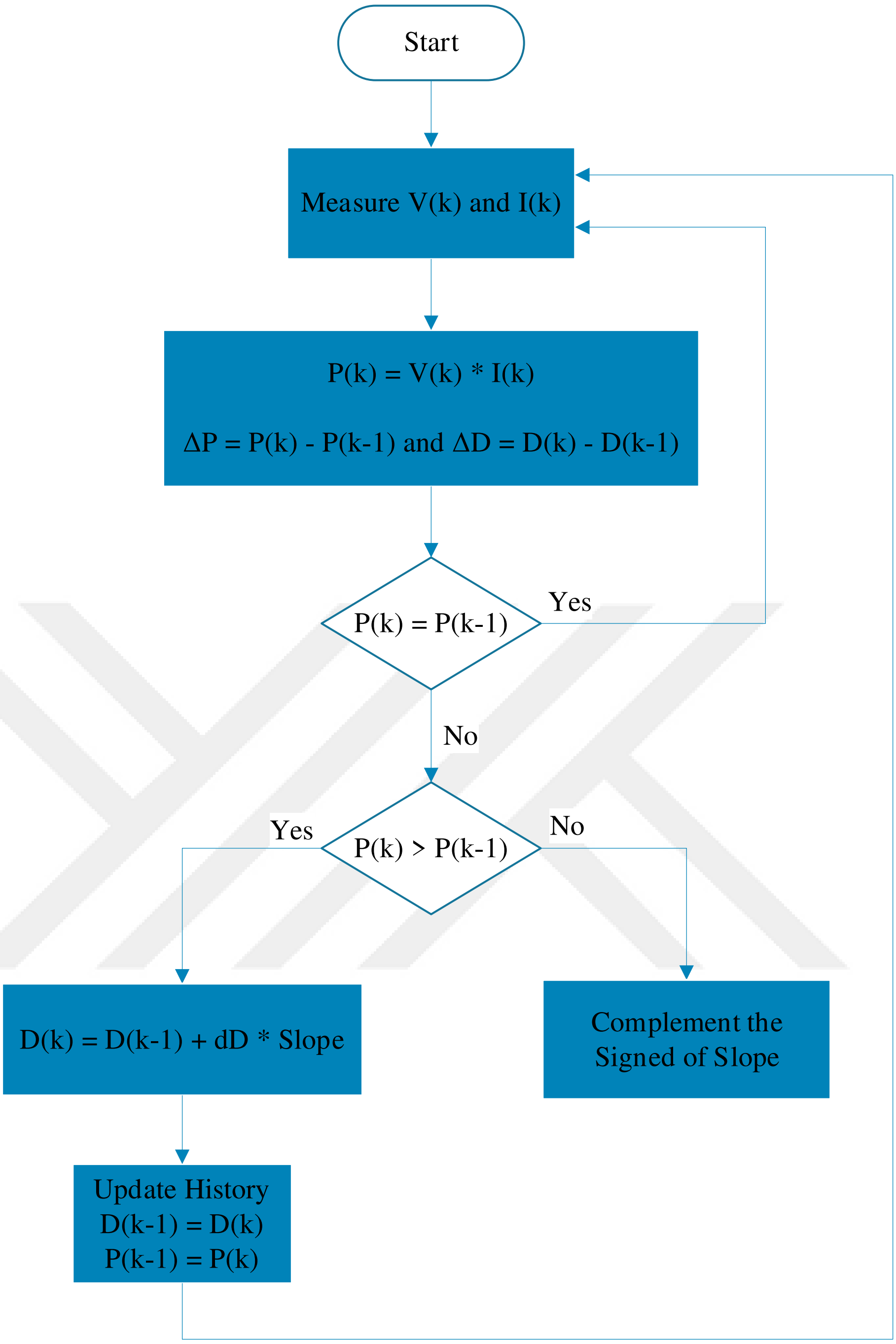

Figure 2.33. MPPT control algorithm based on Hill Climbing

Beta (β) Algorithm

One of the quickest tracking algorithms, this method quickly does an initial MPP computation using a variable coefficient (Jain and Agarwal, 2004; Jain and Agarwal, 2007). Jain and Agarwal provide a description of the beta technique (Ali et al., 2020). The panel's voltage and current values are utilized to calculate the value of β. This value is then included in a standard closed loop with a fixed reference (Podder et al., 2019).

In this method, Beta value is calculated with the following equation:

$$\beta = ln\frac{I_{PV}}{V_{PV}} - \left(\frac{q}{k \times T \times \eta}\right) \times V_{PV} \qquad (2.12.)$$

In this formula;

q: Electric Charge,

k: Boltzmann's Constant

T: Ambient Temperature (Kelvin)

η: Diode Quality Factor (Jain and Agarwal, 2004)

The approach is used with any standard MPPT method, such as Hill Climbing, Perturb & Observe, Incremental Conductance, etc., for increased efficiency and quicker MPP tracking. Once the Beta value has been determined, its stability is examined. A classic MPPT approach is used if the Beta value is in the stable region. If the Beta value is unstable, the duty cycle is controlled using the error indicated in below equation:

$$Error = \beta_{min} - \beta_{max} \qquad (2.13.)$$

The assessment process is then repeated in order to calculate the beta value (Pradeep et al., 2015; Li et al., 2015). Flow chart of the Beta Algorithm is shown in Figure 2.34. (Verma et al., 2016).

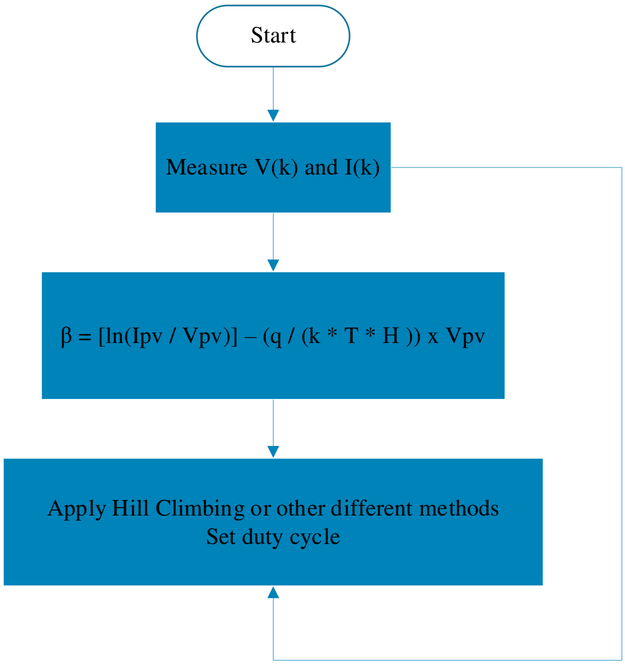

Figure 2.34. Flowchart of Beta Algorithm

Current Sweep Algorithm

In this procedure, the requisite *I-V* curve is found by using the Photovoltaic array's current sweep waveform (Bhatnagar and Nema, 2013). Using the module's current operating circumstances, the current sweep approach draws the characteristic curve *I-V* of the array or module. With the help of the following equation, this technique takes the voltage and current and changes them as a predefined function of time (Ali et al., 2020).

$$i(t) = f(t) \tag{2.14.}$$

The sweep is constantly performed until it achieves the necessary Maximum Power Point in order to obtain the voltage at MPP (Bhatnagar and Nema, 2013). Since the current is more sensitive to variations in solar irradiation, it is swept instead of changing the voltage (Ali et al., 2020). Since the Current Sweep MPP tracking manages the array current, it cannot be done continually. The MPP is calculated using this tracking's interpretation of the PV system's *I-V* characteristic (Moring and Pols, 2012; Tsang and Chan, 2015). This approach has a slower pace, is more difficult to execute, and suffers power losses during sweeping. Nevertheless, it works well for tracking the actual Maximum Power Point (Bhatnagar and Nema, 2013).

One Cycle Control Algorithm

Nonlinear control techniques include One Cycle Control (OCC). It works by integrating a variable's value (current or voltage) to get the variable's value to match a reference value (Verma et al., 2016). Typically utilized in single-stage grid-connected PV systems, the OCC approach is a non-linear MPPT technique (Sreeraj et al., 2013). As seen in Fig. 2.35. (Yang and Smedley, 2004; Sreeraj et al., 2013), a One Cycle Control-based technique is used to apply to a grid-connected solar PV system (Yang and Smedley, 2004; Sreeraj et al., 2013).

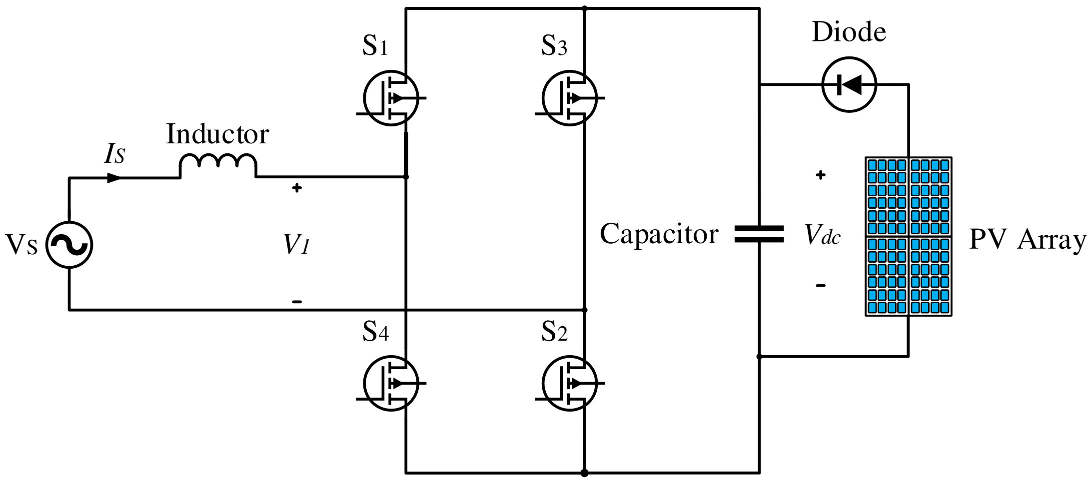

Figure 2.35. An inverter linked to the single phase grid is shown using a solar power system

The functioning of MPPT is carried out using a single stage inverter (Yang and Smedley, 2004; Sreeraj et al., 2013). According to the One Cycle Control approach, the single-stage inverter's output current is said to be regulated by the of reference current and reference voltage. As shown in Figure 2.36. (Ribeiro et al., 2009), it is employed to obtain the Maximum Power Point (Esram and Chapman, 2007; Ribeiro et al., 2009).

To get the most output power possible from the PV system, the single stage inverter's output current can be adjusted in accordance with the voltage of the PV array (V_{PV}) (Fortunato et al., 2008; Chatterjee and Mohanty, 2018). High dependability, robustness, and cost-effectiveness are all benefits of the one cycle control approach (Basha and Rani, 2020). Applying a one cycle control MPPT approach can increase the speed of Maximum Power Point Tracking (Carvalho et al., 2016). Additionally, no Phase-Locked Loop (PLL) controller is needed with this technique to connect the grid and inverter. One Cycle Control (OCC) Maximum Power Point Tracker (MPPT) technique's main flaw is its moderately inefficient power point tracking (Basha and Rani, 2020).

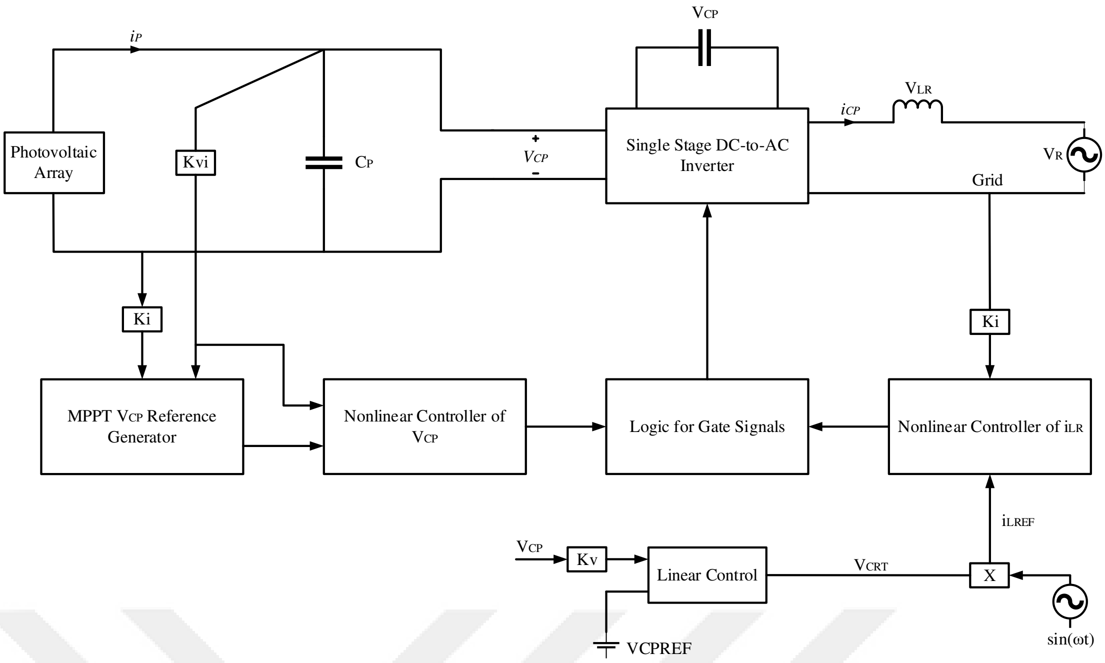

Figure 2.36. Single-stage inverter design for One Cycle Control

Ripple Correlation Control Algorithm

This technique makes use of the signal ripple that power converters naturally produce (Bhatnagar and Nema, 2013). A development in this area is the use of ripple content, which was created in the PV system for the MPP approach (Bollipo et al., 2021). Typically, Equation 2.15. of the Maximum Power Point corresponds to the Ripple Correlation Control (Ali et al., 2020).

$$\frac{\Delta P}{\Delta t} \times \frac{\Delta V}{\Delta t} \quad \text{or} \quad \frac{\Delta P}{\Delta t} \times \frac{\Delta I}{\Delta t} = 0 \qquad (2.15.)$$

An optimization may be realized from the ripple, which is seen as a disturbance. Power oscillation delivered by an all-pass filter that performs MPPT using ripples: The MPP Equation 2.15. is used in the method (Bhatnagar and Nema, 2013). Ripple Correlation Control technique connects to the PV system using, voltage, high-frequency ripple current or power of power electronic devices. With this control mechanism and a simple analogue controller, the Maximum Power Point may be tracked quickly and accurately (Bollipo et al., 2021). Controlling the ripple correlation involves using the high pass filter's first order function. From the recorded PV power and PV voltage, it produces the ripple in both power and voltage (Boonmee and Kumsuwan, 2013).

As shown in Figure 2.37. (Boonmee and Kumsuwan, 2013), a first order low pass filter function then reduces the ripple caused by PV power ripple and PV voltage ripple (Boonmee and Kumsuwan, 2013).

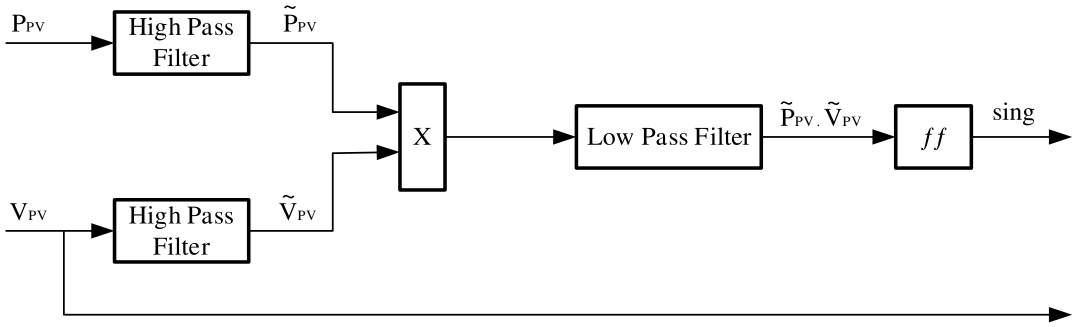

Figure 2.37. Flowchart for the ripple correlation approach

The fundamental approach is to determine the voltage derivative of power d*P* / d*V*, which serves as the primary determinant of the Maximum Power Point. Current controller and voltage controller are components of the power converter. It is equipped with the capacity to sense inverter voltages and provide a reference signal. This method makes use of two sensors to measure the PV current and voltage data. This technique uses a P-Q controller to effectively manage the grid current (Bollipo et al., 2021).

System Oscillation Algorithm

By using a system oscillation approach, solar PV efficiency may be increased (Lasheen et al., 2017). The MPP is not explicitly perturbed by a source of perturbation while using the system oscillation approach. Rather, the MPP module is functional through the utilization of an oscillation in the perturbation (Ali et al., 2020). The maximization of power transmission is the foundation of this technique (Verma et al., 2016).

With this MPPT method, the PV system as a whole will become self-oscillating (Labidi et al., 2019). The duty ratio fluctuates while using this strategy. The oscillation of the parts of an alternating current is compared to this fluctuating duty ratio (Ali et al., 2020). The median converter input voltage is computed in this manner in order to get the duty ratio (Ho et al., 2004; Obaid et al., 2017). The duty ratio in the power transformation step is calculated by comparing the ac part with the median input voltage level (Ho et al., 2004). A fixed ratio between the mean voltage and amplitude of oscillation exists at Maximum Power Point (Labidi et al., 2019).

Consequently, the power transformation stage switch's duty cycle is completely controlled at a predetermined frequency with a tiny amplitude fluctuation (Abdel-Rahim and Haoyu, 2020). The block diagram for the System Oscillation technique, in which a PI controller serves as the error amplifier, is shown in Figure 2.38. (Ali et al., 2020).

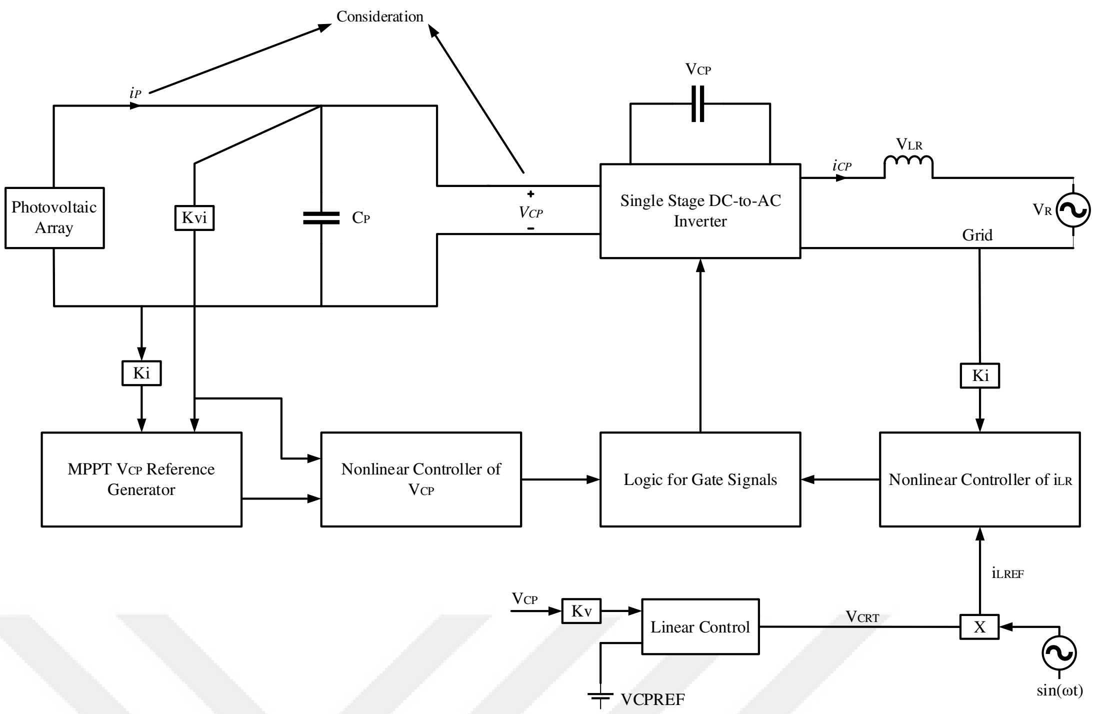

Figure 2.38. Diagrammatic representation of the oscillation technique system

Its purpose is to measure oscillations in the system. By using a fourth-order band-pass filter to eliminate the switching frequency parts, the alternating current (AC) part is produced at the high pass filter output (Yılmaz et al, 2018). Additionally, the peaks of the AC component are eliminated using a peak detector. By means of pulse width modulation, the duty cycle is ascertained by the Error Amplifier’s output (Ali et al., 2020). This method mostly relies on comparing the mean PV output voltage and the ac part (Labidi et al., 2019). This technique simply requires a voltage sensor, and it is simple to put into practice (Verma et al., 2016). Its tracking of the Maximum Power Point without the need for system estimates is its main benefit. Reduced design costs are one of this controller’s benefits. It works better for tracking the Maximum Power Point of solar photovoltaic systems with non-uniform irradiation. The state space-based Maximum Power Point Tracking controller’s drawback is that it is solely dependent on the PV array type chosen (Abdel-Rahim and Haoyu, 2020).

Slide Control Algorithm

The nonlinear system is controlled via the slide control approach. Regarding MPPT, there are two ways in which this control method might be applied. There are two types of modes: approaching and sliding. The power changes zero when it comes to voltage or current at the Maximum Power Point (Miao et al, 2004; Song et al., 2006). The rapid loop provides great real-time reaction while tracking the vicinity of the Maximum Power Point. Simultaneously, the slow loop reduces the steady-state error by using a small increase in step size in the MPPT method. As seen in Figure 2.39. (Vazquez et al., 2015; Levron and Shmilovitz, 2013), the Slide Control Method is set up with two types of control loops: slow and quick (Vazquez et al., 2015).

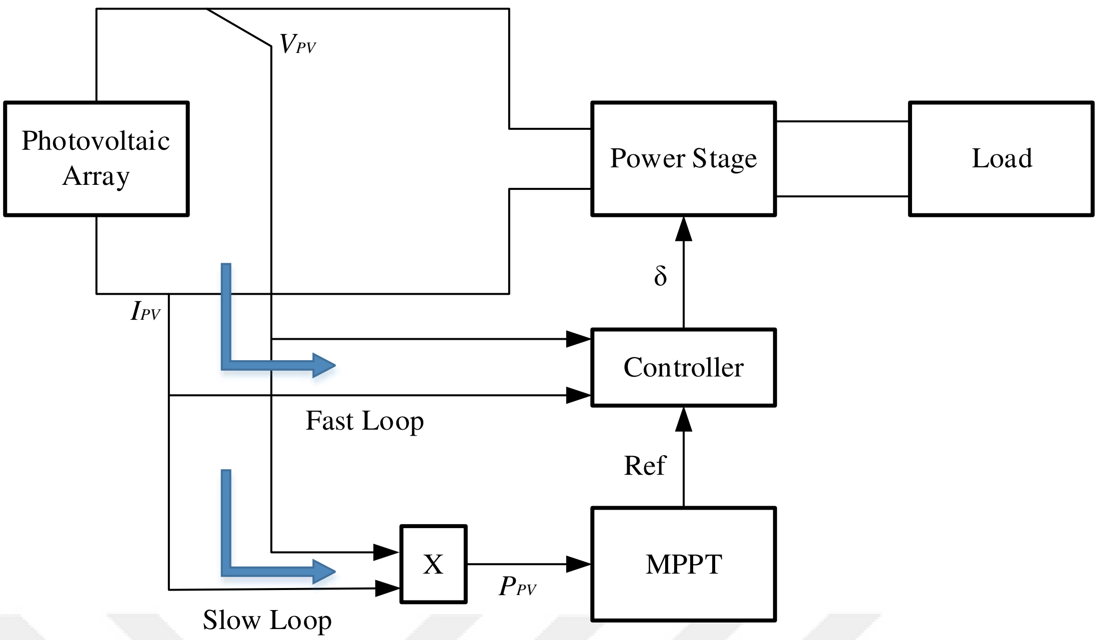

Figure 2.39. Schematic representation of the slide control method system

The switched mode converters may be controlled properly with the slide control approach. In non-linear control systems, this technique is easy to use and demonstrates excellent stability and quick reaction times (Levron and Shmilovitz, 2013).

State Space Algorithm

Linear state equations are used in the design of the Maximum Power Point Tracking controller, which is based on an estimated state space (Labidi et al., 2019). The process is predicated on the photovoltaic system with DC-to-DC converter being mathematically modelled as Equation 2.16. (Verma et al., 2016).

$$\dot{x}(t) = Ax(t) + B(t)u(t) + D\varepsilon(t) \quad (2.16.)$$

By turning the system into a linear model, the approach helps to approximate it. Furthermore, it facilitates the utilization of linear control techniques (Jamil et al., 2013; Hossain et al., 2018). It provides an accurate tiny signal model at comparatively lower frequencies and is used to construct DC-to-DC converters (Ali et al., 2020). Through the employment of a highly effective converter, solar energy is rendered more efficient through this way (Abdel-Rahim and Haoyu, 2020). Situations of imbalance include variations in temperature, load variations, and solar radiation-induced changes in I_{PV} or V_{PV}. These factors make it necessary for MPP to be precisely monitored while maintaining a steady output voltage. These factors make it necessary for MPP to be precisely monitored while maintaining a steady output voltage (Ali et al., 2020). In this technique, a mean value method is used to give the analytic solution of a point which is near to the true Maximum Power Point (Abdel-Rahim and Haoyu, 2020).

This controller has the benefit of being less expensive to develop. It performs better in Maximum Power Point Tracking when solar PV has non-uniform irradiation (Basha and Rani, 2020). This process guarantees system stability. This approach can also be used in environments with rapidly changing conditions (Solodovnik et al., 2004). It also offers great efficiency and less steady-state fluctuations over the Maximum Power Point. However, its Maximum Power Point Tracking performance is just relatively small (Basha and Rani, 2020).

This algorithm's drawback is that it only relies on the kind of PV array used. This method's drawback is that freestanding photovoltaic systems cannot be utilized with it (Adak et al., 2019).

Variable Step Size Incremental Resistance Algorithm

Solar PV systems wobble about their genuine MPP when functioning. The system temperature rises as a result. Transmission losses also rise in addition. For step size perturbation, the Incremental Resistance approach involves the Perturb & Observe Maximum Power Point Tracking method. The overall architecture became more complex and expensive as a consequence. The paper (Ali et al., 2020) uses a VSS-INR MPPT approach to get around this problem. It is employed to extract the solar photovoltaic systems peak output under various temperature and irradiance circumstances (Basha and Rani, 2020).

The P&O technique is typically used in combination with the variable step size incremental resistance approach. This technique was chosen to solve a significant drawback: the point of operation fluctuation around the Maximum Power Point (MPP) in both stable state and changing state scenarios. Reduced system effectiveness results from part of the obtainable energy being wasted by these operating point fluctuations (Ram et al., 2017). The perturbation level is automatically adjusted using the Incremental Resistance approach based on the degree of variation and the distance from the Maximum Power Point. Equation 2.17., which states that the derivative (∂P / ∂V or ∂P / ∂I) may be utilized to regulate and determine the variable increment value, is one of the features that distinguish the VSSIR (Raedani and Hanif, 201). Using Equation 2.17., the duty cycle is adjusted in this approach (Basha and Rani, 2020).

$$\delta(k) = \delta(k-1) \pm N \times \left(\frac{P(k)-P(k-1)}{V(k)-V(k-1)}\right) \qquad (2.17.)$$

The converter duty cycles at instants k and (k−1) are represented by the terms δ and δ (k−1). Before the next step size is formed in Equation 2.17., the input signal is regulated to a suitable scale using a scaling factor N (Ahmet and Shoyama, 2011). The diagram of this method is shown in Figure 2.40. (Basha and Rani, 2020).

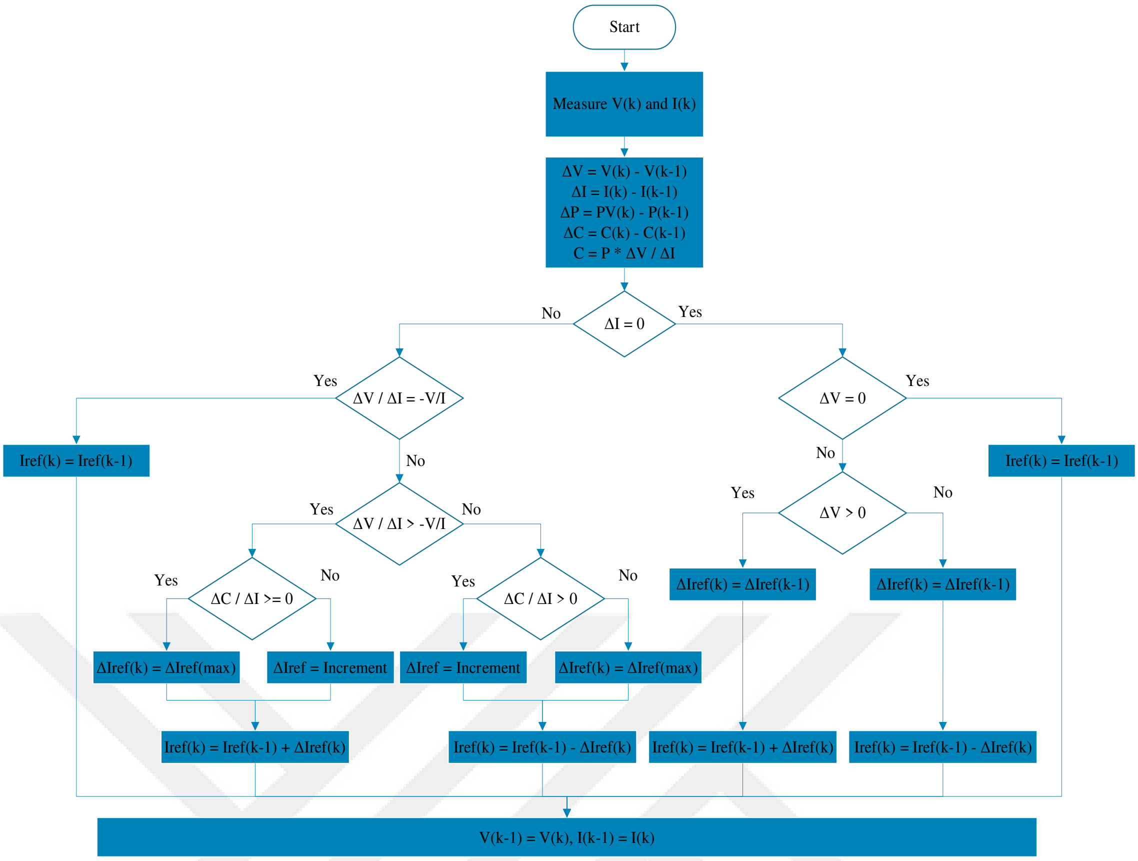

Figure 2.40. Schematic diagram of VSS-INR MPPT controller

The advantages of the VSS-INR MPPT technique over P&O, IC, and HC MPPT techniques are fast tracking speed, automatic perturbation high accuracy in Maximum Power Point Tracking, and less implementation cost. Additionally, for both online and offline usage, the VSS-INR approach is applied (Basha and Rani, 2020).

Linear Current Control Algorithm

Non-linear aspects are present in both the energy conversion mechanism and solar PV power. The *I-V* features, temperature variations, irregular solar irradiance, and time-varying all contribute to its occurrence. Among the issues raised and looked into the most in the planning and development phases of Maximum Power Point Tracking is this nonlinear behaviour (Ali et al., 2020). A simpler linearization procedure is utilized in an LCC method to successfully linearize non-linear situations (Souza et al., 2018). This approach uses mathematical formulas to linearize the power & current variables in order to determine the Maximum Power Point (Pan et al., 1999, Tan et al., 2005). This approach takes use of the typical curve's linear connection between *I* and *V*. (Podder et al., 2019). The intersection of two curves is determined via the linearized approach, also known as the linear current control (Ali et al., 2020). A straight line can be used to depict the maximum output power curve (Pan et al., 1999).

At varying irradiance levels, the *P-I* curve, represented by $f(P, I) = 0$, is the first line. The MPP line intersects and is considered as a linear line at the second curve, the V_{MPP} curve, at $dP / dI = 0$. It can be seen as in Figure 2.41. (Pan et al., 1999).

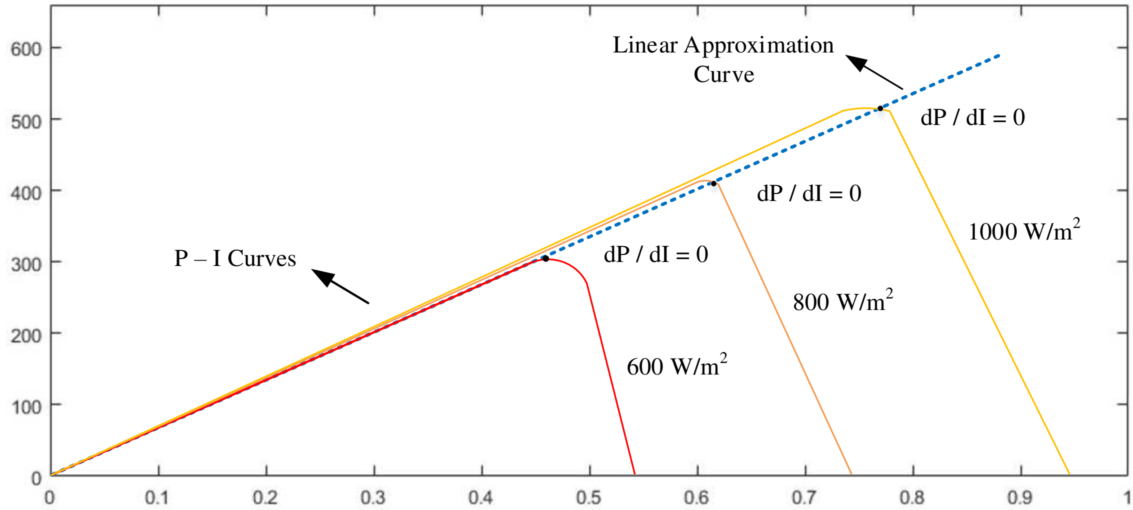

Figure 2.41. Current linearization in a LCC

A basic analog circuit is utilized to determine where the two curves stated above cross (Verma et al., 2016). Discovering a transistor amplifier's operating point for a given load is similar to this process. The position at which the load current-voltage profile and the transistor current-voltage profile contact is the operational point (Pan et al., 1999). Improved insolation conditions are required for this approach to become linear (Podder et al., 2019).

Variable Inductance Algorithm

With this technique, the Maximum Power Point Tracking controller and variable inductor are added to the DC-to-DC buck converter in place of the constant inductor (Lonlong et al., 2011). In a DC-to-DC converter, the total inductor size is reduced by 75% when a variable inductor is used instead of a constant inductor. A lower inductance value will be enough in situations when the solar current is expected to be strong. On the other hand, a higher inductance is needed in the event of lesser insolation (Verma et al., 2016). A connection between the PV current and the inductor's lowest value is established by this way. Utilizing the inductor to achieve Maximum Power Point Tracking allows for a scientific demonstration of it (Karami et al., 2016; Zhang et al., 2010). The following Equation 2.18. gives the minimum inductance value:

$$L_{min} = \frac{\delta^2 (1-\delta) \times V_{PV}}{2 \times f_s \times I_{PV}} \quad (2.18.)$$

Figure 2.42. (Verma et al., 2016) depicts the schematic representation for this procedure. In spite of variations in solar insolation, this approach is dependable and strong (Verma et al., 2016).

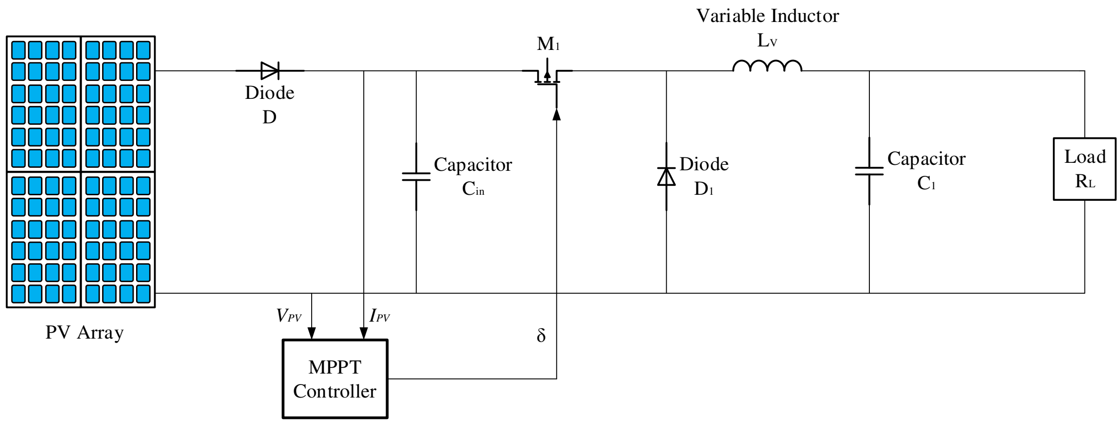

Figure 2.42. Schematic for the variable inductor control method

DC Link Capacitor Droop Algorithm

A converter that converts DC-to-DC is utilized in conjunction with the DC-link Capacitor Droop Control Algorithm. The duty cycle ratio for steady output and improved power quality is calculated using the power balance theory. Equation 2.19. yields the duty cycle (Prasad et al., 2019; Khatib et al., 2017).

$$\delta = 1 - \frac{V_{cell}}{V_{Link}} \tag{2.19.}$$

By varying the duty ratio "δ," the boost converter's output is maintained constant, and this approach is founded on the power equilibrium at DC-link (Verma et al., 2016). The energy balance standard at the DC-link is necessary for this technology to function (Joshi and Arora, 2017). As seen in Figure 2.43. (Ali et al., 2020), the solar energy system and the AC system are connected in parallel. The voltages in the DC-link in this circuit are represented by V_{Link} and the photovoltaic cell by V_{cell} (Ali et al., 2020).

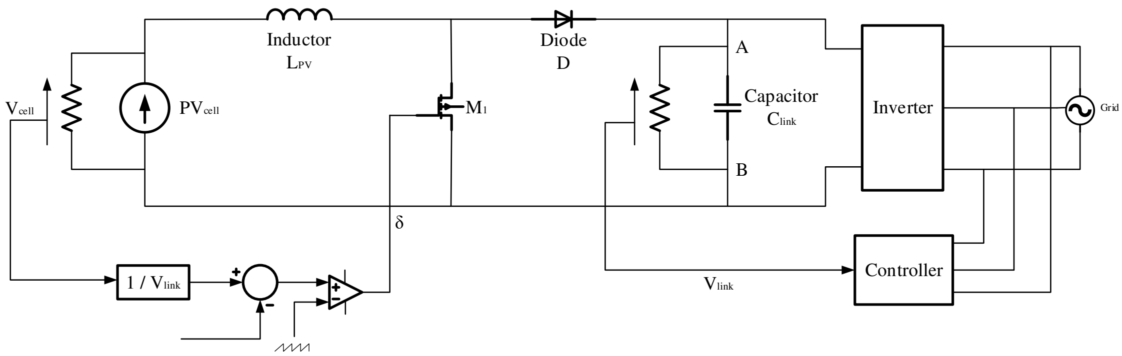

Figure 2.43. Circuit schematic for DC Link Capacitor Droop algorithm

It demonstrates how the inverter receives the boost converter's output via connections "*a*" and "*b*". By raising the amplitude of the AC system's line current, the array's operational power may be enhanced (Verma et al., 2016). When the PV's output power is lower than P_{MAX}, line current rises cause the power to rise while V-link stays constant. The V-link begins to decline after reaching its highest level of power. As a result, the state of balance is upset, which may be managed by altering the boost converter's duty ratio. Therefore, it is possible to reach the maximum power point in a state of equilibrium at a constant V-link (Matsui et al., 1999; Kitano et al., 2001).

This layout uses a feed-forward loop to maintain a constant line voltage thanks to the boost chopper. By using a feedback loop, the pulse-width modulation (PWM) regulates the voltage applied to the load. The DC-to-AC inverter's ripple voltage is lessened by the DC-link capacitor. Additionally, it offers a waiting time during which there is an instantaneous high-low oscillation of sunshine (Podder et al., 2019). Only PV systems that are linked to the AC system line may use this method (Francis et al., 2014).

Feed Back Control Algorithm

Nonlinear power-voltage and current-voltage characteristics are provided by solar PV. Because of this, operating the solar PV system near to the maximum power point is challenging (Basha and Rani, 2020). Based on current or voltage, Figure 2.44. (Verma et al., 2016) illustrates how power increased continuously until it reached the Maximum Power Point, at which point it decreased (Bleijs and Gow, 2001).

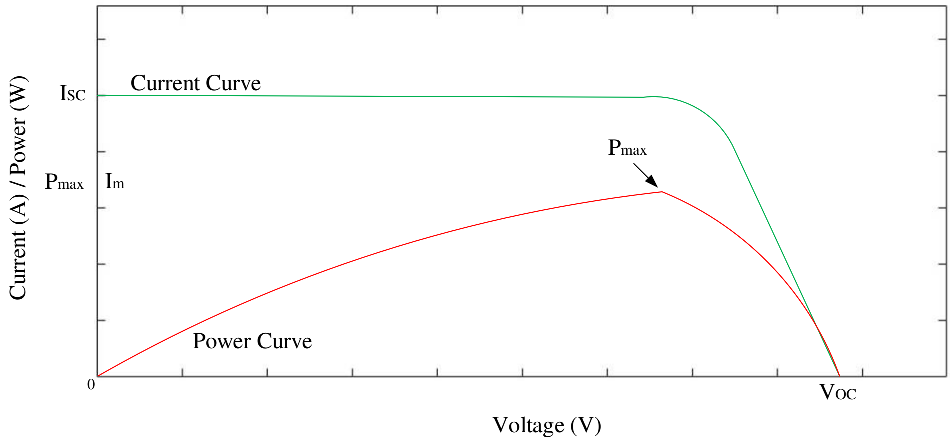

Figure 2.44. Characteristics of solar cells related to power, voltage, and current

This approach compares two successive powers in the above scenario. However, in contrast to traditional techniques, the Maximum Power Point is determined by taking into account the slope's magnitude (Bleijs and Gow, 2001). PV curve's Maximum Power Point slope (dP / dV or dI / dV) is used in this procedure. In Figure 2.45. (Park and Song, 2009), the feedback control is utilized to push it to zero (Park and Song, 2009).

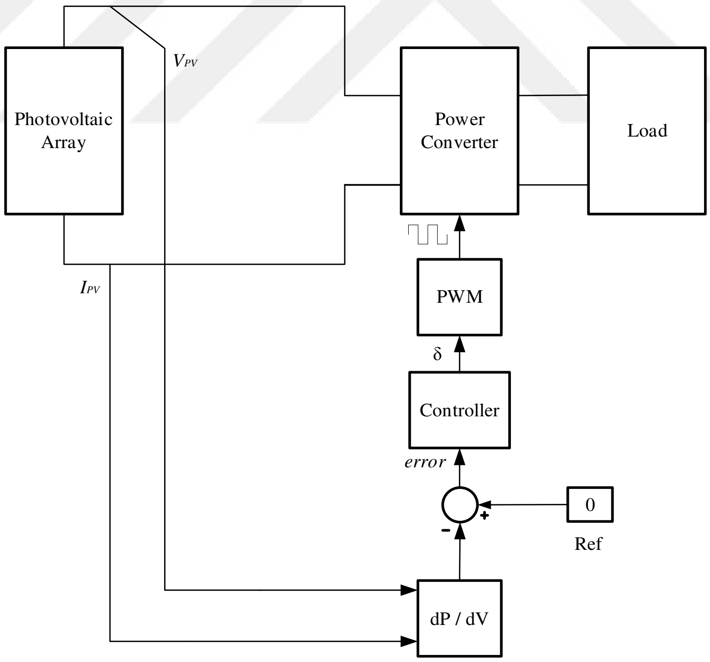

Figure 2.45. Block diagram of Feedback Control Algorithm

The literature has presented a control approach where in the task step size is adjusted by the incremental MPPT method based on dP / dV. There have also been other suggested feedback control methods (dP / dV or dI / dV), including employing linearization methods to calculate dP / dV (Abdel-Salam et al., 2018; Fesharaki et al., 2017).

Using a feedback controller, as seen in Figure 2.46. (Basha and Rani, 2020), one may determine the slope d*P* / d*V* of the *P*-*V* statistics (Basha and Rani, 2020).

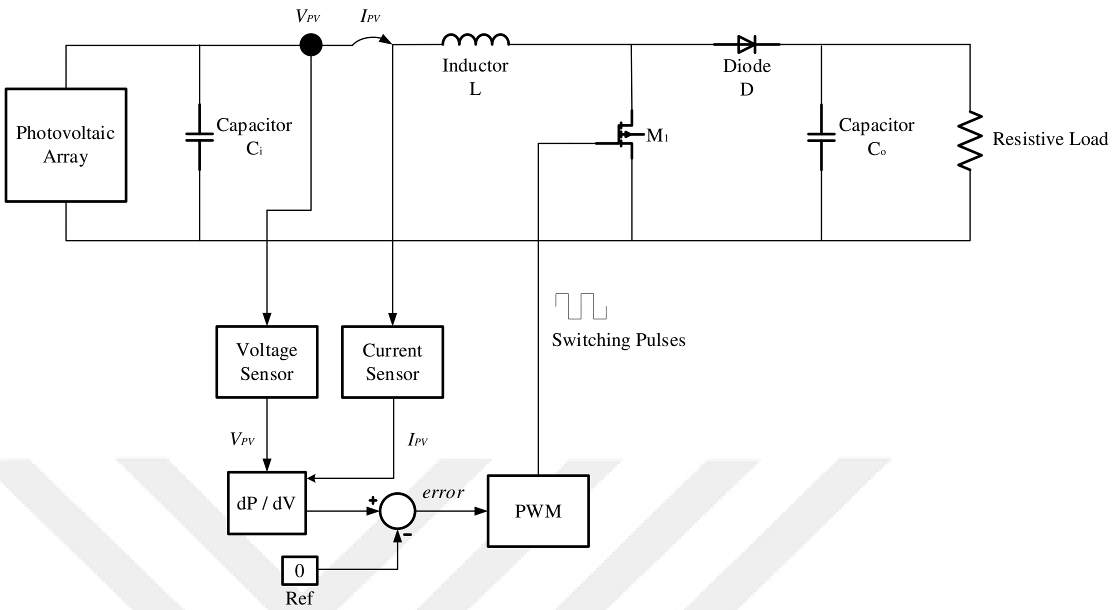

Figure 2.46. A Maximum Power Point Tracking Controller based on VSS Feedback Controller

The slope of the power-voltage and current-voltage characteristics is set to zero based on Figure 2.46. (Basha and Rani, 2020).

To find the subsequent duty cycle, a few calculated indications from the past can be kept. Figure 2.46. (Basha and Rani, 2020) shows that in order to attain the Maximum Power Point, it is either increased or decreased based on the recorded cycle data (Ali et al., 2020).

The duty ratio is modified in accordance with the tracking error, which is calculated using the formula in Equation 2.20. below (Verma et al., 2016).

$$\epsilon = K_c \int K_P \left(\frac{dP}{dI}\right) dt \tag{2.20}$$

The duty cycle stage is automatically modified depending on the slope of solar PV's nonlinear properties with various irradiance and temperature circumstances (Basha and Rani, 2020). The approach is cell-independent and is capable of quickly recognizing the Maximum Power Point (Park and Song, 2009). The feedback control algorithm has multiple benefits, including high Maximum Power Point tracking performance, strong converging speed, medium tracking speed, and fewer steady-state fluctuations over Maximum Power Point (Basha and Rani, 2020).

Three Point Weight Comparison Algorithm

Hsiao and Chen (2002) introduced their "Three Point Comparison Perturb & Observe" approach (Mohanty et al., 2014). This approach works on the same idea as the Perturb & Observe algorithm. However, just the two working points and related powers are checked out in Perturb & Observe algorithm. By periodically varying the solar PV voltage at the terminals at spots *A*, *B*, and *C*, this approach performs comparisons (Hsiao et al., 2002). The Maximum Power Point power-voltage graph is the focal point of the Three Point Comparison method, which examines power at three points (Podder et al., 2019). The following operating point, *B*, is determined by perturbing the present working point; *A*. Contrary to point *B*, point *C* is twice perturbed (Hsiao et al., 2002). Therefore, nine such scenarios need to be run through the control system in order to find the Maximum Power Point (Karami et al., 2016). For each of point *A*, point *B*, and point *C*, the control parameter is perturbed on three occasions independently (Ali et al., 2020). These situations are seen in Figure 2.47. (Ali et al., 2020).

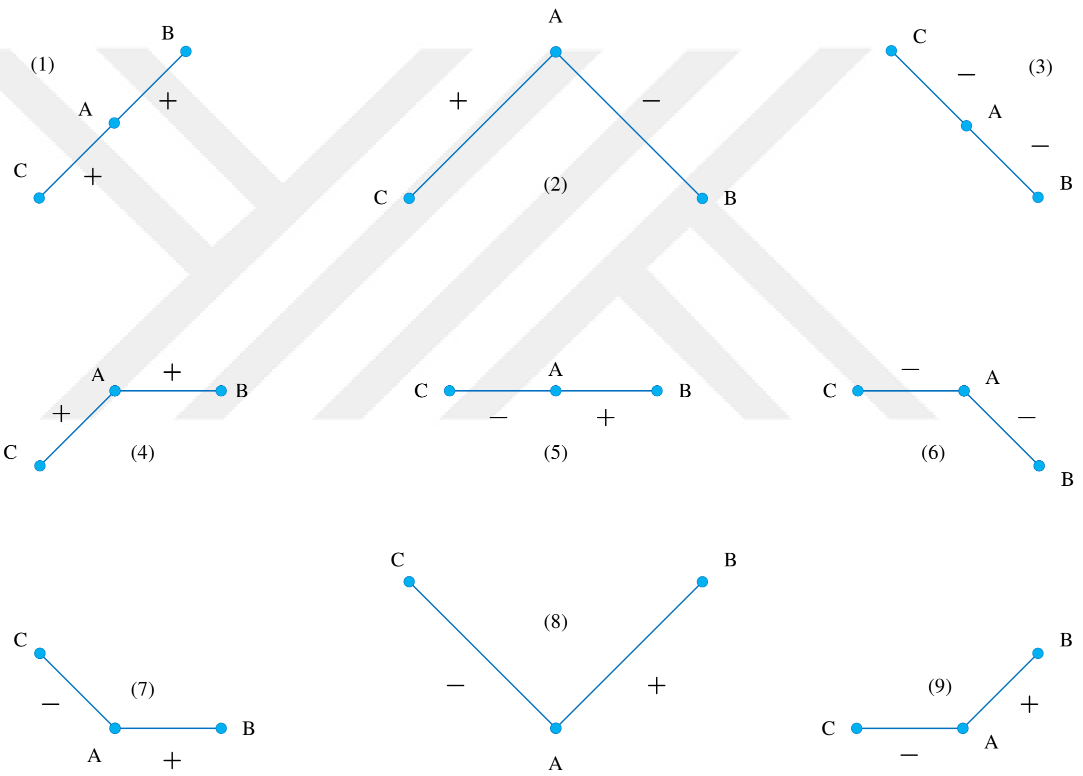

Figure 2.47. Possible circumstances for a Three Point Comparison

On a regular basis the V_{PV} is perturbed and compared with the P_{PV} at three sites, *A*, *B*, and *C*, using the Three Point Comparison technique. The disturbance begins at point *A* and moves to point *B* in the initial phase. It then goes from *A* to *C*. Later on, it is disturbed from *B* to *A* in the opposite way. For each duty cycle step size, it calculates *C* to *A*. Positive condition is achieved if *B*'s computed wattage equals or exceeds *A*'s, while negative condition is achieved otherwise. The outcome for *A* to *C* be positive if *C*'s computed power in watts is smaller than *A*. The outcome be negative in the opposite situation. Duty cycle will rise if two of the three measures are positive. If not, there will be a reduction in duty cycle (Ali et al., 2020). The Maximum Power Point is attained in the third scenario if the measured values have different polarities. It also implies that the duty cycle doesn't change (Hsiao et al., 2002). Compared to the "Perturb & Observe Algorithm", this technique is faster and more appropriate for rapidly changing circumstances (Verma et al., 2016).

Steepest Descent Algorithm

Perturb & Observe and Hill Climb power point tracking techniques have several disadvantages. The Steepest Descent Method, which was recently suggested in a work (Park and Song, 2009), was employed to get over these problems (Basha and Rani, 2020). The gradient descent scheme, sometimes referred to as the steepest descent approach, is an optimization method used in practical math (Xiao et al., 2007). The first order method of optimization is this one. A local minimum of a function can be found by following steps that are proportionate to the gradient's negative (Verma et al., 2016). The Maximum Power Point is found in phases using the Steepest Descent technique, which uses a single derivative method for optimization of the solar system (Pradhan and Subudhi, 2012). The gradient of the function $f(V, P) = dP / dV$ is where it is constructed (Ali et al., 2020). This technique is used to locate the closest local Maximum Power Point, in addition Equation 2.21. provides the gradient of the function (Verma et al., 2016).

$$V_{k+1} = V_k + \left|\frac{dP}{dV}\right| \frac{V = V_k}{k_\epsilon} \tag{2.21.}$$

To operate the Maximum Power Point Tracking, one must determine the point at which dP / dV or the function equals minimal, or zero (Verma et al., 2016). In this case, the gradient value corresponds to the next step size, which is determined by the step size corrector k. The derivation is represented by dP / dV (Xiao et al., 2007; Pradhan and Subudhi, 2012). PV open circuit voltage (V_{OC}) is used in the gradient descent computations. The operational voltage (V) falls between 0 and V_{OC}. Equation 2.22. shows that the power change is a function that decreases with respect to voltage (Ali et al., 2020).

$$\frac{dP^2}{dV^2} \quad \text{and} \quad \frac{dP}{dV} \tag{2.22.}$$

In order to avoid fluctuations and maximize power around the Maximum Power Point, the gradient descent approach is employed. With rapidly fluctuating weather, our Maximum Power Point Tracking method makes sense (Podder et al., 2019). Less speed for maximum power point tracking is the technique's downside (Basha and Rani, 2020).

Analytical Solution Algorithm

The mean value theorem is the foundation of this method (Podder et al., 2019). The Maximum Power Point is tracked using the real analysis means value theorem in the analytical solution approach (Ali et al., 2020). A solar photovoltaic system's efficiency can be increased by the employment of an efficient converter in the analytical solution approach (Abdel-Rahim and Haoyu, 2020). The PV system's voltage and current, as well as the controller's duty ratio, are the independent variables in this technique. The dependent factor that is employed is the output power. The term "bracketed technique" is another name for this approach (Podder et al., 2019). The precise expression for a single point in a tiny radius ball, ε, that is located in a tiny circle yields the Maximum Power Point (Rodriguez and Amaratunga, 2007). Equation 2.23. is used to determine the precise position of the little ball in radius (Ali et al., 2020).

$$i = -\frac{I_L}{V_{OC}}v + I_L \tag{2.23.}$$

The solar cell current I_L is what creates the straight line L_1 in this instance. Dependent on I_{SC} and V_{OC} is the L_1 straight line. Equation 2.24. is used to generate a second parallel straight line, L_2. To compute the tiny radius, ε, it is tangent to the present curve (Ali et al., 2020).

$$\epsilon > (v_{PV}^* + i_{PV}^* \times R_s) - (V_{MPP} + i_{MPP} \times R_s) \tag{2.24.}$$

In this region, the crossing sites of L_2 (v^*_{PV}, i^*_{PV}) and $\varepsilon > 0$ are in close proximity to the true maximum power point (Ali et al., 2020).

Less steady state fluctuations over the Maximum Power Point and great efficiency are the benefits of this method. However, the tracking speed is mediocre (Basha and Rani, 2020).

Temperature Based Algorithm

This approach measures the temperature of solar photovoltaics. The method for obtaining temperature-dependent changes in the Maximum Power Point is identical to that of the constant voltage approach (Verma et al., 2016). The photovoltaic array-module surface temperature is represented by T in the Temperature Based Approach. Equation 2.25.'s voltage/temperature coefficient value is utilized to track the Maximum Power Point (Vicennte et al., 2015).

$$V_{MPP(T)} = V_{MPP(T_{ref})} + uV_{MPP}(T - T_{ref}) \tag{2.25.}$$

The reference temperature in relation to the Maximum Power Point is determined by Equation 2.25. (Correa-Betanzo et al., 2018). The Maximum Power Point voltage under typical testing circumstances is shown below as $V_{MPP(T)}$. As per the datasheet, $V_{MPP(Tref)}$ represents the maximum power point voltage. The expression for the temperature coefficient is uV_{MPP} (Vicente et al., 2015). A temperature sensor takes the place of a current sensor. The voltage converter and the voltage sensor are both adjusted on the Photovoltaic panel's top surface. The schematic representation of a temperature-based method is shown in Figure 2.48. (Correa-Betanzo et al., 2018).

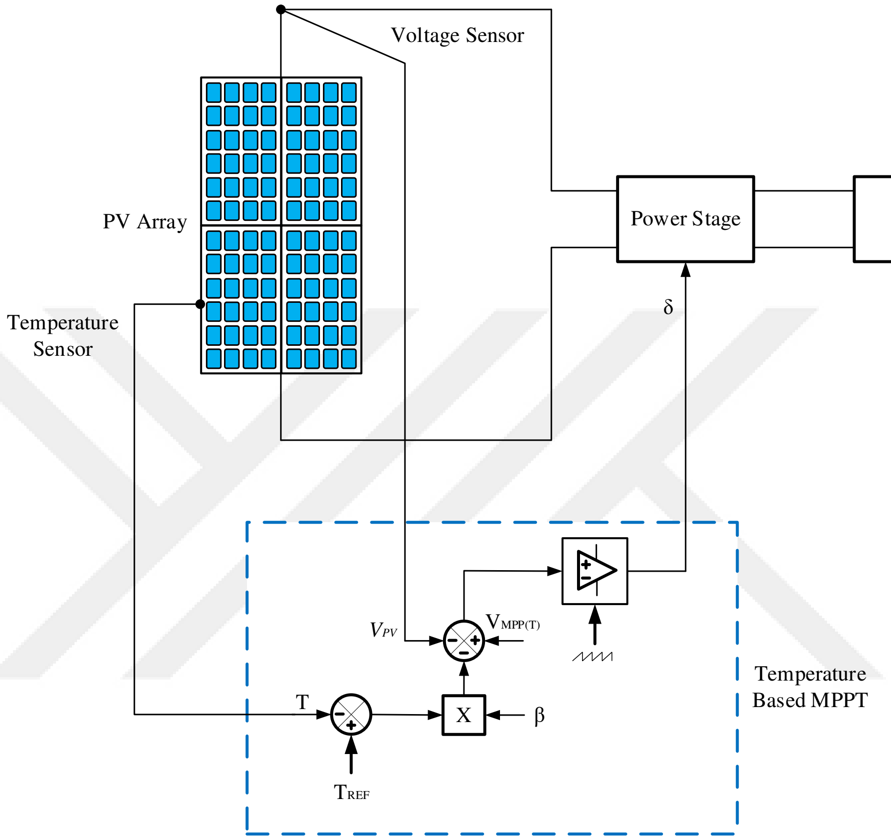

Figure 2.48. A temperature-based approach's schematic

The intended output voltage is retained by the voltage control converter main. It determines the ideal voltage by measuring the surface temperature. It is instantly maintaining the ideal voltage by controlling the converter's input voltage. There won't be tracking failure when the Maximum Power Point is restrained (Ali et al., 2020). This approach requires little circuit and is straight forward to set up. However, voltage and the temperature must be watched in this approach (Verma et al., 2016).

Bisection Search Algorithm

In order to choose a subinterval to monitor the Maximum Power Point, the Bisection Search Theorem (BST algorithm) continually splits an interval in half. The Intermediate Value Theorem forms the basis of this approach (Ali et al., 2020). A compelling argument for applying this theory is made by researchers Eiselt and Sandblom (2007). A modified approach of it is provided in a study article by John and Kurtis (2004) (Podder et al., 2019). Finding any function's roots in the range [*a*, *b*] using mathematics is one method (Wangpeng et al., 2010). The above theorem tells us where the root of any possible range for the real variable (x) is by using the formula $y = f(x)$. It may be said that function f is continuous. Its definition falls between [a, b]. There are opposing signs for $f(a)$ and $f(b)$ (Ali et al., 2020). Inside the range [0, V_{OC}], the equation for the function is $\Delta P / \Delta V$ (Wangpeng et al., 2010). The answer is then represented by the root x (Verma et al., 2016). With this procedure, the interval's end points are systematically changed to be closer to zero. It's as Figure 2.49. (Wang et al., 2010) illustrates (Ali et al., 2020).

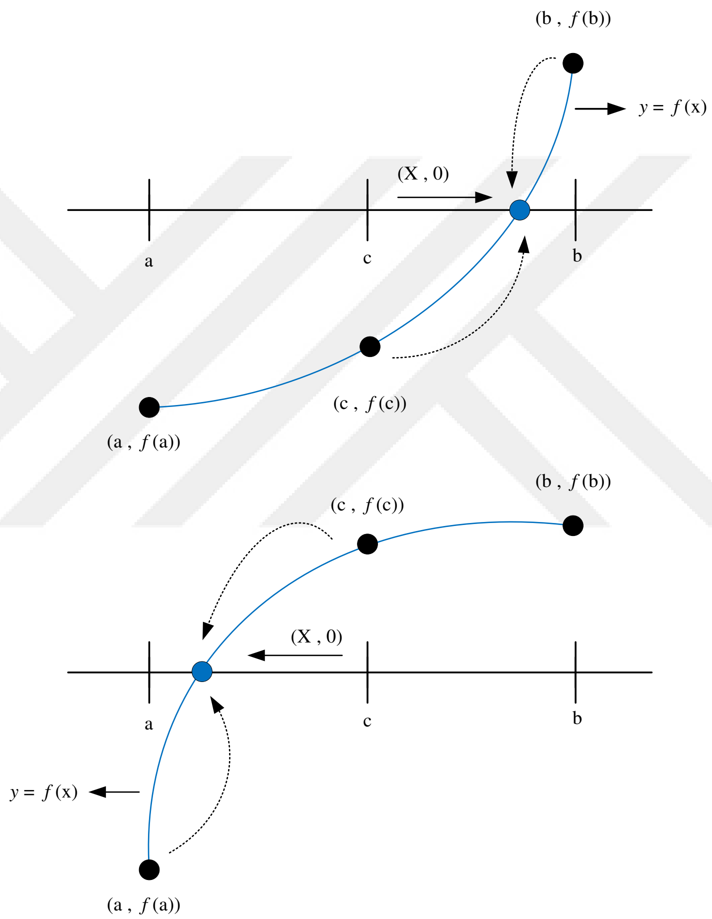

Figure 2.49. Illustration of the Bisection Search Theorem

Each stage decreases the size of a range which includes 0 function f. Until the gap is narrow enough to determine the Maximum Power Point, the process is repeated (Ali et al., 2020).

Maximum Power Point is the point at which the function $\Delta P / \Delta V$ becomes zero (Verma et al., 2016).

A more effective numerical method for locating conditional roots to follow the actual Maximum Power Point is the Bisection Search Theorem (Wang et al., 2010). The implementation of this approach is inexpensive. This is an easy method to implement. Maximum Power Point tracking requires fewer sensors and a faster approach. Calculations of derivatives are not needed (Podder et al., 2019).

Particle Swarm Optimization Algorithm

Kennedy and Eberhartin proposed this optimization method in 1995, and it is used to address problems having several local points (Koad et al., 2017). It was created by observing how creatures, such fish flocks and birds, interact with one another. This method is and stochastic and evolutionary. In the algorithm, the population is made up of individuals known as particles. Random velocity values are assigned to each particle that represents the potential answer. The search region is then searched with these particles. Every particle exchanges the knowledge it has acquired from both itself and its neighbour's flight experiences. Each particle then modifies its location. Each particle advances to the global optimal point in this way (Sundareswaran et al., 2015). Consequently, the local and global best solutions have an impact on a particle's position (Ishaque et al., 2012). A collection of random particles is used to initiate the algorithm, which then updates generations to find the optimal solution. The individual and global optimal values are used to update every single particle in each cycle. The optimal solution (which is fitness) this particle has attained thus far is known as the personal best value, or P_{best}. The optimal answer (fitness) for the entire group is the global best value (which is G_{best}) (Wei et al., 2017). The algorithm is constantly updated according to two different formulas. These are velocity update and position update.

Velocity update formula is as Equation 2.26.

$$v_i = w \times v_i + c_1 \times r_1 \times (pbest_i - x_i) + c_2 \times r_2 \times (gbest - x_i) \quad (2.26.)$$

Position update formula is as Equation 2.27.

$$x_i = x_i + v_i \quad (2.27.)$$

If the parameters here need to be explained,

v_i: The particle's velocity vector,
x_i: The current position of the particle,
w: Coefficient of inertia,
c_1, c_2: Cognitive and social component coefficients,
r_1, r_2: Random numbers (between zero and one) that randomize particle motion,
$gbest$: The best position of the entire solutions,
$pbest$: The best position of the particle is,

can be expressed as (Wei et al., 2017). The algorithm diagram of the PSO algorithm is as in Figure 2.50. (Hsu et al., 2010).

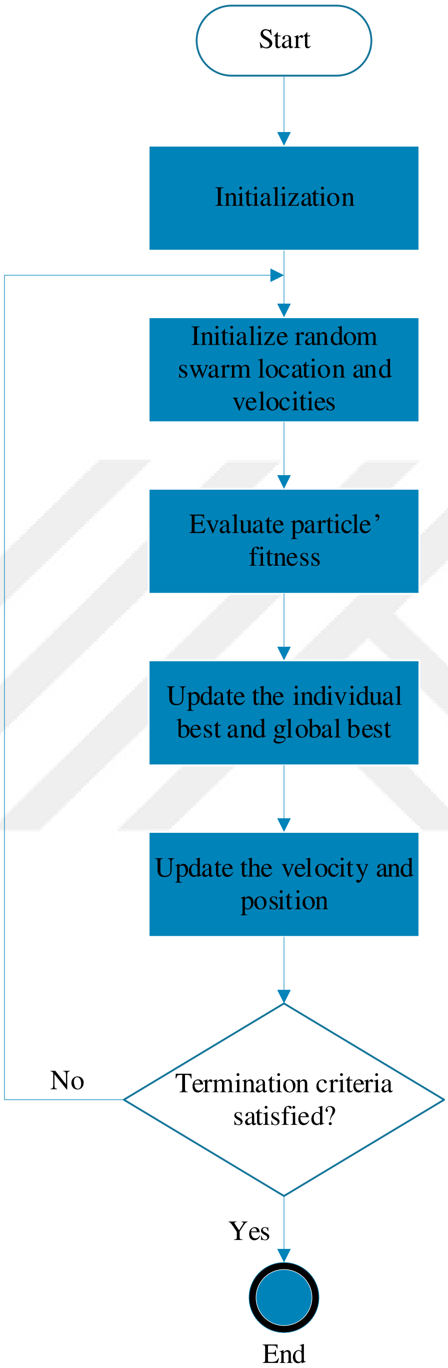

Figure 2.50. Particle Swarm Optimization MPPT algorithm flow chart

Off-line MPPT Algorithms

In these control algorithms, unlike online algorithms, the current and voltage values taken from photovoltaic panels are not measured continuously. In these methods, which are referred to as model-based methods, voltage, current, temperature, radiation, etc. other information is used. The desired MPPT is tried to be reached by using the data and sample collection that are pre-set to suit the desired purpose as input. Below, offline algorithms from MPPT methods that can be used under uniform radiation conditions are mentioned.

Constant Voltage Algorithm

The ratio of the voltage of the array at MPP (V_{MPP}) to its open-circuit voltage V_{OC} is approximately a constant and generally around 0.76 time of the V_{OC} of the solar module in any given solar insulation. The basis for the Constant Voltage (CV) algorithm lies in this (Hohm and Ropp, 2003). In other word,

$$\frac{V_{MPP}}{V_{OC-K}} < 1 \qquad \text{(Assumed 0.76)} \qquad (2.28.)$$

The block diagram representation for the MPPT control with Constant Voltage (CV) is given in Figure 2.51. (Mohanty et al., 2014).

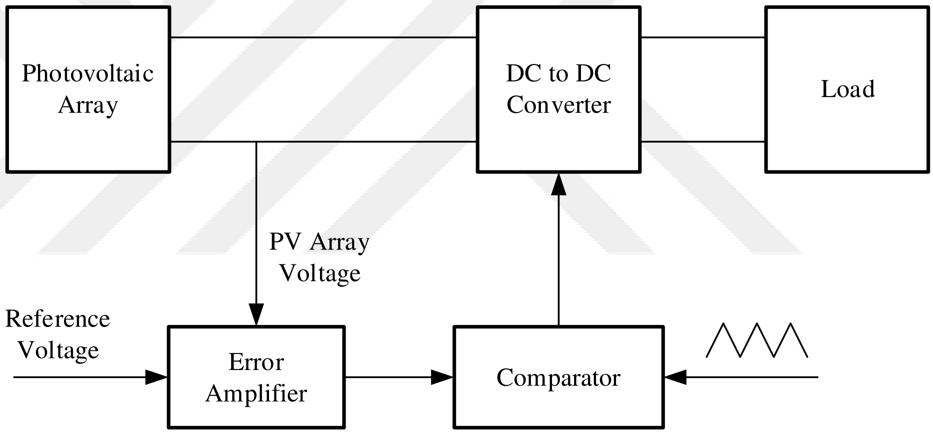

Figure 2.51. Control topology for the constant voltage based MPPT

Constant Voltage control can be easily implemented with analog hardware (Mohanty et al., 2014). The sensed PV array voltage is compared with the reference voltage to generate an error signal, which controls the duty cycles (Vasant and Pawar, 2017). The Constant Voltage (CV) algorithm can be implemented using the flow given below in Figure 2.52. (Vasant and Pawar, 2017).

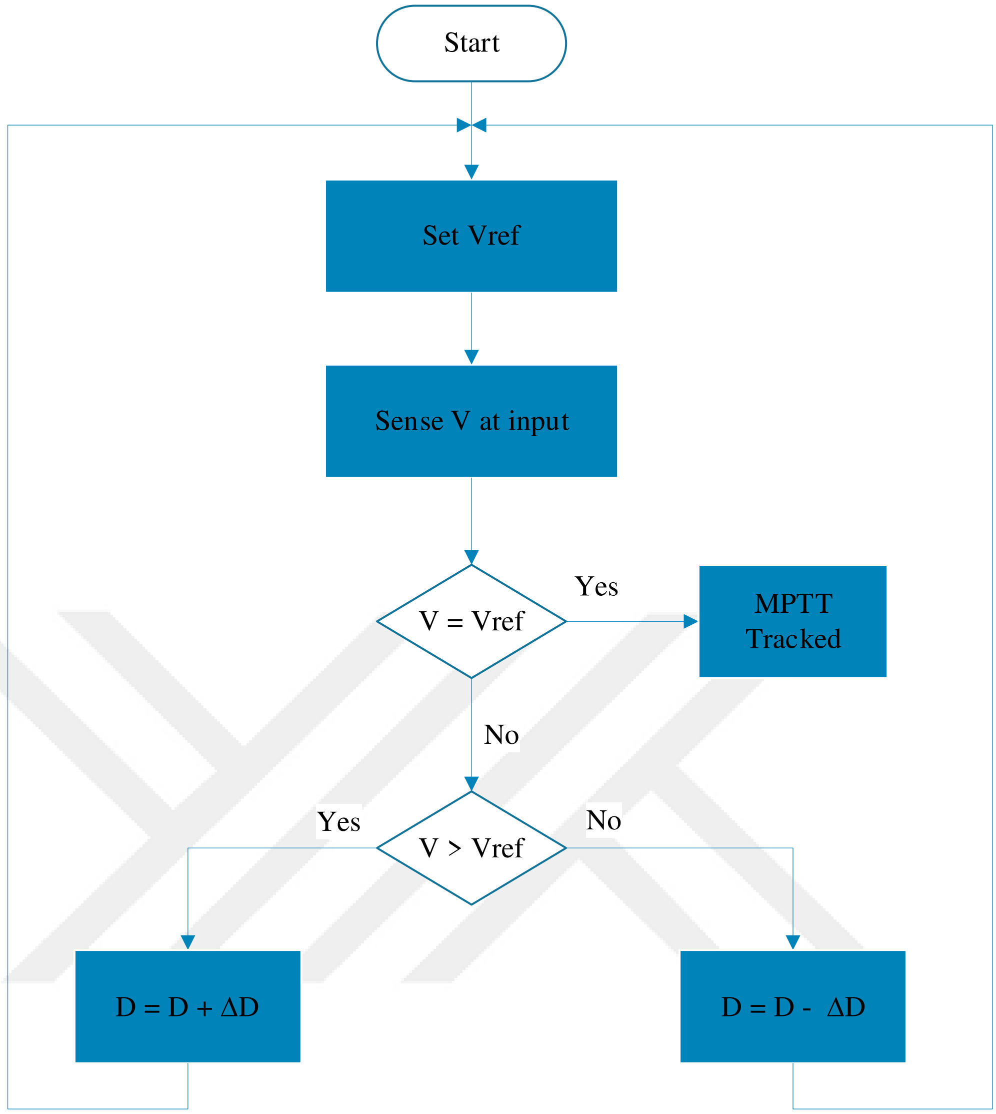

Figure 2.52. Flow diagram of constant voltage algorithm

Constant Current Algorithm

Constant Current (CC) method is based on the same phenomenon of the Constant Voltage (CV) method. In the Constant Voltage (CV) method the PV array operates at the constant voltage and in this method PV array operates at the constant current. The Maximum Power Point arrives between 78% and 92% of the short circuit current I_{SC} thus the sensed parameter is short circuit current. Equation 2.29. shows this situation (Verma et al., 2016).

$$I_{ref} = K_2 \times I_{SC} \quad \text{where} \quad K_3 = 0.78 \times 0.92 \qquad (2.29.)$$

The current is measured periodically when the PV array/module is under a short circuit condition via a power switch. In both CV and CC methods, only one sensor is required (voltage or current) (Yılmaz et al., 2018).

Curve Fitting Algorithm

According to the approximate curve fitting approach, the tracking points in the study report were approximated using (Ausias et al., 2007). The difference between the observed and expected global points is obtained using this approach. Both operational voltage and global power are evaluated and are minimized throughout this procedure (Rahesh and Mabel, 2015). One offline method of Maximum Power Point Tracking is the Curve Fitting method. Because of the erratic nature of the weather, it is based on the solar module's non-linear feature (Ali et al., 2020). Solar photovoltaics has a nonlinear property. It may be quantitatively represented by applying the curve fitting technique (Salas et al., 2006; Leedy et al., 2013). To create a mathematical model that describes the output qualities, whole the production information and production data is needed (Ali et al., 2020). The technique relies on a solar generator's power-to-voltage characteristic (Salas et al., 2006; Leedy et al., 2013; Masoum and Dehbonei, 1998). Equation 2.30. is utilized in the computation of the typical of the solar module. Here, the coefficients that were obtained by collecting the P_{PV}, I_{PV}, and V_{PV} are a, b, c, and d (Salas et al., 2006).

$$P_{PV} = aV_{PV}^3 + bV_{PV}^2 + cV_{PV} + d \quad (2.30.)$$

Sampling values inside the necessary interval yields this information (Dadje et al., 2016). The relationship between array voltage and P_{PV} as well as temperature has also been demonstrated (Verma et al., 2016). In below Equation 2.31., it can be found maximum power voltage (Masoum and Dehbonei, 1998).

$$V_{MPP} = \frac{-b \pm \sqrt{b^2 - 3ac}}{3a} \quad (2.31.)$$

In actuality, to identify a precise Maximum Power Point, the procedure needs to be performed every few milliseconds (Dadje et al., 2016). An inherent drawback of the curve fitting approach is its high data requirements for the system. In order to calculate Maximum Power Point, precise knowledge of physical characteristics is also necessary (Ali et al., 2020). The quantity of specimens determines the degree of precision (Dadje et al., 2016). Due to the variance between ideal and practical circumstances, this approach becomes sluggish and ineffective (Ali et al., 2020).

Pilot Cell Algorithm

Constant Current or Constant Voltage can be applied in a Pilot Cell methodology. Instead of using the PV array or module, a pilot cell is used in this calculation of the V_{OC} (Esram and Chapman, 2007; El-Dein et al., 2012). The FOCV algorithm and this technique are identical. There, the main distinction is that V_{opt} does not cause the whole PV panel to be open circuit. Rather, it is computed just using the V_{OC} of just one PV cell, without taking other PV cells into account. This goes by the name "pilot" as well. The disruptions that occur when measuring voltage are one of the main drawbacks of fractional open circuit voltage. By using the pilot technique, these disruptions are avoided (Tozlu and Calik, 2021). This number has to be multiplied by a constant K_3 value in order to determine the pilot cell's V_{OC} value. This is what Equation 2.32. illustrates (Ali et al., 2020).

$$V_{ref} = K_3 \times V_{OC(pilotcell)} \quad \text{where} \quad K_3 \approx constant < 1 \tag{2.32.}$$

Predefining the constant allows it to follow the array's Maximum Power Point regardless of insolation or temperature fluctuations (Chandra and Gaur, 2018). Therefore, every solar module and pilot cell must be corrected in turn. The system's energy costs are rising as a result (Ali et al., 2020). Additionally, the specifications of the pilot solar cell and the photovoltaic module it represents must match (Chandra and Gaur, 2018). Nevertheless, in situations like partial shade, this approach performs less well (Tozlu and Calik, 2021).

Look-up-table Algorithm

Look Up Table is an offline approach that is the result of reducing the time required for processing of the control circuit (Bollipo et al., 2021). This approach compares the array's measurements with data that have been recorded in the past. This allows MPP to be suitable with the array's working point (Desai and Patel, 2007). A maximum power point for a particular solar photovoltaic array may be found in the database that has been maintained (Verma et al., 2016). The voltage and current of the photovoltaic module were measured using the lookup table approach. Next, a calculation is made to monitor the Maximum Power Point (Ali et al., 2020). In Figure 2.53. (Tozlu and Calik, 2021), which displays the process diagram for the Look Up Table. A table is developed based on the data collected from solar systems in every potential meteorological condition (Tozlu and Calik, 2021).

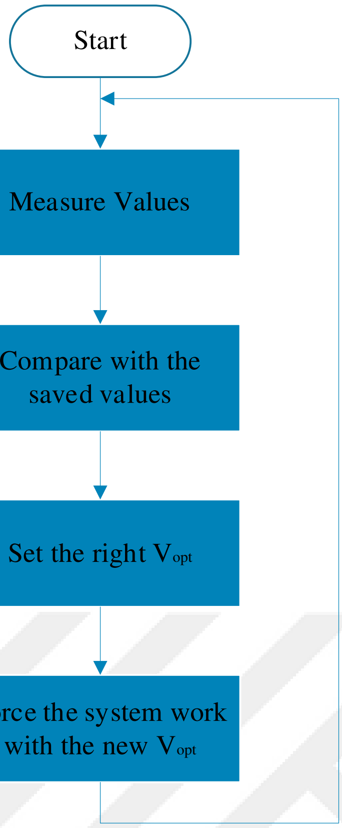

Figure 2.53. Look Up Table approach

Consequently, a lot of information is kept in look up storage for precise Maximum Power Point tracking and improved accuracy (Ali et al., 2020). Every session, which was the next V_{opt} level is calculated by contrasting the stored data and the real values (Tozlu and Calik, 2021). Equation 2.33. characterizes P_{max} as an equation that depends on two parameters in this approach (Bollipo et al., 2021).

$$V_{PV} \times I_{MPP} = f(P_{max}) \tag{2.33.}$$

Figure 2.54. (Bollipo et al., 2021) shows the block structure depiction of the technique (Bollipo et al., 2021).

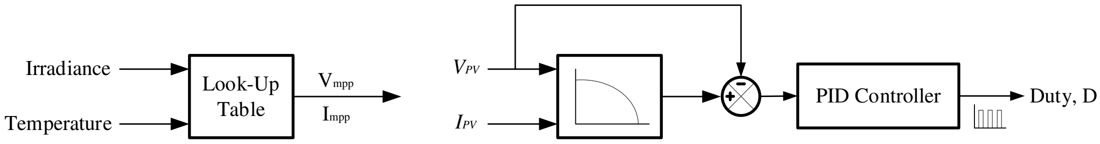

Figure 2.54. Maximum Power Point Tracking schematic using a “Look Up Table”

The DC-to-DC converter's Duty Cycle is changed using a PID controller. The predefined baseline value will be reached if the solar source's power and current are both "0" (Kota and Bhukya, 2016).

Load Voltage & Load Current Algorithm

The underlying premise of this approach is that a lossless converter's energy output maximization will likewise result in its input power maximization (Tozlu and Calik, 2021). Rather of measuring the current or voltage from the solar system, the Maximum Power Point is monitored by measuring the load current or voltage. Figure 2.55.a. (Ali et al., 2020) shows the Maximum Power Point for this approach.

The technique optimizes solar power in four distinct load-connected configurations. In that order, they are current source, resistive source, voltage source, and resistive and voltage source. Figure 2.55.b. (Ali et al., 2020) illustrates it.

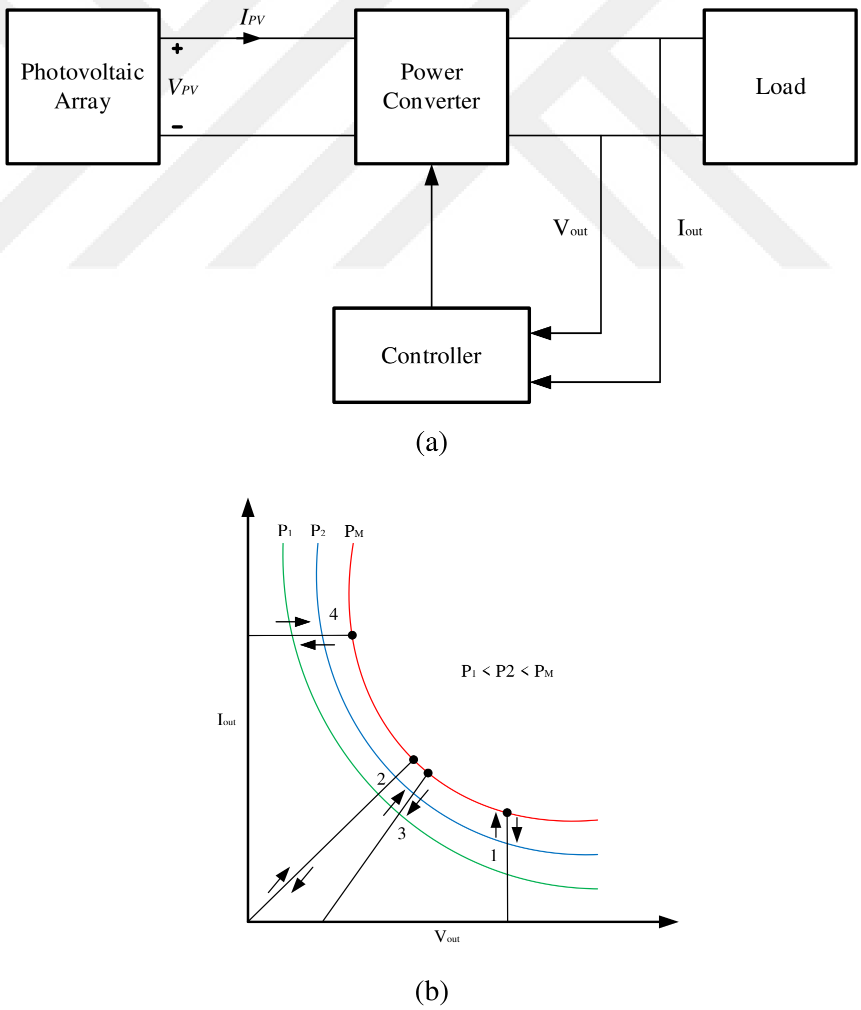

Figure 2.55. (a) The load voltage and load current approach, (b) Alternative arrangements for load systems

According to the parameters of the load, the maximum load voltage or current is achieved. Both output voltage and output current can be utilized to maximize the effects of resistive or voltage source load (Ali et al., 2020). As a result, it is presumable that the input power likewise maximizes (Tozlu and Calik, 2021).

Any loads using a single load sensor can benefit from the load voltage and load current maximizing techniques (Ali et al., 2020). Because the converter is not lossless, Maximum Power Point cannot be properly tracked, which represents one of the approach's main drawbacks. It is possible to reduce losses by improving the converter's effectiveness, although doing so would raise pricing (Tozlu and Calik, 2021).

PV Output Senseless Algorithm

Both current and voltage must be detected in order to use the conventional maximum power point tracking approach. Due to its complexity, it might not be able to track the Maximum Power Point under irregular meteorological circumstances (Ali et al., 2020). Thus, in order to follow the Maximum Power Point with no detecting current or voltage, massive solar systems employ the photovoltaic output senseless approach (Shabaan et al., 2018). Figure 2.56. (Tozlu and Calik, 2021) depicts the process diagram of the procedure, which is typically used to huge systems (Tozlu and Calik, 2021).

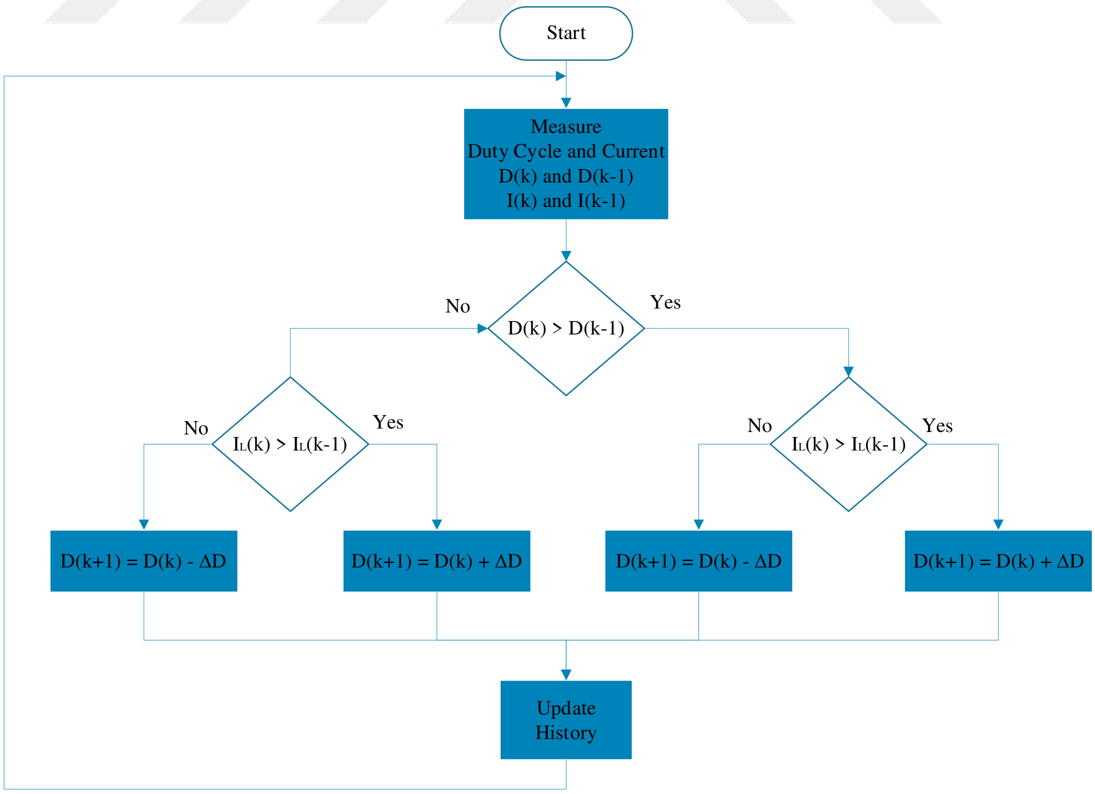

Figure 2.56. Output senseless algorithm schematic

To determine the Maximum Power Point, this approach takes into account a single factor the load current. However, as Figure 2.57. (Ali et al., 2020) illustrates, it is only relevant to photovoltaic systems that include just one phase DC-to-AC converter (Ali et al., 2020).

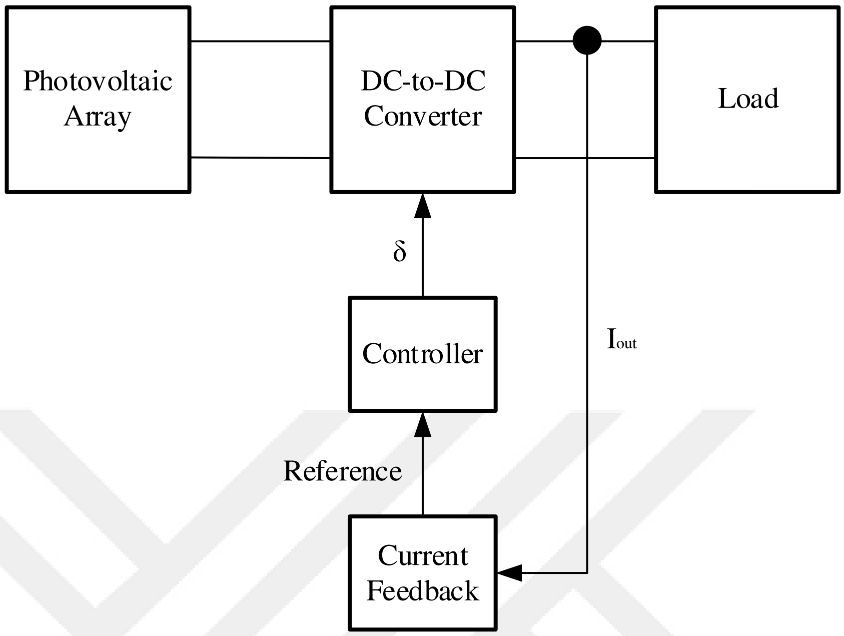

Figure 2.57. Control schematic for the output sensors technique

The decrease in voltage at the output of massive solar energy sources is minimal. In this instance, the maximum current and power may be thought of as being exactly proportionate (Tozlu and Calik, 2021). To track the Maximum Power Point, it is also expected that the power of the load is proportionate to the power of the photovoltaic array. For the purpose of adjusting the load current in relation to the PV array/module output voltage, the duty cycle variation is monitored (Ali et al., 2020). The DC-to-AC converter's output current, or load current, rises while the voltage falls as the duty cycle rises. Therefore, it is possible to determine the relationship between voltage and duty cycle (Ching-Tsai et al., 1993). First, a comparison is made between the information from the old and new duty cycles. The mistake is then reduced by using the load current as an evaluation (Almutairi et al., 2020). A fall in duty cycle causes a fall in current following the maximum power point, or moving out of it (Verma et al., 2016). Shadowing and abrupt changes in the atmosphere are promptly handled by this approach. The photovoltaic part of the structure does not need to observe anything (Kim et al., 2009).

2.4.2. MPPT Algorithms under non-Uniform Radiation

Hybrid MPPT Algorithms

In non-uniform radiation conditions, there are more MPP points than normal in the power-voltage graphs of PV panels. Since the global maximum power point and local maximum power points are present together, MPPT tracking becomes difficult and cannot be done properly. There are large losses in the system that does not work at the MPPT point. Hybrid algorithms with various advantages have been developed for situations where the traditional single algorithm is insufficient (Ali et al., 2020). Hybrid algorithms are derived by combining multiple algorithms such as direct algorithms and indirect algorithms. Hybrid methods provide faster approach to the MPP point. The pertubation rate can be selected variably when performing power point tracking. Disturbances in the system occurring in the MPPT phase are monitored by direct algorithms. In power tracking, predictions are made with an indirect algorithm (Jasim and Shepetov, 2017). Examples of hybrid algorithms are given in Figure 2.58. (Ali et al., 2020).

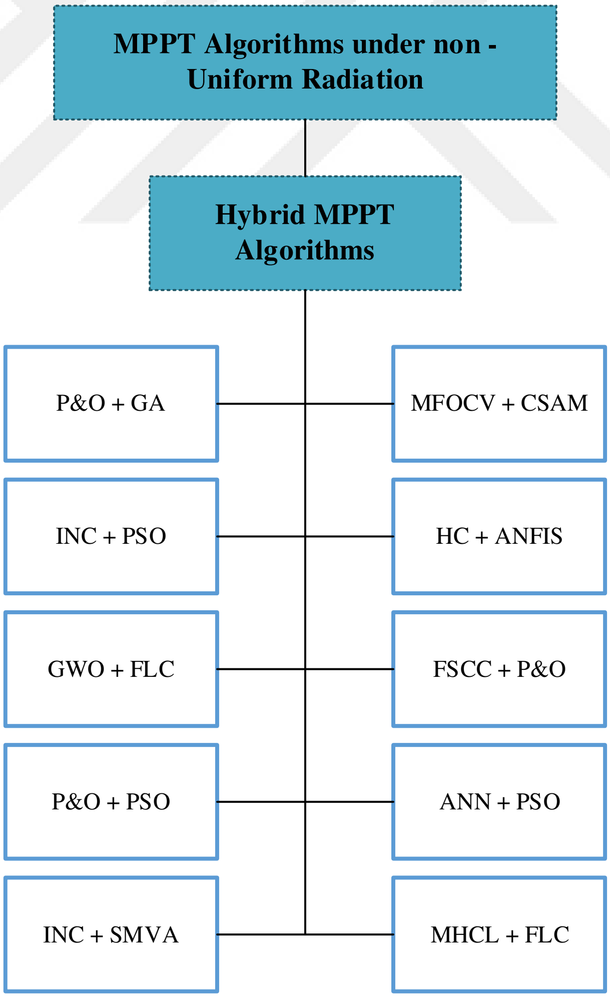

Figure 2.58. Hybrid algorithm examples

2.4.3. Comparison of MPPT Methods in the Literature

Numerous methods, PV modelling approaches, array designs, and controller topologies have all been thoroughly investigated up to this point (Tozlu and Calik, 2021). It is becoming more difficult for designers to select the best option for their particular applications, even if a variety of approaches are offered for non-uniform insolation circumstances (Erdem, 2017). The most important requirements and needs for any particular application are efficiency, category, cost, PV array dependency, precision, partial shading fitness, difficulty of implementation, market available, stages of energy transfer, detectors needed, grid connection, analog or digital structure, convergence speed, range of efficiency and popularity (Erdem, 2017; Dadje et al., 2016; Verma et al., 2016). Considering some of the priorities and needs here, a comprehensive explanation table of MPPT methods used in partial shading situations in the literature has been prepared according to various categories, as in Table 2.2. (Omar et al., 2023; Erdem, 2017; Tozlu and Calik, 2021; Maoa et al., 2020; Ali et al., 2020; Pawar et al., 2017; Singh and Singh, 2019; Bingöl and Özkaya, 2019).

Table 2.2. Comparison of MPPT methods in the literature in terms of various features

MPPT Algorithm	Required Sensors and Input Parameters	Tracking Accuracy to GMPP	Tracking Speed	Dependency of PV Array	Efficiency	Implementation Comlexity	Cost
Perturb and Observe (P&O)	V - I	Medium	Slow	No	High	Low	Low
Hill Climbing (HC)	V - I	Medium	Medium	No	High	Low	Low
Sliding Mode Control (SMC)	V - I	Medium	Fast	No	High	High	Expensive
Switching Ripple Correlation	V - I	Medium	Fast	No	High	Medium	Medium
Fractional Open Circuit Voltage (FOCV)	V	Low	Medium	Yes	Low	Low	Low
Incremental Conductance (IncC)	V - I	High	Medium	No	High	Medium	Medium
Fractional Short Circuit Voltage (FSCV)	I	Low	Medium	Yes	Low	Low	Low
Constant Voltage (CV)	V	Low	Fast	Yes	Low	Low	Low
Particle Swarm Optimization (PSO)	V - I	High	Fast	No	High	High	High
Modified PSO	V - I	High	Fast	No	High	High	High
Genetic Algorithm (GA)	V - I	High	Medium	No	High	High	High
Ant Colony Optimization (ACO)	V - I	High	Fast	No	High	High	High
Gray Wolf Optimization (GWO)	V - I	High	Fast	No	High	Medium	High
Artificial Bee Colony (ABC)	V - I	High	Fast	No	High	High	High
Fuzzzy Logic (FL)	V - I	High	Medium	Yes	Low	Medium	Medium
Bat Algorithm (BA)	V - I	High	Fast	No	High	High	High
Cuckoo Search (CS)	V - I	High	Fast	No	High	Medium	Medium
Firefly Algorithm (FA)	V - I	High	Fast	No	High	Medium	Medium
Artificial Neural Network (ANN)	V - I - G	High	Fast	Yes	Low	High	High
Kalman Filter (KF)	V - I	High	Fast	No	High	High	Medium
Look Up Table (LUT)	V - I	Low	Fast	Yes	Medium	Low	Low
PV Output Senseless	I	Medium	Medium	Yes	High	Medium	Medium
Three-Point Weight Comparison (TWC)	V - I	Medium	Slow	No	High	Low	Low
Constant Current (CC)	I	Low	Fast	Yes	Low	Low	Low
Beta Algorithm	V - I	Medium	Fast	No	High	Medium	Medium
Current Sweep	V - I	Medium	Medium	No	Medium	Medium	Medium
Steepest Descent	V - I	Medium	Medium	Yes	High	Medium	Medium
One Cycle Control	I	Medium	Fast	No	High	Medium	Medium
Temperature Based	V - T	Medium	Medium	Yes	High	Medium	High
Pilot Cell	V	Medium	Fast	Yes	Low	Medium	High
Bisection Search Theorem	V - I	Medium	Medium	No	High	Medium	Medium
Analytical Solution	V - I	Medium	Medium	No	High	Medium	Low
Feedback Control	V - I	Medium	Medium	No	High	Medium	Medium
DC-Link Capacitor Droop	V - I	Medium	Medium	No	High	Medium	Medium
Linear Current Control	V - I	High	Fast	Yes	High	Medium	Medium
Variable Inductance	V - I	Medium	Medium	No	Medium	Medium	Medium
Curve Fitting	V - T	Low	Fast	Yes	Medium	Medium	Medium
Variable Step Size Incremental Resistance	V - I	Medium	Fast	No	High	Medium	Medium
Load Voltage and Load Current	V - I	Medium	Slow	No	Medium	Low	Low
Slide Control	V - I	Medium	Fast	No	High	Medium	Medium
State-Space	V - I	Medium	Medium	Yes	High	Medium	Medium
Parasitic Capacitance	V - I	Medium	Medium	No	Medium	Medium	Expensive

3. DESIGN STAGE OF PROPOSED SYSTEM

3.1. Design of Proposed PV System

A solar energy system using the proposed Perturb & Observe and Particle Swarm Optimization hybrid MPPT algorithm developed in this part of the thesis was created in the MATLAB/Simulink simulation program. The created system consists of solar panel array, DC-to-DC boost converter, DC-to-DC boost converter control circuit sections.

To summarize the working logic of the system, first of all, the voltage and current values produced from the solar panel array are measured. PV arrays are created by making certain numbers of series and parallel connections for a selected power level. Measurement values are monitored with the developed MPPT algorithm. With the MPPT algorithm, the reference voltage for the DC-to-DC boost converter control circuit is determined. Using the specified reference voltage and the voltage measured from the PV array, a switching signal is generated in the DC-to-DC boost converter control circuit. With this signal produced, the switching element on DC-to-DC boost converter is operated. The reference voltage that will produce the switching signal is taken from the output of the function block in MATLAB/Simulink. The determined MPPT Algorithms are prepared as MATLAB code in the MATLAB Function block.

In accordance with the operating logic of the DC-DC boost converter, the DC voltage generated in the PV array is increased using this switching signal. The block diagram of the applied PV system is as in Figure 3.1.

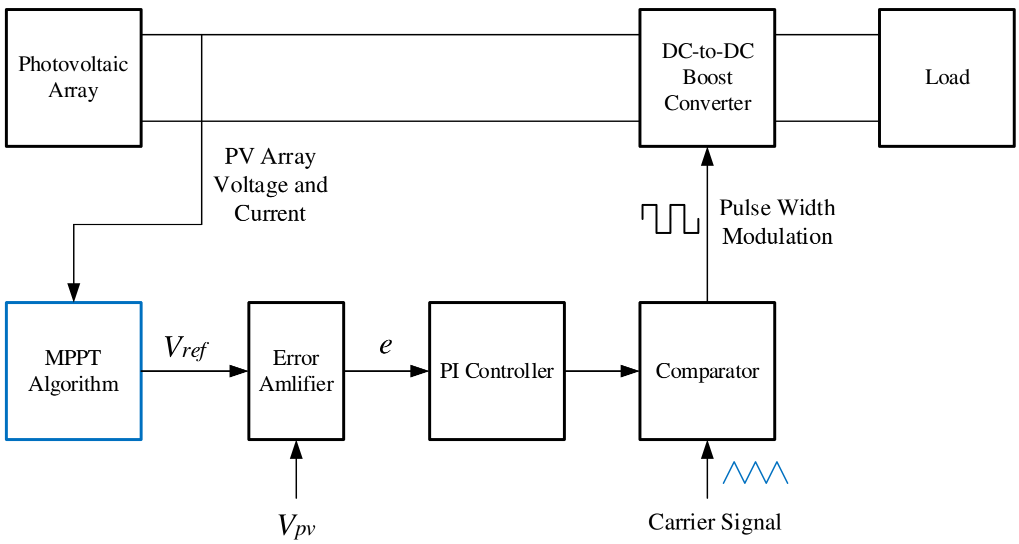

Figure 3.1. Representation of the designed PV System

3.2. Features of PV Array

In this thesis work, Helios Energy Europe 96M420 model PV panels were selected in the created system. The output power values of PV panels are 420 watts. The open circuit voltage of the selected PV panel is 60.55 V. The short circuit current of the panels is 9 A. MPP operating voltages are 49.53 volts. MPP operating currents are 8.48 Amps.

While creating arrays in the PV system, series and parallel connections were prepared. The number of serially connected PV panels in an array became 7 and the number of parallel connected PV arrays was 4. The total number of panels appears to be 28. Initially, the radiation value of each panel was entered as 1,000 W/m^2. 25 degrees Celsius was selected as temperature data. Table 3.1. Label information of the PV panel used is included.

Table 3.1. Label information of Helios Energy Europe 96M420 model PV panels

Features of PV Panel	**Values**
Power at STC	420 W
Power at PTC	375.5 W
Maximum Power (P_{max})	420.0144 W
Open Circuit Voltage (V_{OC})	60.55 V
Short Circuit Current (I_{SC})	9 A
Voltage at Maximum Power Point (V_{mpp})	49.53 V
Current at Maximum Power Point (Impp)	8.48 A
Temperature Coefficient of V_{OC}	-0.364 %/C°
Temperature Coefficient of I_{SC}	0.088 %/C°
Maximum Power Temperature Coefficient	-0.47 %/C°
Nominal Operating Cell Temperature	46.9 C°
Cell Type	Monocrystalline
Number of Cells	96
Maximum System Voltage	1,000 V
Length	1,980 mm
Width	1,300 mm
Module Area	2.57 m^2
Series Fuse Rating	15 A
Peak Efficiency	%16.23
Weight	31.3 kg

The following graphs showing the Power-Voltage and Current-Voltage characteristics of the PV panels used in the system are as shown in the Figure 3.2.

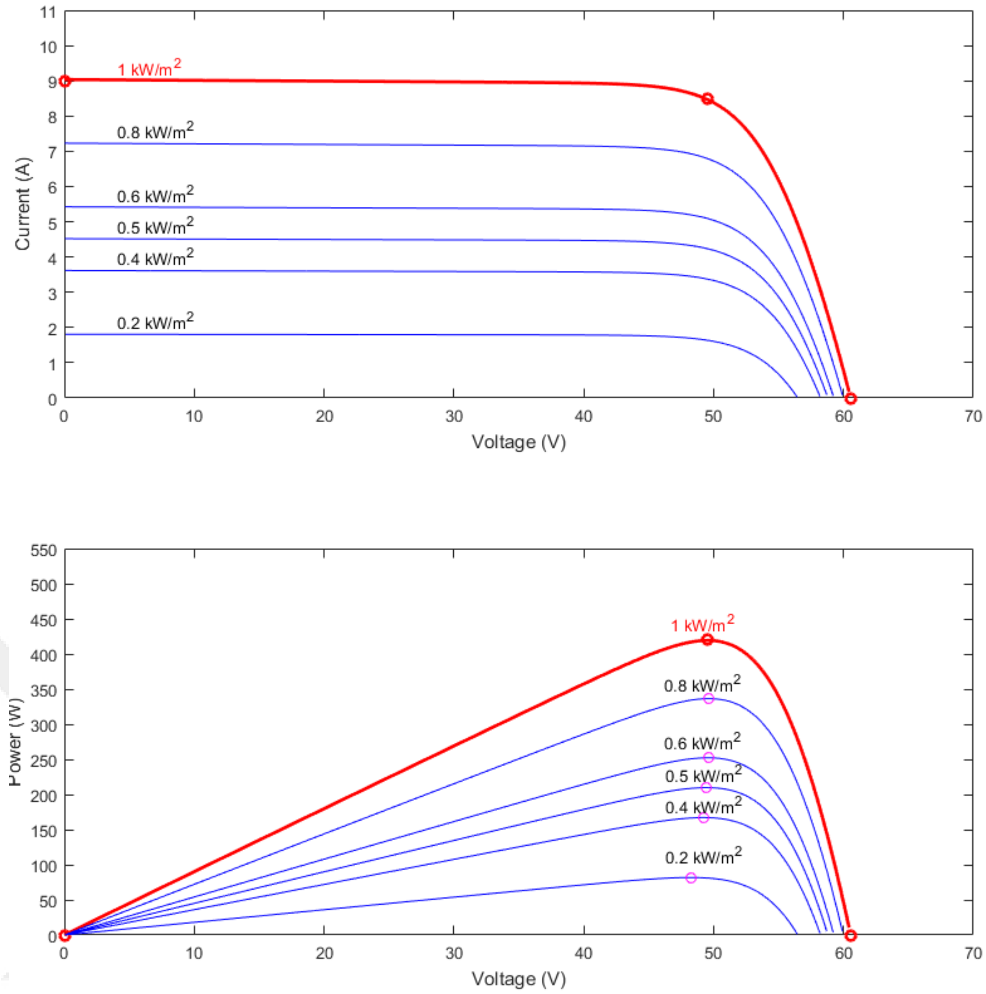

Figure 3.2. Power-Voltage and Current-Voltage characteristics of PV panels used in the system

The total DC output voltage of the system is given in the following Equation 3.1.

$$Total\ Output\ Voltage\ =$$
$$Number\ of\ Panels\ Connected\ in\ Series \times\ Panel\ Output\ Voltage$$

$$Vpv = 7\ \times 49.53\ V\ = 346.71\ V \qquad (3.1.)$$

The total DC output current of the system is shown below in Equation 3.2.

$$Total\ Output\ Current\ =$$
$$Number\ of\ Panels\ Connected\ in\ Parallel\ \times\ PV\ Panel\ Current$$

$$Ipv = 4 \times 8.48\ A = 33.92\ A \qquad (3.2.)$$

The total DC output power of the system is shown below in Equation 3.3.

$$Total\ Output\ Power\ =\ Number\ of\ Panels\ \times\ PV\ Panel\ Power$$

$$Ppv = 28\ \times 420.0144\ W = 11.760\ kW \tag{3.3.}$$

Table 3.2., which contains the information about the PV array in the designed PV system, is given below.

Table 3.2. Information about the PV array used in the designed system

Features of PV Array	
Maximum Output Power at STC	11,760.4032 W (P_{max})
Number of Series Connected Panels in a String	7 pieces
Number of Parallel Connected Strings	4 pieces
Total Number of Panels	28 pieces
Total Output Voltage	346.71 V (V_{MPP})
Total Output Current	33.92 A (I_{MPP})

3.3. Design of DC-to-DC Boost Converter

A DC-to-DC boost converter was used in the PV system created for simple, fast and reliable power transfer and voltage increase. The DC-to-DC boost converter has a structure consisting of five parts. These are inductor, capacitor, diode, switching element (usually IGBT) and output resistor. In this part of the system, the PV array is connected to the DC-to-DC boost converter through a parallel connected capacitor in the middle. This capacitor is used to correct the input voltage imbalance and reduce voltage fluctuations. The input capacitor value was selected as 1 mF. In this simulation, IGBT/Diode element is used for switching for DC-to-DC boost converter.

In this designed system, the PV Array output voltage was selected as 346.71 V. This value will be the input voltage of the DC-to-DC boost converter. The DC voltage will be increased with this converter and 540 V DC voltage will be obtained at the output. The switching frequency required for the switching element in the circuit was selected as 20 kHz. The parameters used in designing the DC-to-DC boost converter used in the system are shown in the equations below.

The Output Current of the converter is shown below in Equation 3.4.

$$Output\ Current\ = \frac{Pout}{Vout} = \frac{11.760{,}4032\ W}{540\ V} = 21.7785\ A \tag{3.4.}$$

The Load Resistor value of the converter is shown below in Equation 3.5.

$$Load\ Resistor\ Value\ = \frac{Vout}{Iout} = \frac{540\ V}{21.7785\ A}\ = 24.7951\ \Omega \tag{3.5.}$$

The Duty Cycle of the converter is shown below in Equation 3.6.

$$Duty\ Cycle\ = \left(1 - \frac{Vin}{Vout}\right) = \left(1 - \frac{346.71\ V}{540\ V}\right) = 0.3579\ = 35.79\% \tag{3.6.}$$

The Voltage Ripple of the converter is shown below in Equation 3.7.

$$Voltage\ Ripple = 0.01 * 540\ V\ = 5.4\ V \tag{3.7.}$$

The Current Ripple of the converter is shown below in Equation 3.8.

$$Current\ Ripple = 0.1 * 21.7785\ A\ = 2.1779\ A \tag{3.8.}$$

The Capacitor Value of the converter is shown below in Equation 3.9.

$$Capacitor\ Value = \frac{Iout \times \left(1 - \frac{Vin}{Vout}\right)}{fsw \times \Delta Vout} = \frac{21.7785\ A \times \left(1 - \frac{346.71\ V}{540\ V}\right)}{20\ kHz \times 5.4\ V} = 72.181\ \mu F \tag{3.9.}$$

The Inductor Current Ripple of the converter is shown below in Equation 3.10.

$$Inductor\ Current\ Ripple = \ \Delta IL\ = 0.01\ \times Iout\ \times \frac{Vout}{Vin} =$$

$$0.01\ \times 21.7785\ A\ \times \frac{540\ V}{346.71\ V} = 0.3392\ A \tag{3.10.}$$

The Inductor Value of the converter is shown below in Equation 3.11.

$$Inductor\ Value = \frac{Vin \times (Vout - Vin)}{fsw \times \Delta IL \times Vout} = \frac{346.71\ V \times (540\ V - 346.71\ V)}{20\ kHz \times\ 0.3392\ A \times 540\ V} = 0.0183\ H \tag{3.11.}$$

Table 3.3. shows the parameter values of the DC-to-DC boost converter.

Table 3.3. Parameters of DC-to-DC Boost Converter

Parameters	
Input Voltage	346.71 V
Output Voltage	540 V
Input Current	33.92 A
Output Current	21.7785 A
Voltage Ripple	5.4 V
Current Ripple	2.1779 A
Inductor Value	0.0183 H
Capacitor Value	72.181 µF
Load Resistor Value	24.7951 Ω
Inductor Current Ripple	0.3392 A
Switching Frequency	20 kHz

Figure 3.3 shows the DC-to-DC boost converter used in the designed circuit.

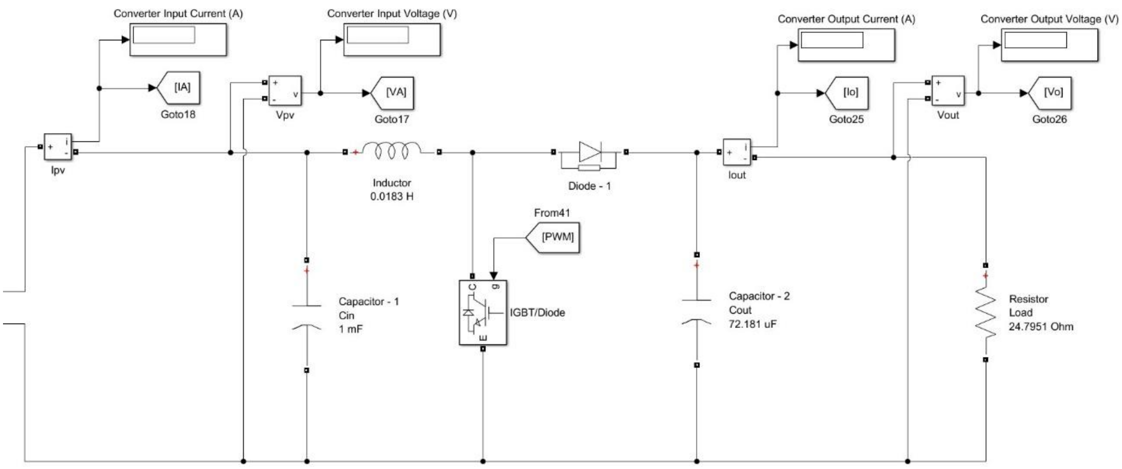

Figure 3.3. DC-to-DC boost converter used in the designed circuit

As the operating logic of the control circuit of the DC-to-DC boost converter, firstly the switching element receives the reference voltage coming from the MATLAB function block that runs the MPPT algorithm. Then an error is generated from this reference voltage with the measured voltage of the PV array. This error reaches the PI controller. The signal from the PI controller output is compared with the 20 kHz triangle wave. As a result, the PWM signal that will trigger the switching element is generated. Figure 3.4. shows the example DC-to-DC boost converter control circuit.

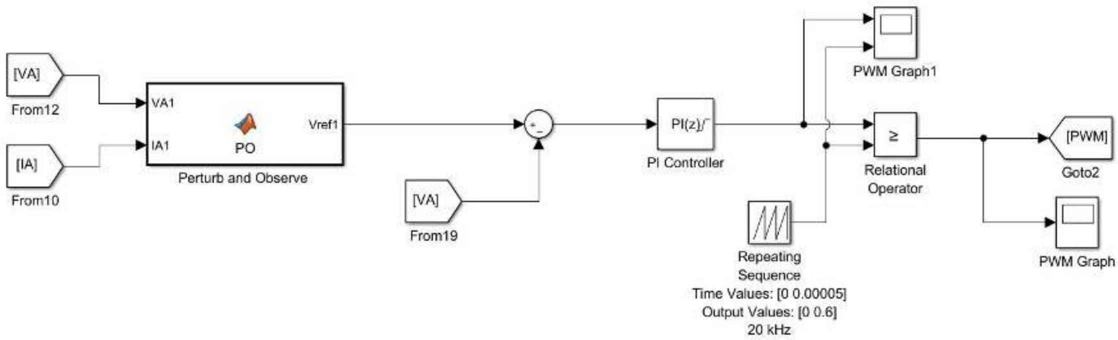

Figure 3.4. Example control circuit of DC-to-DC boost converter circuit

3.4. Design of Proposed MPPT Algorithms

In this section of the thesis, MPPT algorithms determined for the PV system were created using function blocks in the MATLAB/Simulink environment. Each function block contains the MATLAB code containing the relevant algorithm. The created MPPT algorithms are hybrid in structure and are created by combining more than one MPPT algorithm. In these function blocks, MPP tracking is done and Vref, which is the reference voltage at the outputs, is produced. The reference voltages generated here will then be sent to the DC-to-DC boost converter control circuit.

Summary, the current and voltage values of the PV array were measured in this structure. The measured values were processed with the MPPT algorithm and a reference voltage was produced as a result. This reference signal was used for the DC-to-DC boost converter. The block diagram of the created example algorithm block is shown in Figure 3.5.

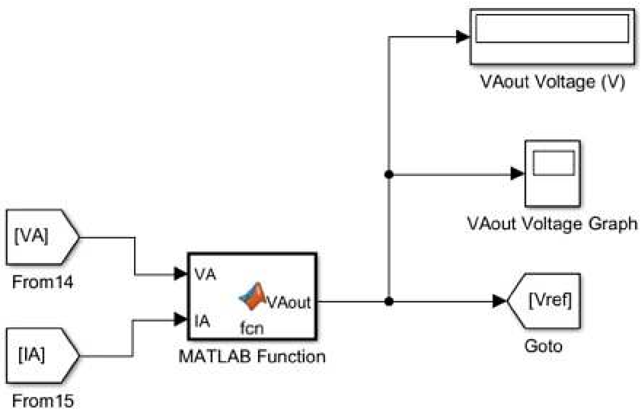

Figure 3.5. Block Diagram of example MPPT method

3.4.1. Design of Perturb & Observe MPPT Algorithm

Perturb & Observe MPPT algorithm is a traditional online MPPT algorithm. It is one of the most studied and implemented MPPT methods due to its simple structure and low cost. This algorithm is mentioned in detail in section 2.4.1. If the working logic of the algorithm is briefly summarized, power is calculated using the voltage and current values measured from the PV array.

Power and voltage values are compared with the previous power and voltage values. Duty cycle or reference voltage value is adjusted according to the direction of decrease or increase of power and voltage. In this prepared structure, a MATLAB code containing Perturb & Observe algorithm is prepared in MATLAB function block.

In this study, the reference voltage value is adjusted. For this reason, a PI controller was needed first to generate the PWM signal. After the PI controller, the PWM signal was generated and DC-to-DC boost converter switching was performed. In the PWM generation stage, a carrier signal with a peak value of 0.6 and a frequency of 20 kHz was used. The structure of Perturb & Observe MPPT algorithm created in MATLAB/Simulink is shown in Figure 3.6.

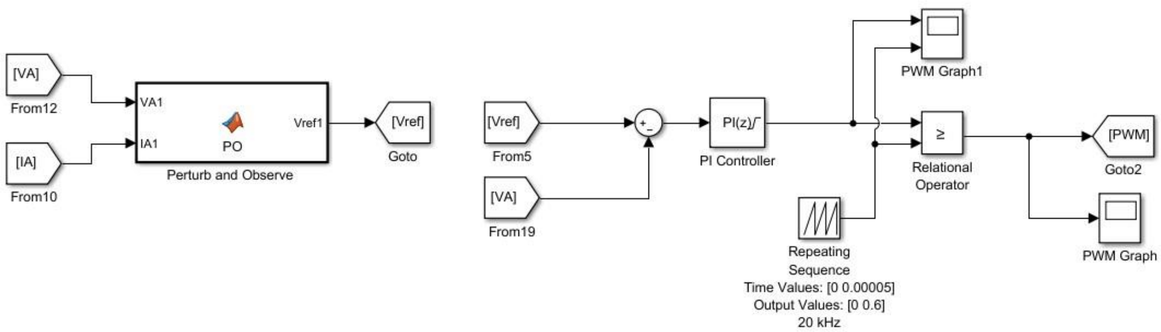

Figure 3.6. Implementation of Perturb & Observe MPPT algorithm in MATLAB/Simulink

3.4.2. Design of Kalman Filter and Perturb & Observe Hybrid MPPT Algorithm

This algorithm is created by combining the Kalman Filter and the Perturb & Observe MPPT algorithm. An efficient hybrid method is created by combining the good aspects of both algorithms. The Kalman filter is used to make an accurate estimate in cases of uncertainty or noise. It is a mathematical algorithm in structure and corrects faulty situations in systems. The Kalman Filter examines the previous system state and estimates the next states. It consists of two stages; the first stage is the estimation stage. The second stage is the update section.

In this structure, a MATLAB code containing the Kalman Filter and P&O algorithm is prepared in the MATLAB function block. In this hybrid algorithm, the voltage and current measurements of the PV array are first performed. The power value is calculated using these measurements. In the first stage, the Perturb & Observe method starts the algorithm with the first step. The Perturb & Observe algorithm compares the previous states of the power and voltage values and adjusts the reference voltage. In the second step, the Kalman filter immediately comes into play and monitors the state of the first system. It starts to estimate the next power by accepting the power value as the previous power value. These algorithms work one after the other in order to perform an efficient MPP tracking. In this study, the reference voltage value is also produced. The PI controller was again necessary for this circuit. In the same way, the PWM signal was produced and the DC-to-DC boost converter switching was done. In the PWM production stage, a carrier signal with a peak value of 0.6 and a frequency of 20 kHz was also used. The structure of Kalman Filter and Perturb & Observe Hybrid MPPT algorithm created in MATLAB/Simulink is shown in Figure 3.7.

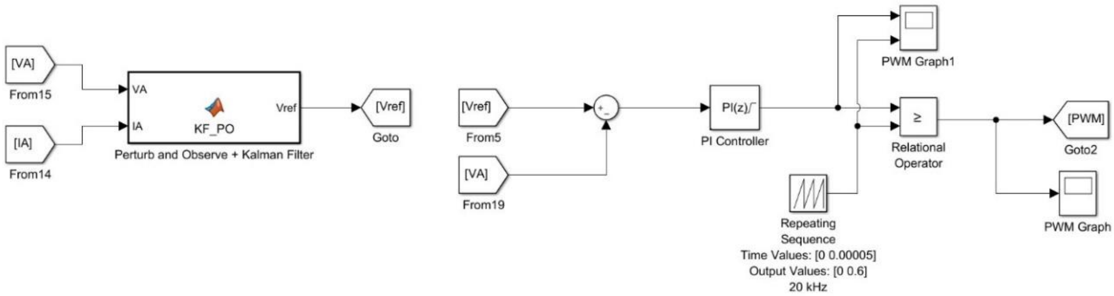

Figure 3.7. Implementation of Kalman Filter and Perturb & Observe Hybrid MPPT algorithm in MATLAB/Simulink

3.4.3. Proposed Algorithm: Design of Perturb & Observe and Particle Swarm Optimization Hybrid MPPT Algorithm

This algorithm is created by combining Perturb & Observe and Particle Swarms Optimization MPPT algorithms. A good hybrid method has been created by using the advantageous aspects of both algorithms. The PSO algorithm is a method created by taking the swarm behaviour of living beings in nature as an example. In this algorithm, a cluster of particles is created. Particles move in the solution space. These particles, which are constantly moving, search for the best solution. In this algorithm, the initial positions are determined randomly. Each particle has speed and position information. Position information also represents a solution. Moving particles make their next moves according to their distance and position to the appropriate value. Speed and positions are constantly updated in the algorithm. The algorithm has various parameters and the algorithm can gain different advantages according to the values of these parameters. As a result, the algorithm continues to do its job until it finds the best solution. In this algorithm, a MATLAB code containing the Perturb & Observe algorithm and the PSO algorithm is prepared in the MATLAB function block. First, voltage and current information are obtained from the PV array. The power value is calculated using these measurements. The Perturb & Observe method starts the algorithm as the first stage. The Perturb & Observe algorithm compares the previous states of the power and voltage information and produces the reference voltage. The generated reference voltage enters the PSO algorithm. Here, the best solution is tried again. Finally, the PSO algorithm produces a suitable reference voltage. These algorithms will work continuously one after the other in order to follow the MPP. In this circuit, like the others, a PI controller is used. The PWM signal is generated in the control circuit and the DC-DC boost converter is switched. The peak value of the carrier signal is selected as 0.6 and its frequency is 20 kHz. The structure of Perturb & Observe and Particle Swarm Optimization Hybrid MPPT algorithm created in MATLAB/Simulink is shown in Figure 3.8.

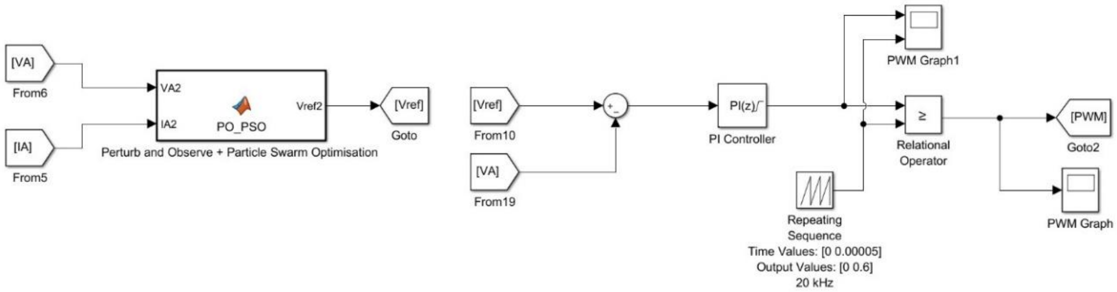

Figure 3.8. Implementation of Perturb & Observe and Particle Swarm Optimization Hybrid MPPT algorithm in MATLAB/Simulink

Figure 3.9. shows the flowchart of the applied P&O and PSO Hybrid MPPT method.

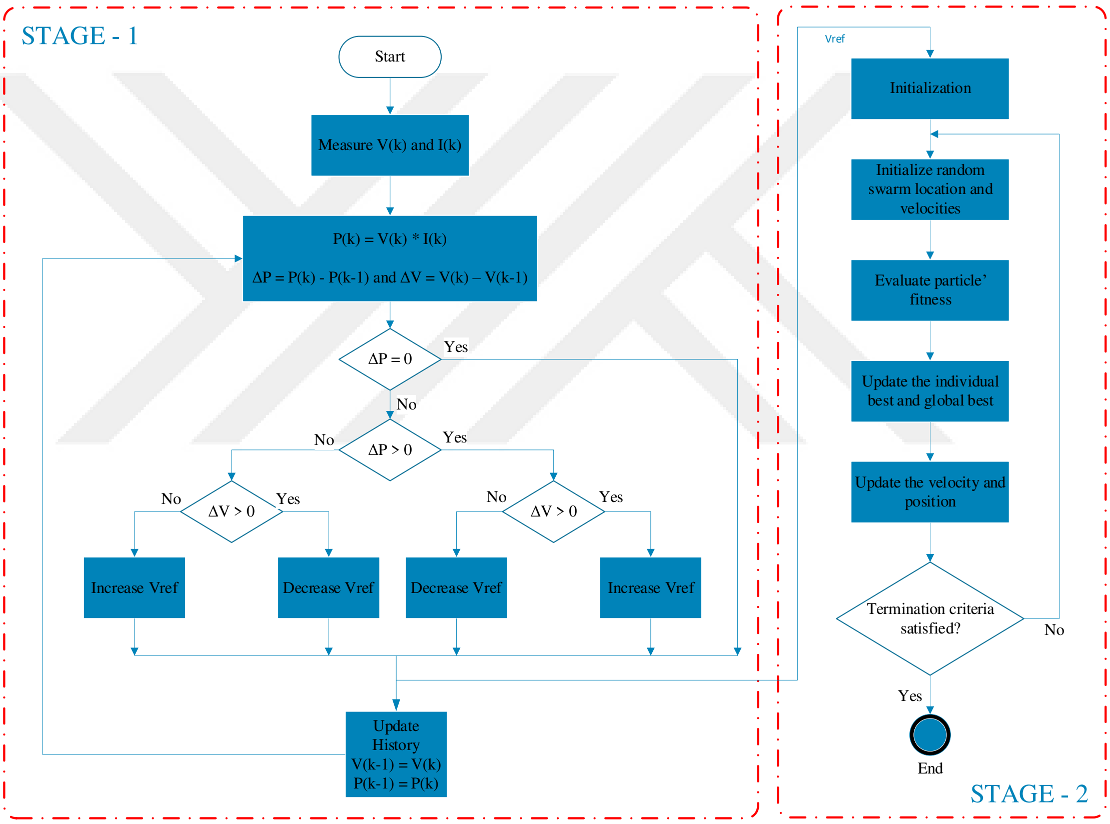

Figure 3.9. Proposed Flowchart of Perturb & Observe and Particle Swarm Optimization Hybrid MPPT

4. CASE ANALYSIS AND SIMULATION RESULTS

In this section, simulations including the MPPT algorithms and the proposed hybrid MPPT method were tested under specified conditions and the results were examined. In all simulations created, the values of other design elements except the MATLAB/Simulink function were the same. Only the MPPT algorithm block used was different. A signal generator was used in MATLAB/Simulink as the radiation source in the simulated PV systems. Simulations including the algorithms mentioned in Section 3 were tested under conditions where 1000 W/m^2, 800 W/m^2, 600 W/m^2, 500 W/m^2 and 900 W/m^2 irradiation values were given. The responses of the algorithms created with this study and the proposed hybrid MPPT method were observed under fixed and variable irradiation conditions. Then, the results were interpreted and the simulation results were compared with the proposed method.

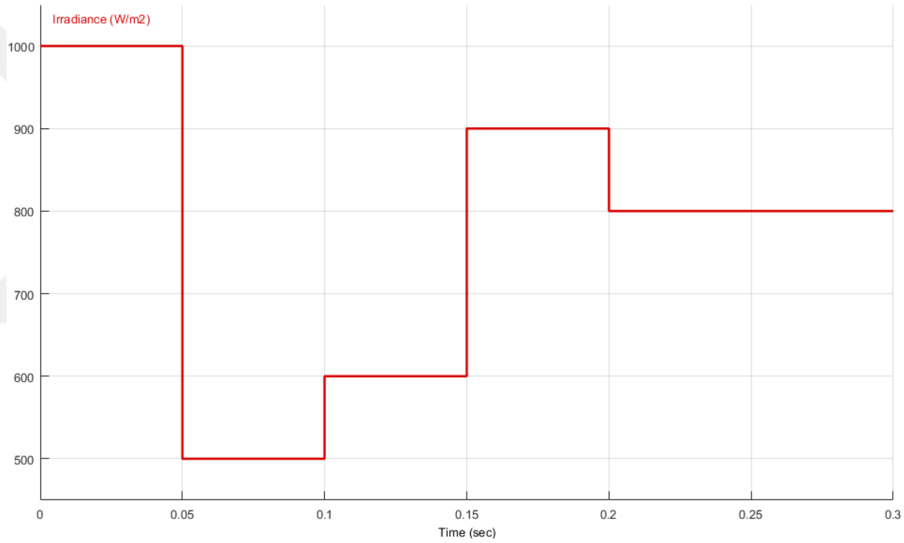

Figure 4.1. Signal graph of the signal generator that produces the irradiation

4.1. Operating Scenario of the Overall System without using an MPPT Controller

This study scenario does not include any MPPT controller, unlike the PV system introduced in Chapter 3. The switching signal of the DC-to-DC boost converter in the system is given directly from the PWM generator. The duty cycle ratio is constant throughout the simulation. The irradiation data from the signal generator seen in Figure 4.1 is given to the system.

The following figures show the PV Array output voltage, current and power. Then, the converter output voltage, current and power graphs are given. PV array output voltage graph for the system without MPPT method under changing irradiation conditions can be seen in Figure 4.2.

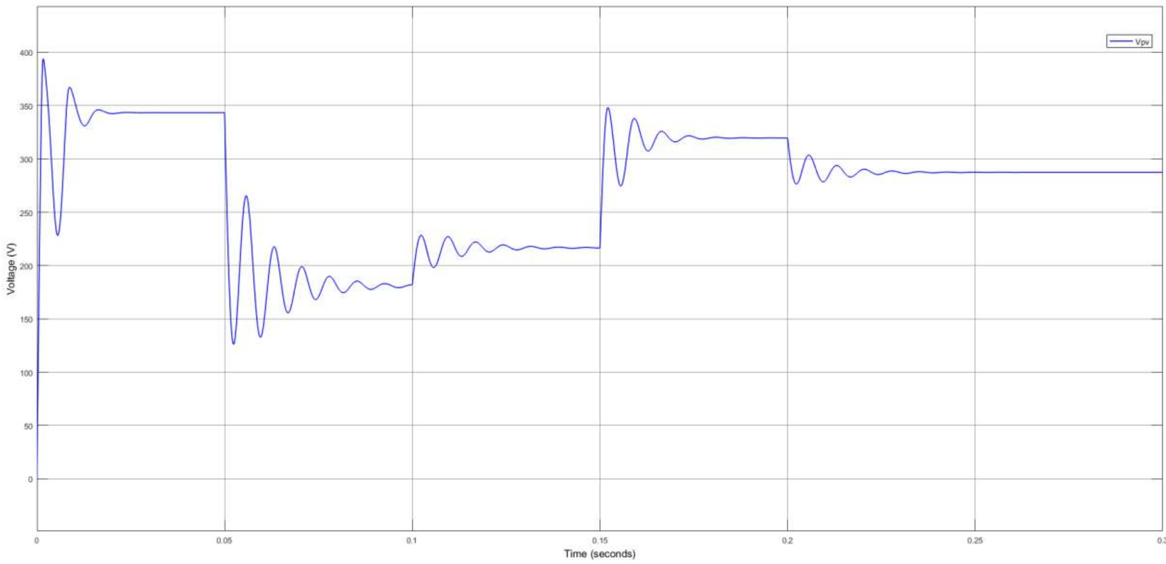

Figure 4.2. PV array output voltage graph for the system without MPPT method under changing irradiation conditions

Figure 4.3 shows the output voltage graph of the converter. Fluctuations appear as distinct dark areas at the boost converter output.

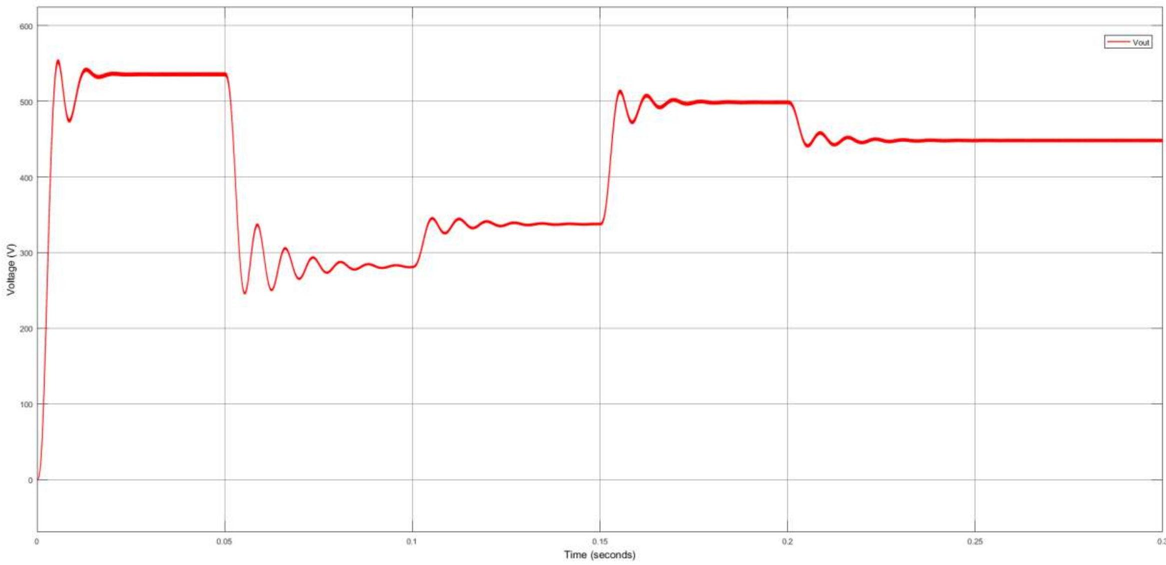

Figure 4.3. Converter output voltage graph for the system without MPPT method under changing irradiation conditions

The PV array output current graph is shown in Figure 4.4.

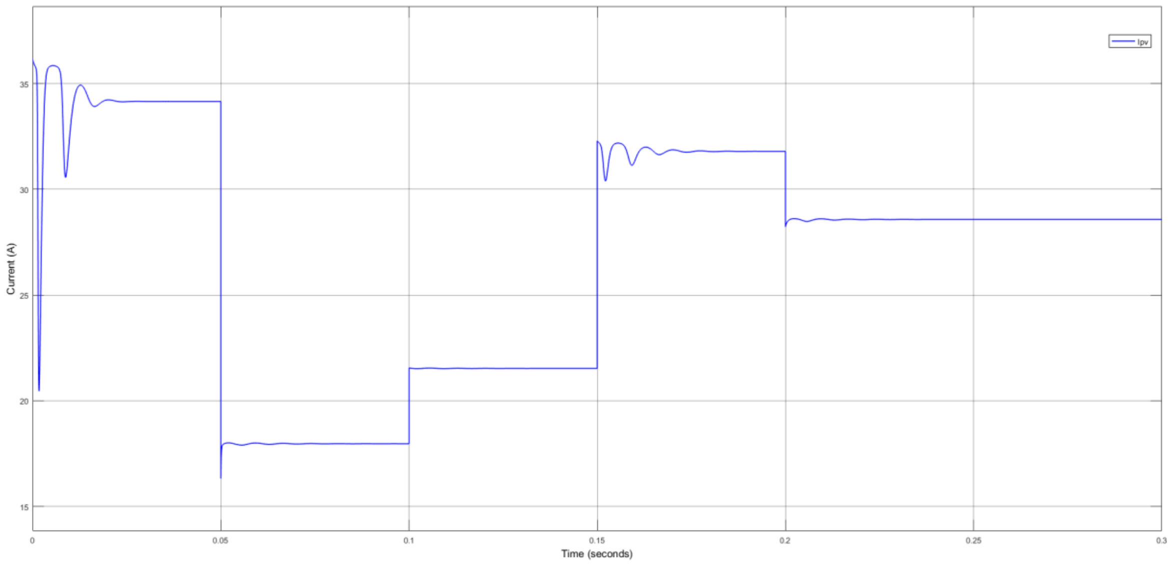

Figure 4.4. PV array output current graph for the system without MPPT method under changing irradiation conditions

Converter Output current graph is shown in Figure 4.5.

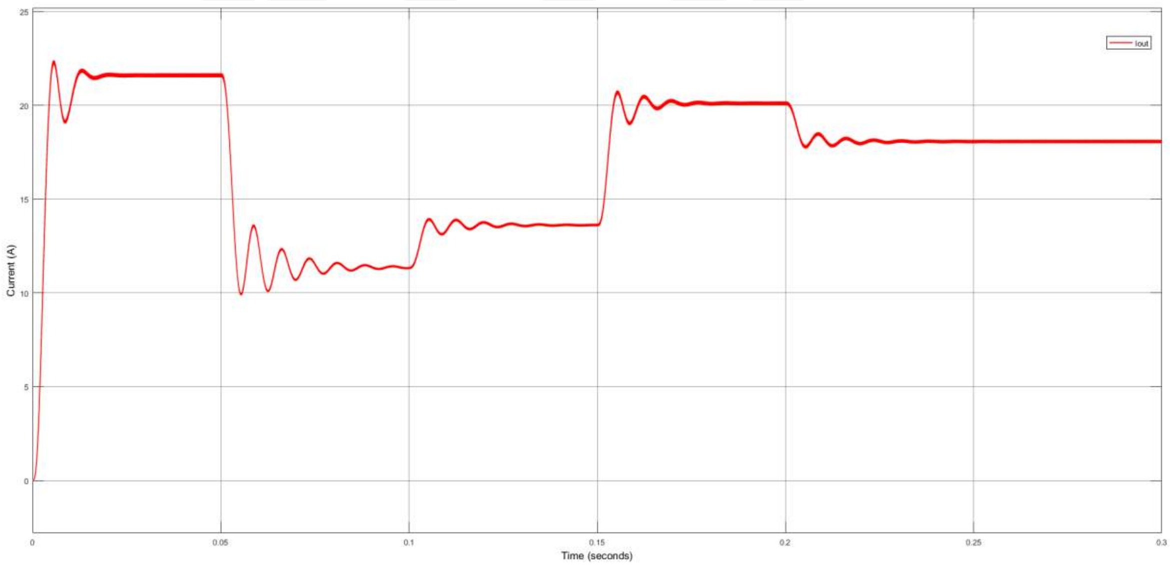

Figure 4.5. Converter output current graph for the system without MPPT method under changing irradiation conditions

Distortions in the converter output current graph, especially at times of irradiation change, can be clearly detected in PV array output current graph.

PV array output power graph as illustrated Figure 4.6.

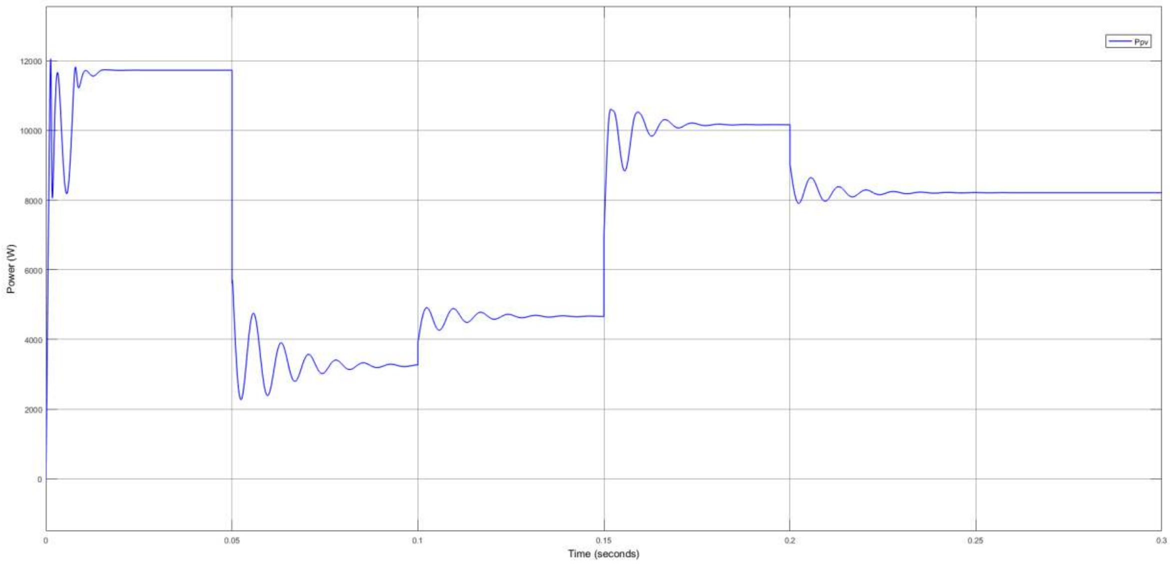

Figure 4.6. PV array output power graph for the system without MPPT method under changing irradiation conditions

The output power graph of the converter is drawn in Figure 4.7.

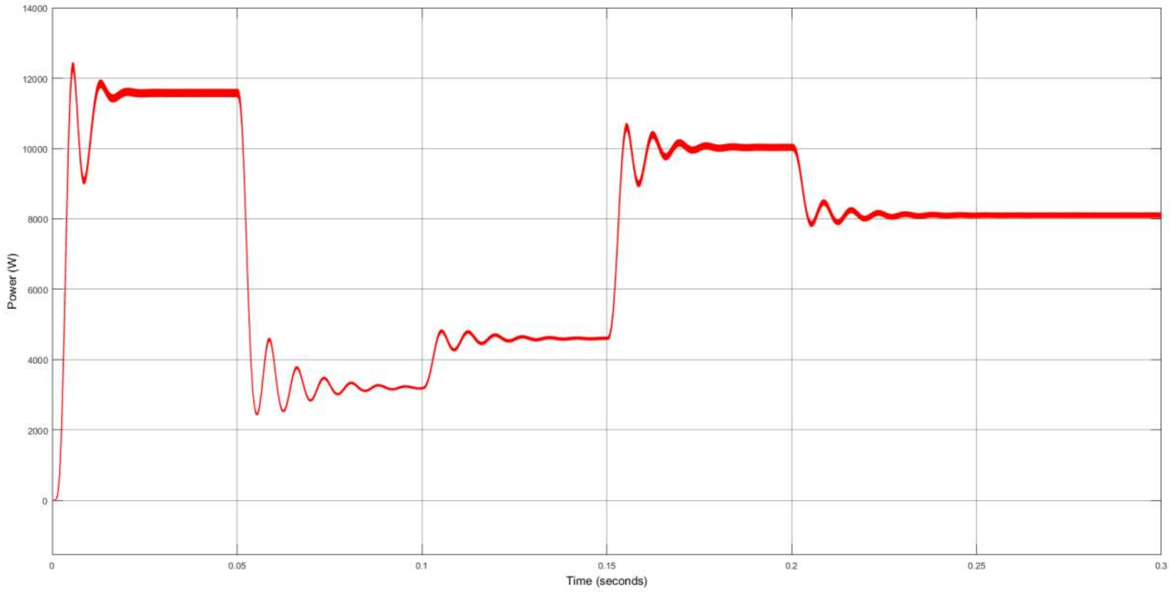

Figure 4.7. Converter output power graph for the system without MPPT method under changing irradiation conditions

When the graphs are examined, it is seen that in every case where the radiation is irregular and changes, the graphs are also distorted in the same way. There is an excessive oscillation in the voltage, current and power values. This shows that the power loss is high.

4.2. Operating Scenario of the Overall System: Perturb & Observe MPPT Algorithm

In this section, the MATLAB/Simulink function block containing the Perturb and Observe Algorithm was run. The algorithm that generates the reference signal passed through the PI controller and comparator to produce the PWM signal. A successful MPPT tracking was performed by switching. The PV array voltage, PV array current and PV array power were examined. In addition, the PV array voltage was compared with the Reference voltage produced in the Perturb & Observe algorithm. It was seen that the reference voltage followed the PV array voltage. The advantageous aspects of this method can be seen for fast needs.

In Figure 4.8, the PV array output voltage graph of the system using the Perturb & Observe MPPT algorithm under varying irradiation conditions can be seen.

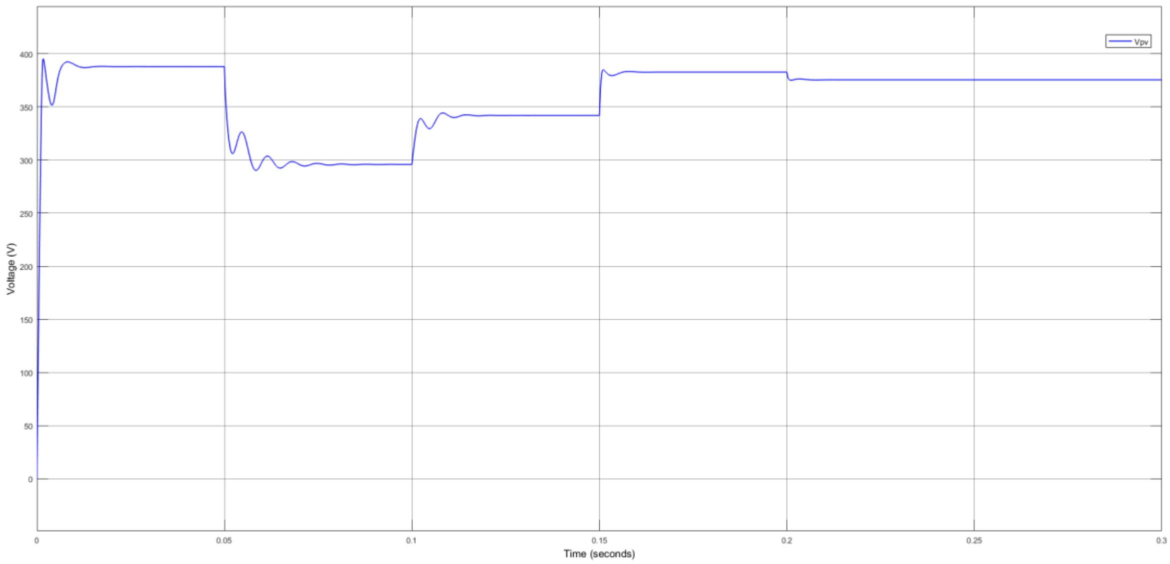

Figure 4.8. PV array output voltage graph for P&O MPPT method under changing irradiation conditions

If Figure 4.8 is examined, the voltage ripple has decreased compared to the simulation case without MPPT.

The output voltage of the converter circuit used is illustrated in Figure 4.9. Converter Output voltage also reaches stable position faster.

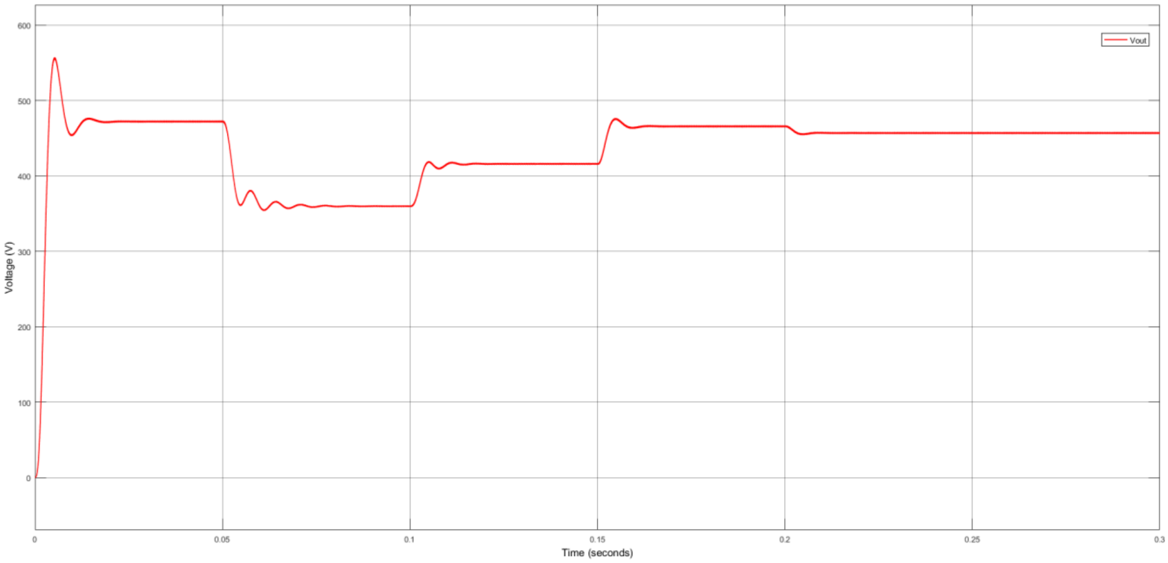

Figure 4.9. Converter output voltage graph for P&O MPPT method under changing irradiation conditions

Figure 4.10. shows the output current of the PV array. Although instantaneous peaks are seen in the power changes in the Converter Output current graph, the signal reaches stable positions very quickly.

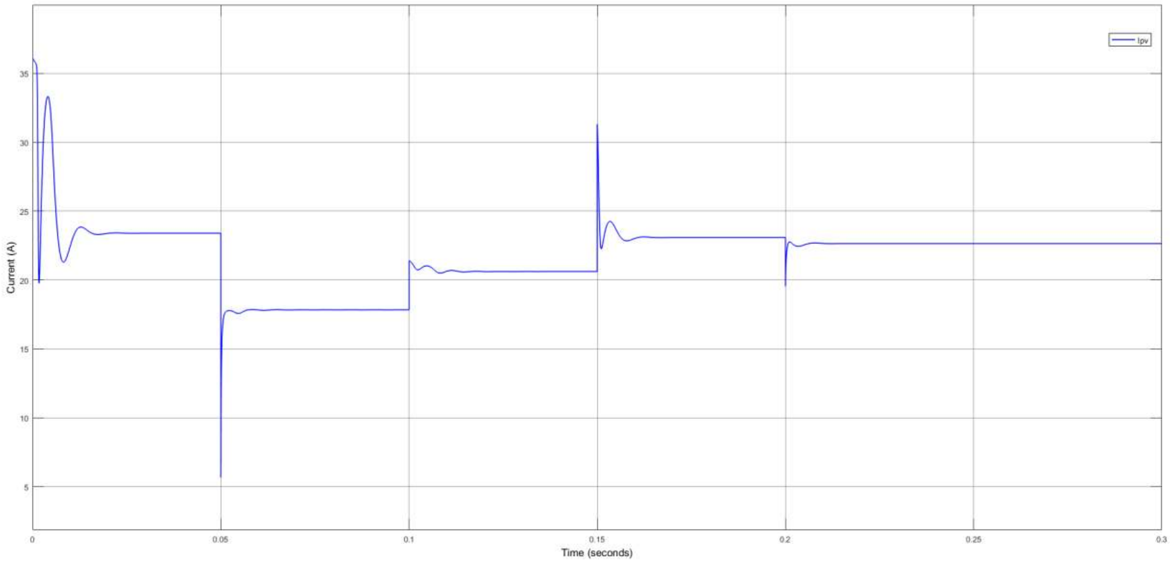

Figure 4.10. PV array output current graph for P&O MPPT method under changing irradiation conditions

The converter output current graph for the Perturb & Observe MPPT method under varying irradiation conditions is shown in Figure 4.11.

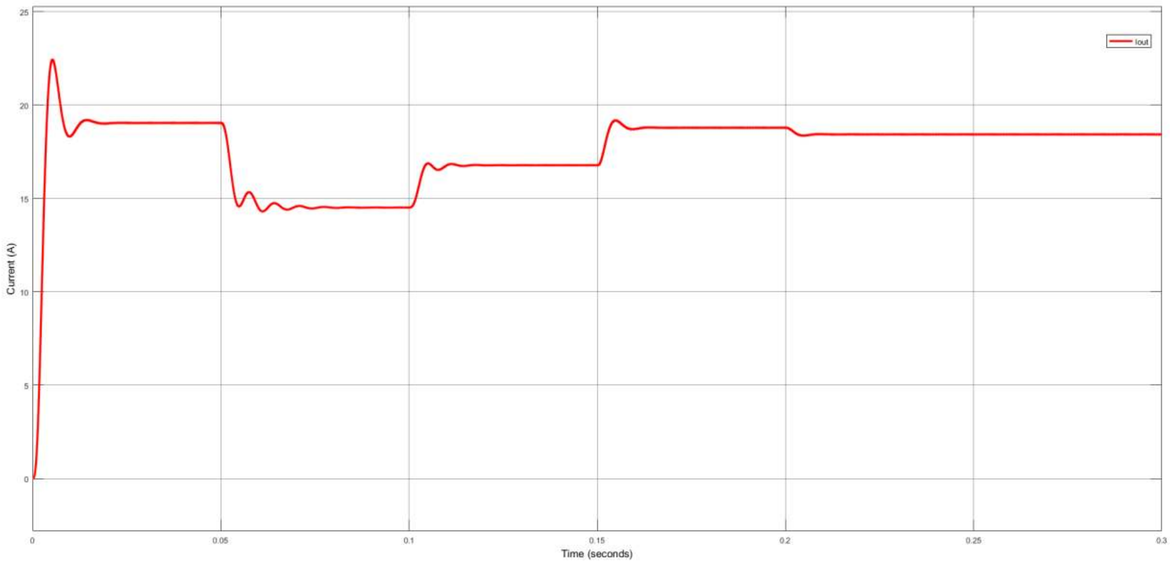

Figure 4.11. Converter output current graph for P&O MPPT method under changing irradiation conditions

If the converter output current graph is examined, there are smoother transitions compared to the non-MPPT method.

PV array output power graph is illustrated in Figure 4.12.

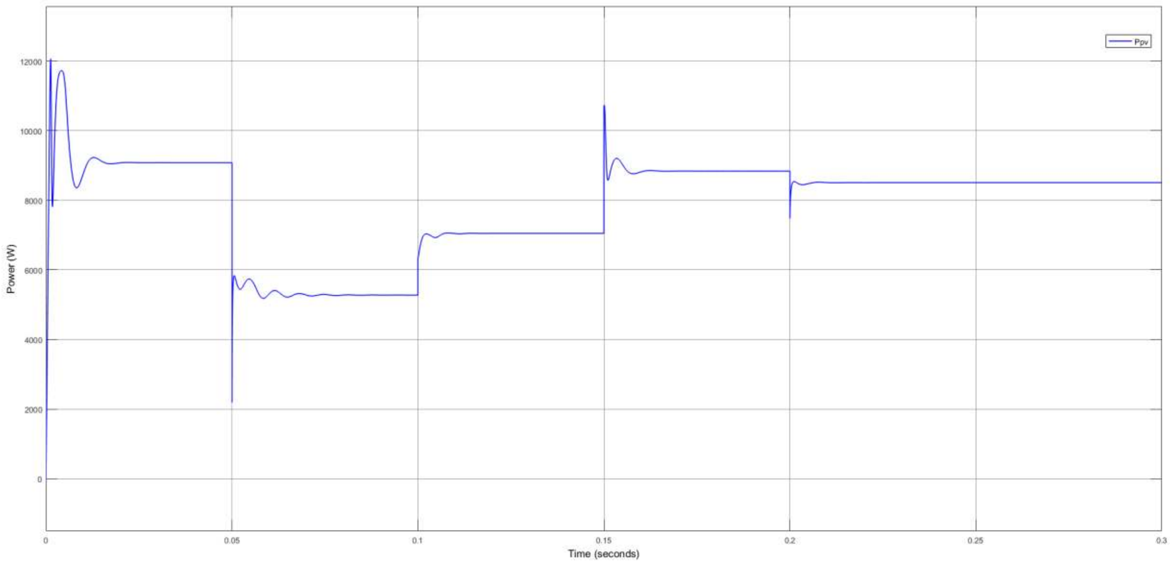

Figure 4.12. PV array output power graph for P&O MPPT method under changing irradiation conditions

The converter output power graph is shown in Figure 4.13 below.

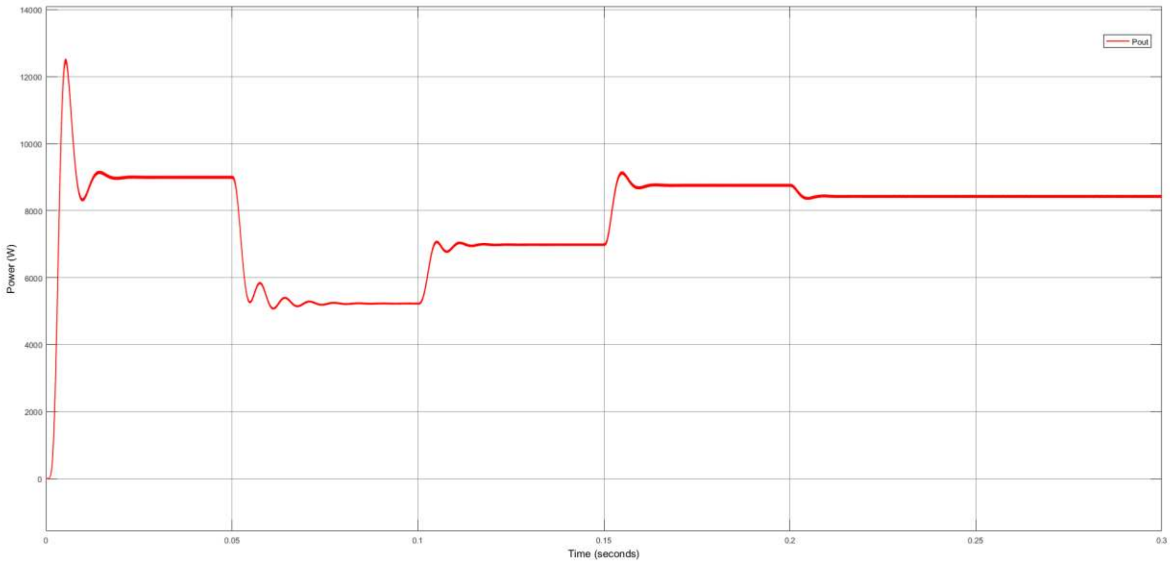

Figure 4.13. Converter output power graph for P&O MPPT method under changing irradiation conditions

If the Converter Power graph is examined, the fluctuation is very little compared to the simulation case without the MPPT algorithm.

PV array output voltage and reference voltage graphs for the Perturb & Observe MPPT method under varying irradiation conditions are shown in Figure 4.14.

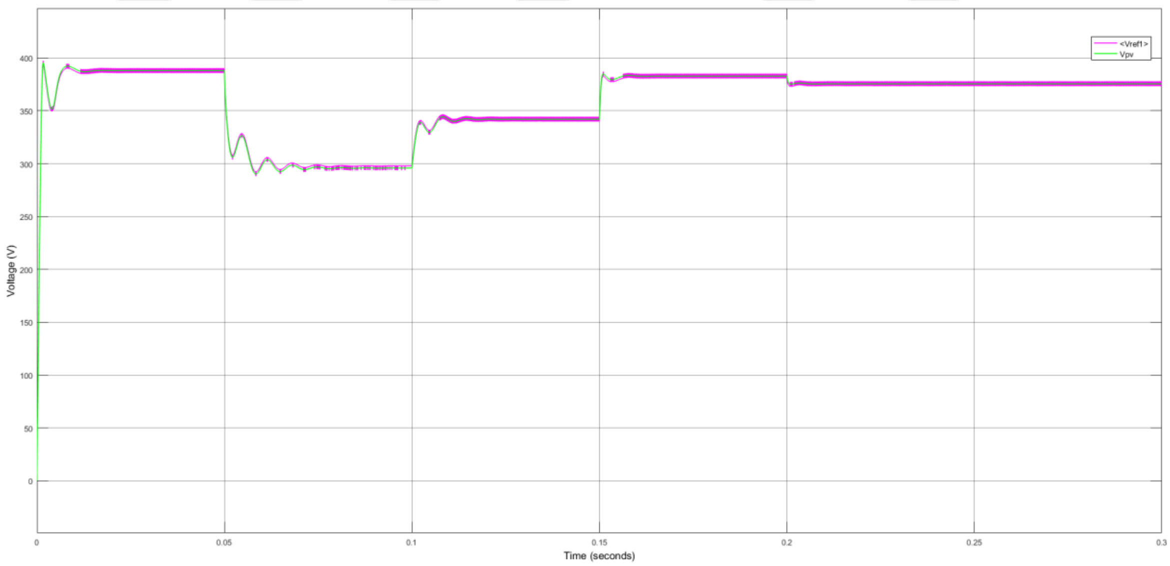

Figure 4.14. PV array output voltage and reference voltage graphs for P&O MPPT method under changing irradiation conditions

The green colour represents the PV array voltage and the purple colour represents the reference voltage generated in the Perturb & Observe Algorithm. It is understood from these graphs that MPPT tracking is done.

The PV array output voltage and reference voltage graphs for the Perturb & Observe MPPT method at the changing irradiation stage are shown in close perspective in Figure 4.15.

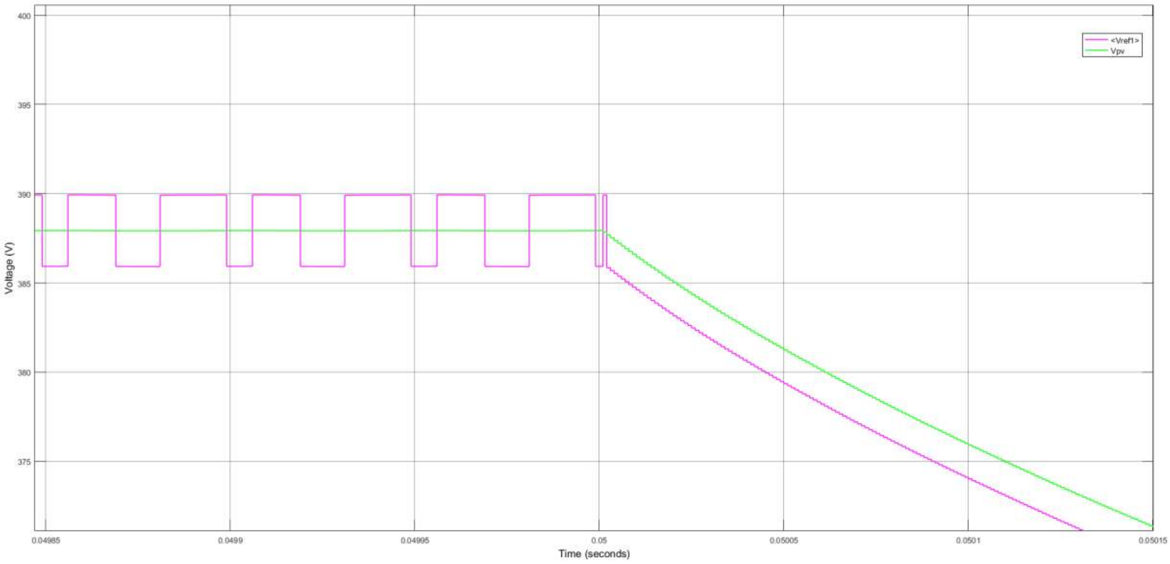

Figure 4.15. PV array output voltage and reference voltage graphs for P&O MPPT method in changing irradiation stage

In this scenario, the MPPT algorithm successfully followed the MPP. Compared to the previous simulation case where the MPPT controller was not used, more stable signals are formed during irradiation changes.

4.3. Operating Scenario of the Overall System: Kalman Filter and Perturb & Observe Hybrid MPPT Algorithm

In this simulation case, a hybrid algorithm where Perturb & Observe and Kalman Filter are created together has been tested. PWM signal was generated using the reference voltage generated by the algorithm. Boost converter was successfully operated and MPP point was attempted to be reached. Simulation graphics were examined and voltage, current, power and reference signal comparisons were made for PV array and DC-to-DC boost converter. Since Kalman Filter is only a mathematical operation, it will be useful to combine it with Perturb and Observe method in a hybrid structure as a low-cost solution.

The PV array output voltage graph for KF and Perturb & Observe Hybrid MPPT method under varying solar conditions is shown in Figure 4.16.

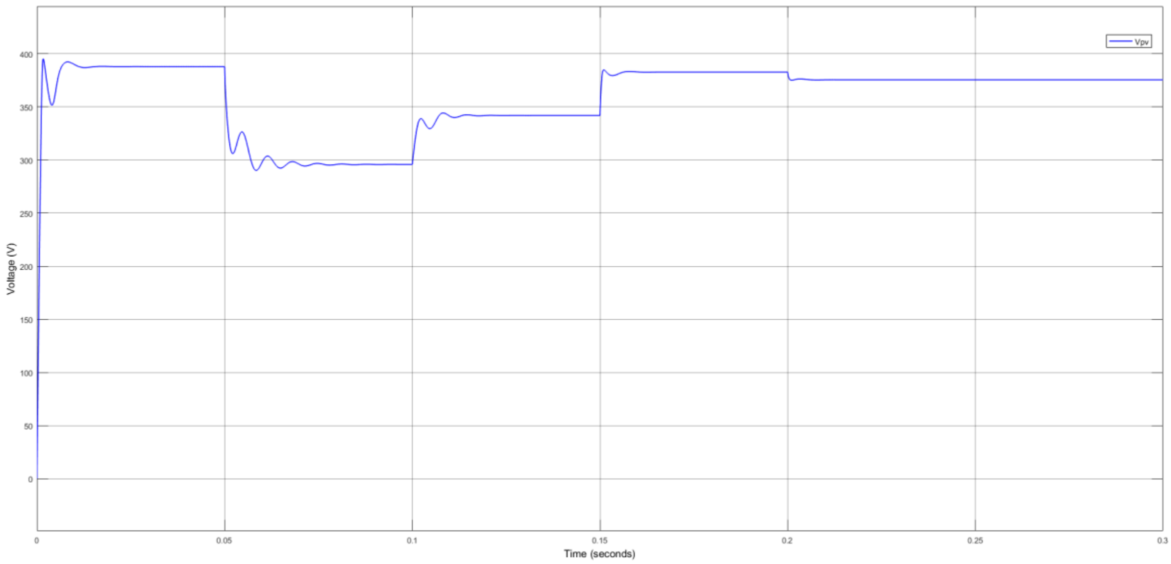

Figure 4.16. PV array output voltage graph for KF and P&O Hybrid MPPT method under changing irradiation conditions

The converter output voltage graph is shown in Figure 4.17.

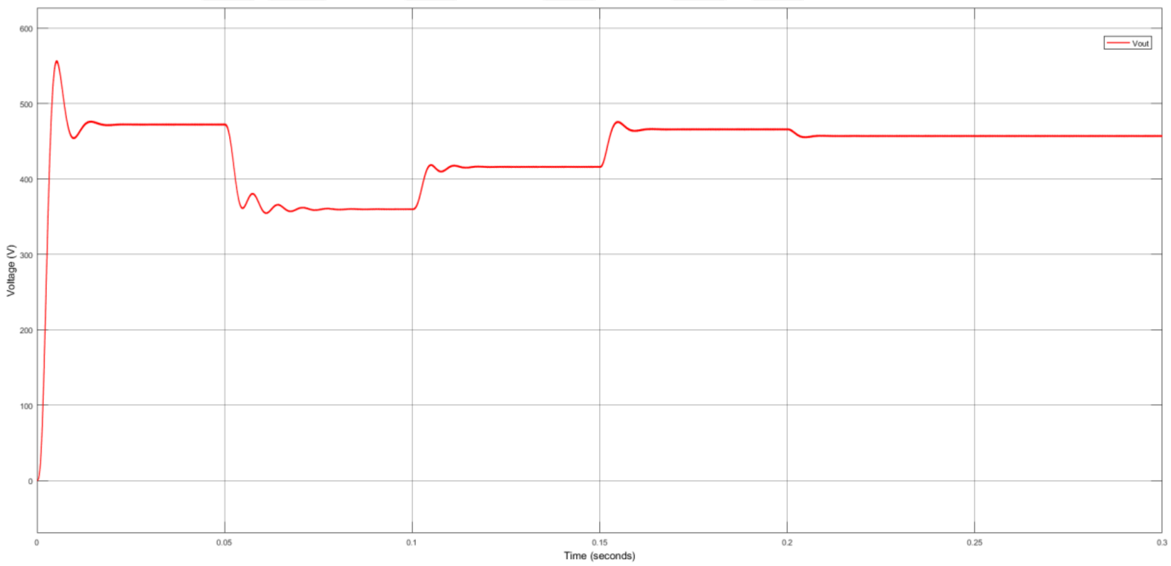

Figure 4.17. Converter output voltage graph for KF and P&O Hybrid MPPT method under changing irradiation conditions

The PV array output current graph for the KF and P&O Hybrid MPPT method under varying irradiation conditions is given in Figure 4.18.

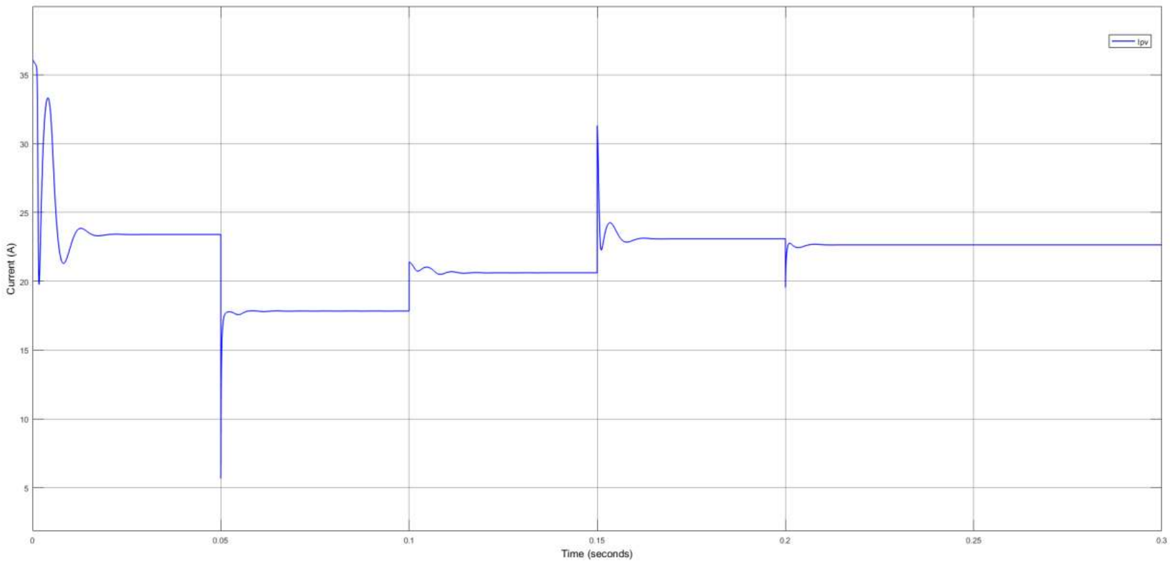

Figure 4.18. PV array output current graph for KF and P&O Hybrid MPPT method under changing irradiation conditions

The Boost Converter output current graph is as shown in Figure 4.19.

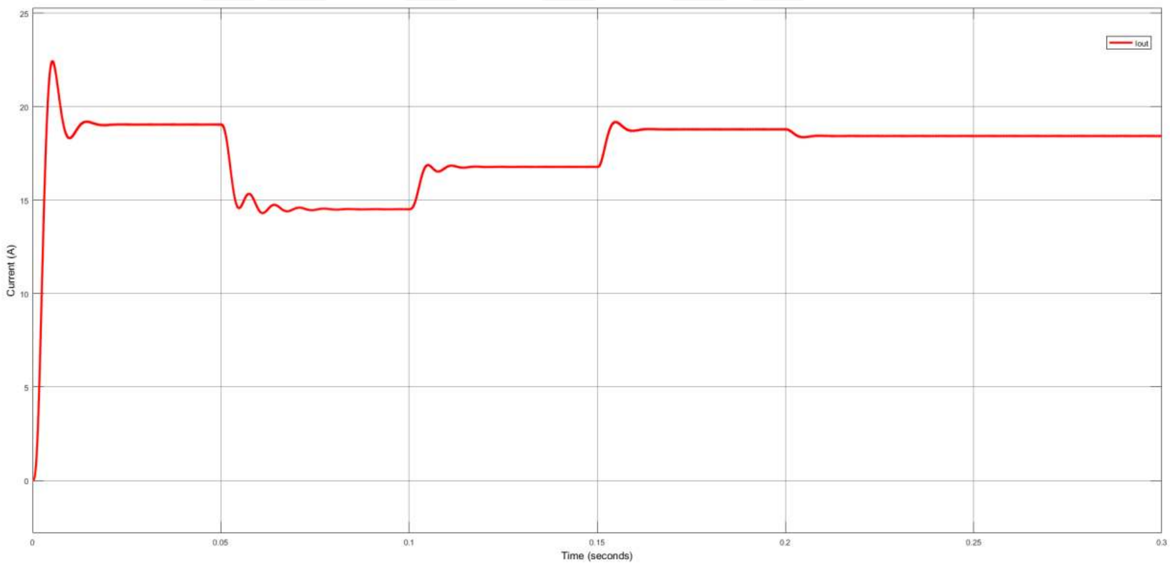

Figure 4.19. Converter output current graph for KF and P&O Hybrid MPPT method under changing irradiation conditions

The graph shown in Figure 4.20 is the PV array output power graph for the KF and P&O Hybrid MPPT method under varying irradiation conditions.

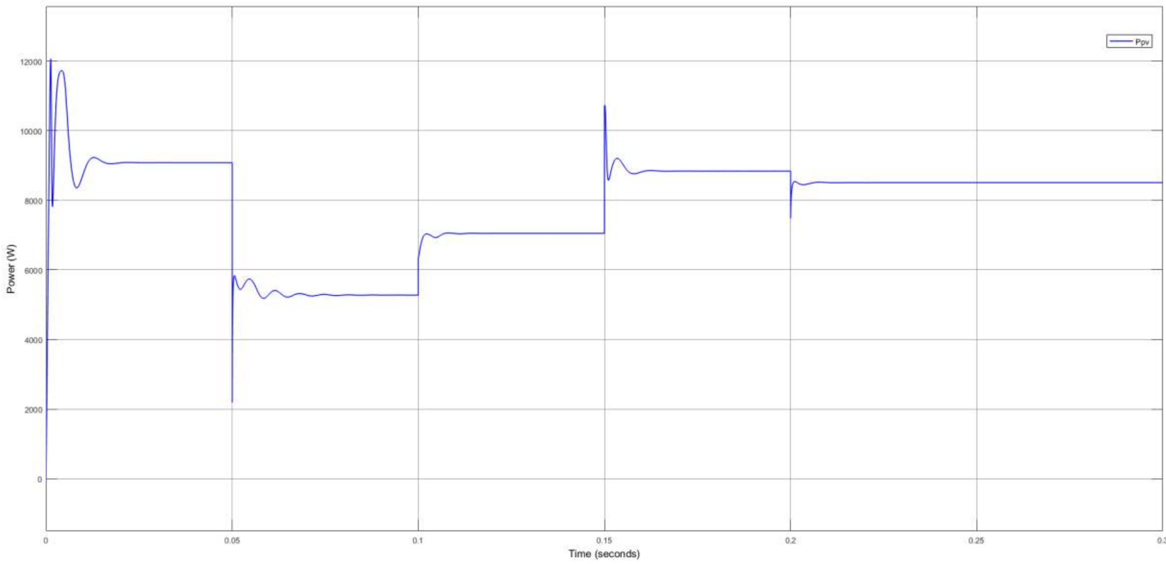

Figure 4.20. PV array output power graph for KF and P&O Hybrid MPPT method under changing irradiation conditions

The converter output power graph for the Kalman Filter and Perturb & Observe Hybrid MPPT method is illustrated in Figure 4.21.

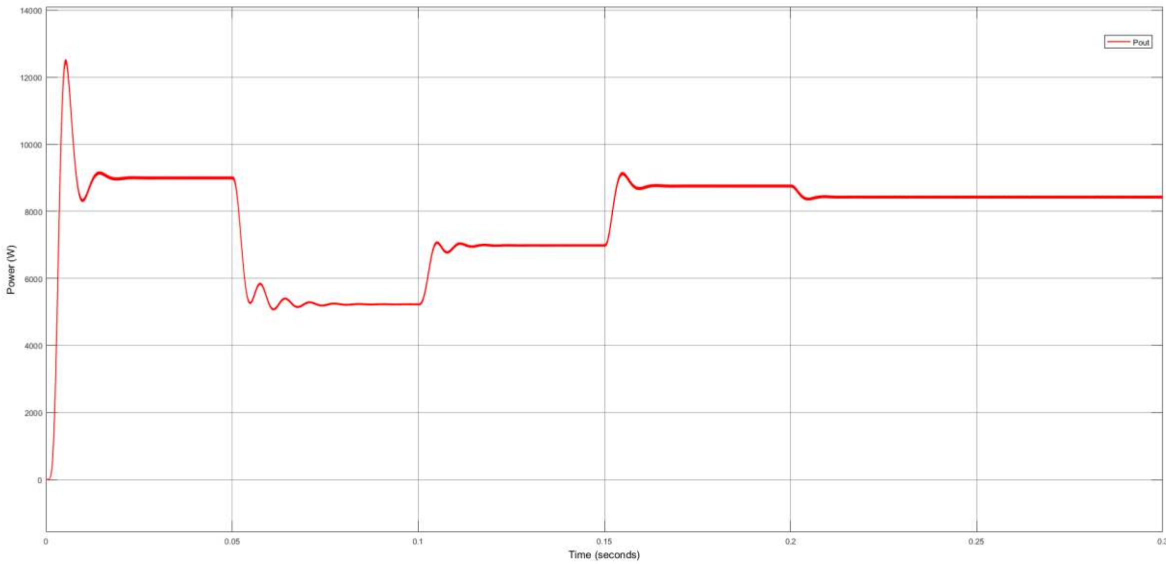

Figure 4.21. Converter output power graph for KF and P&O Hybrid MPPT method under changing irradiation conditions

The graph given in Figure 4.22 is the PV array output voltage and reference voltage graphs. This graph also shows that MPP has been followed successfully. The green colour represents the PV array voltage, and the blue colour represents the reference voltage generated in the MPPT algorithm.

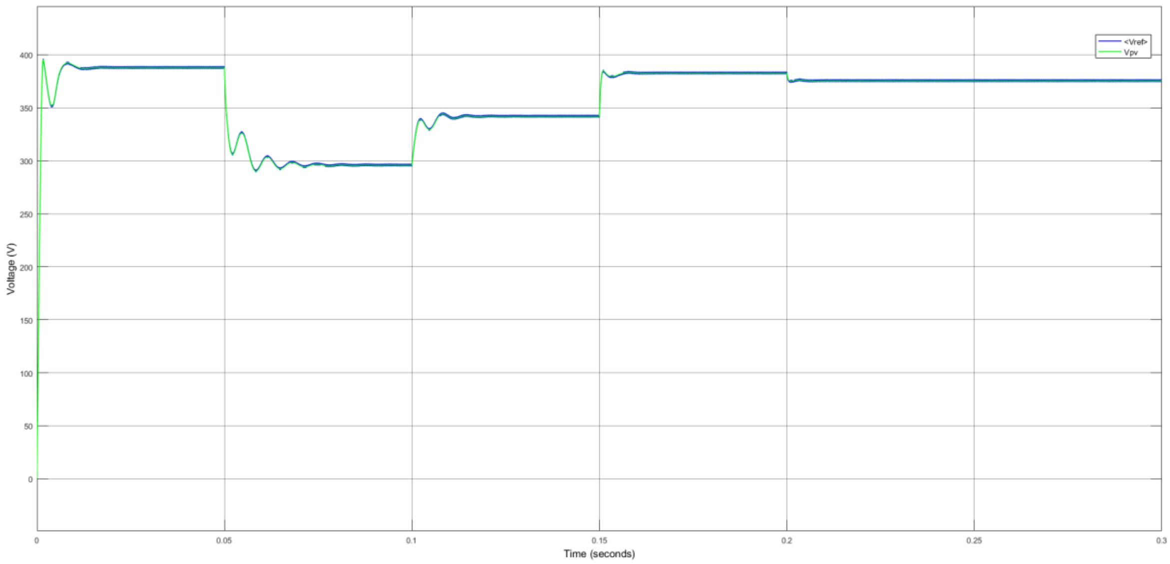

Figure 4.22. PV array output voltage and reference voltage graphs for KF and P&O Hybrid MPPT method under changing irradiation conditions

The PV array output voltage and reference voltage graphs at the changing irradiation stage are shown in close perspective in Figure 4.23.

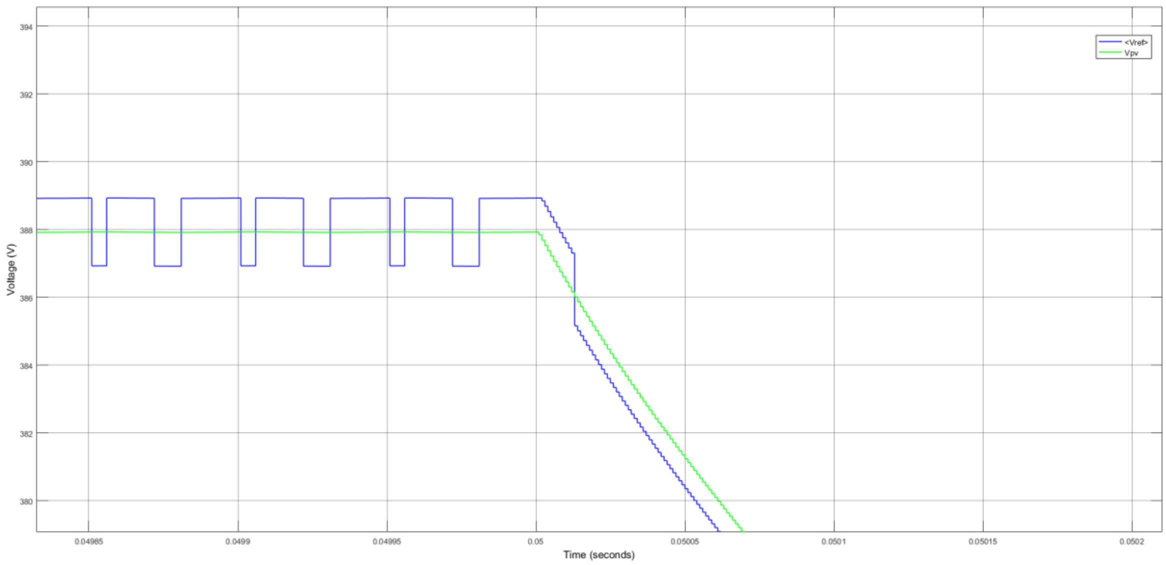

Figure 4.23. PV array output voltage and reference voltage graphs for KF and P&O Hybrid MPPT method in changing irradiation stage

4.4. Operating Scenario of the Overall System: Perturb & Observe and Particle Swarm Optimization Hybrid MPPT Algorithm

In this section, Perturb & Observe and Particle Swarm Optimization Hybrid MPPT Algorithm was tested in the simulation environment using the previously introduced PV system. The algorithm used the reference voltage produced by the algorithm by following the MPP. The PWM signal was generated and the boost converter was operated. The PV array voltage, current and power graphs resulting from the simulation were examined. In addition, the boost converter voltage, current and power graphs were also examined. The PSO algorithm is considered a good method because it performs detailed MPP search.

The graph in Figure 4.24 is the PV array output voltage graph for P&O and PSO Hybrid MPPT method under varying irradiation conditions.

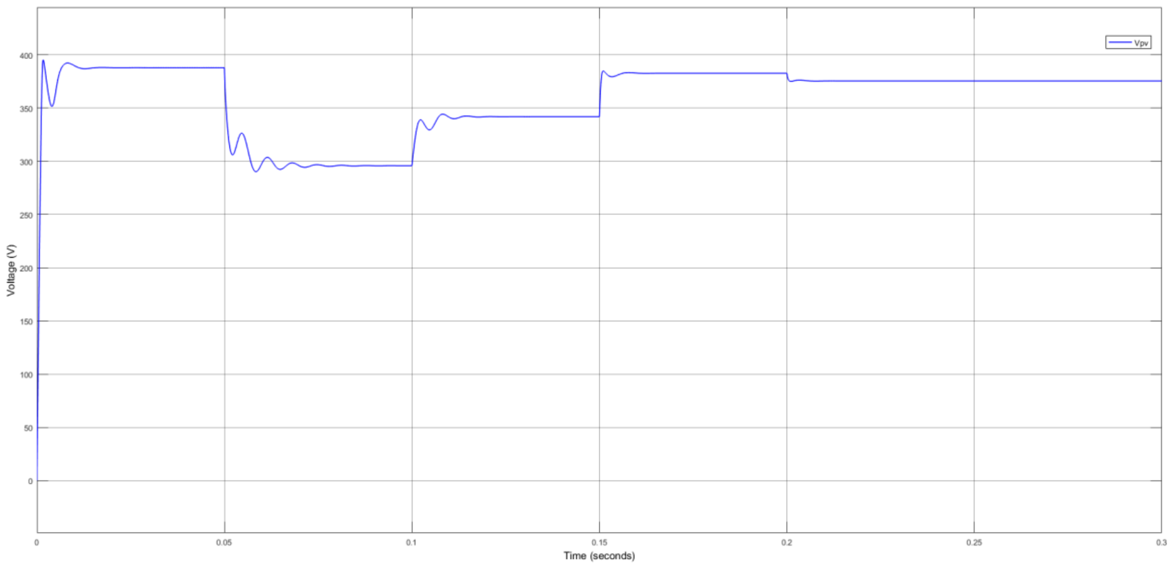

Figure 4.24. PV array output voltage graph for P&O and PSO Hybrid MPPT method under changing irradiation conditions

The graph in Figure 4.25 is the converter output voltage graph.

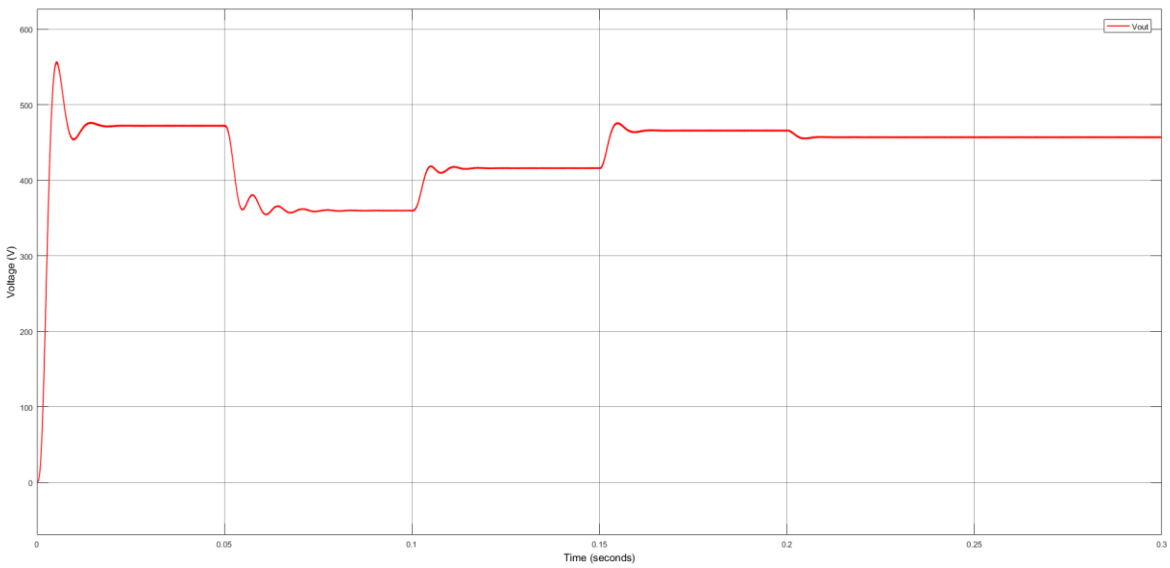

Figure 4.25. Converter output voltage graph for P&O and PSO Hybrid MPPT method under changing irradiation conditions

The PV array output current graph for Perturb & Observe and PSO Hybrid MPPT method under varying irradiation conditions is shown in Figure 4.26.

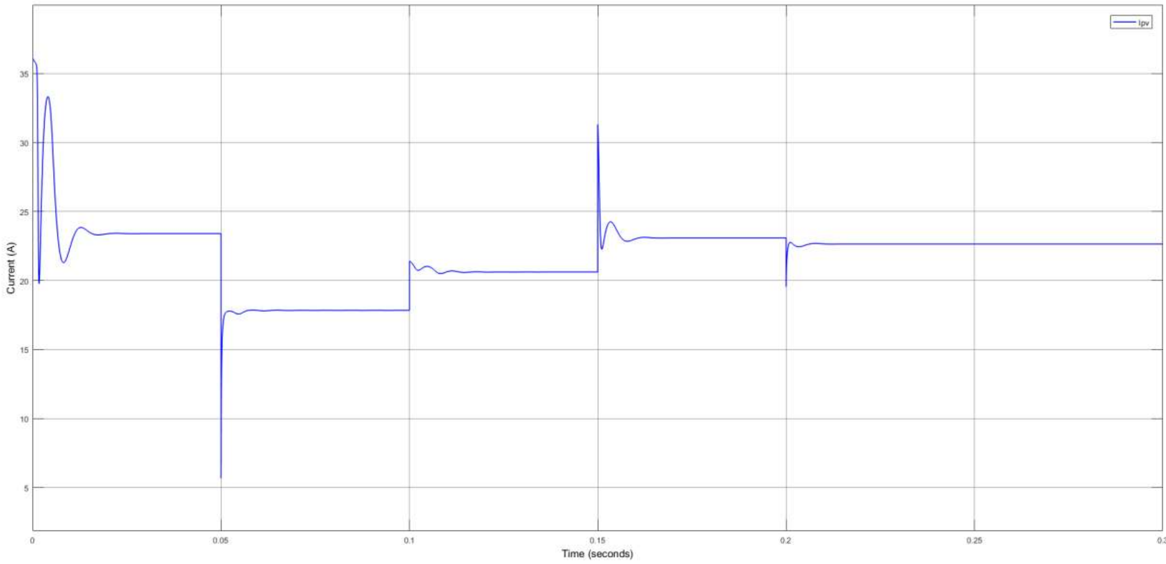

Figure 4.26. PV array output current graph for P&O and PSO Hybrid MPPT method under changing irradiation conditions

The converter output current graph for the Perturb & Observe and PSO Hybrid MPPT method under varying irradiation conditions is shown in Figure 4.27.

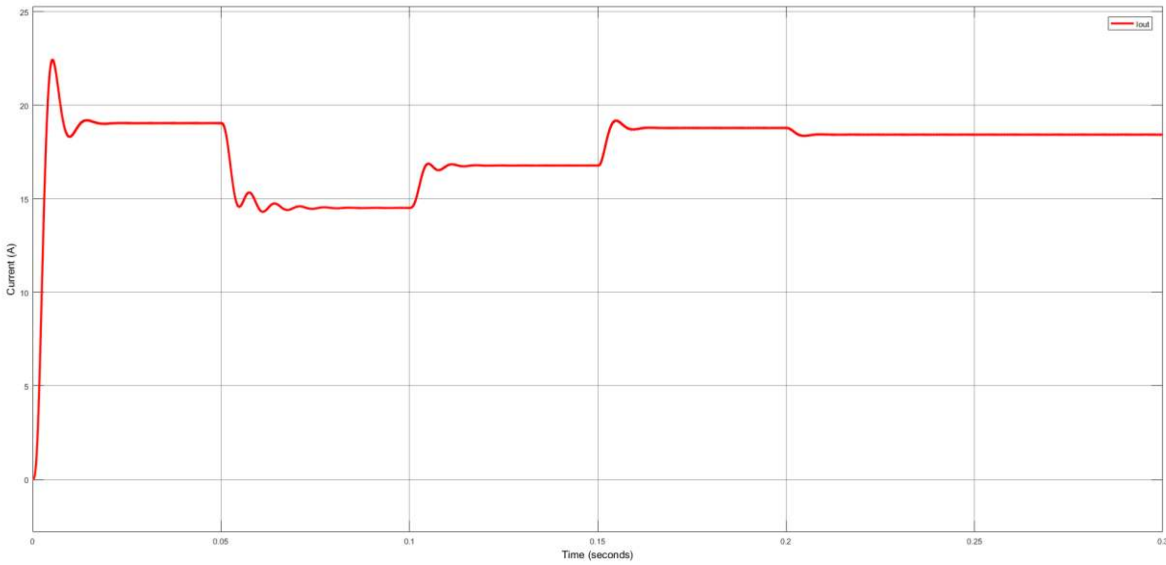

Figure 4.27. Converter output current graph for P&O and PSO Hybrid MPPT method under changing irradiation conditions

The graph in Figure 4.28 is the PV array output power graph.

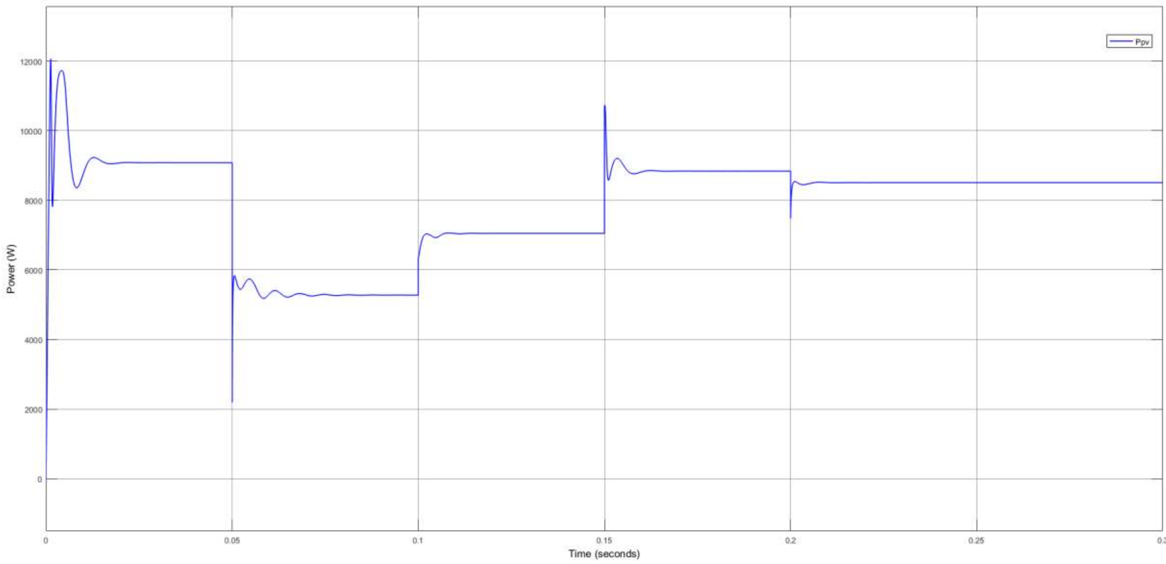

Figure 4.28. PV array output power graph for P&O and PSO Hybrid MPPT method under changing irradiation conditions

The converter output power graph for the P&O and PSO Hybrid MPPT method under varying irradiation conditions is illustrated in Figure 4.29.

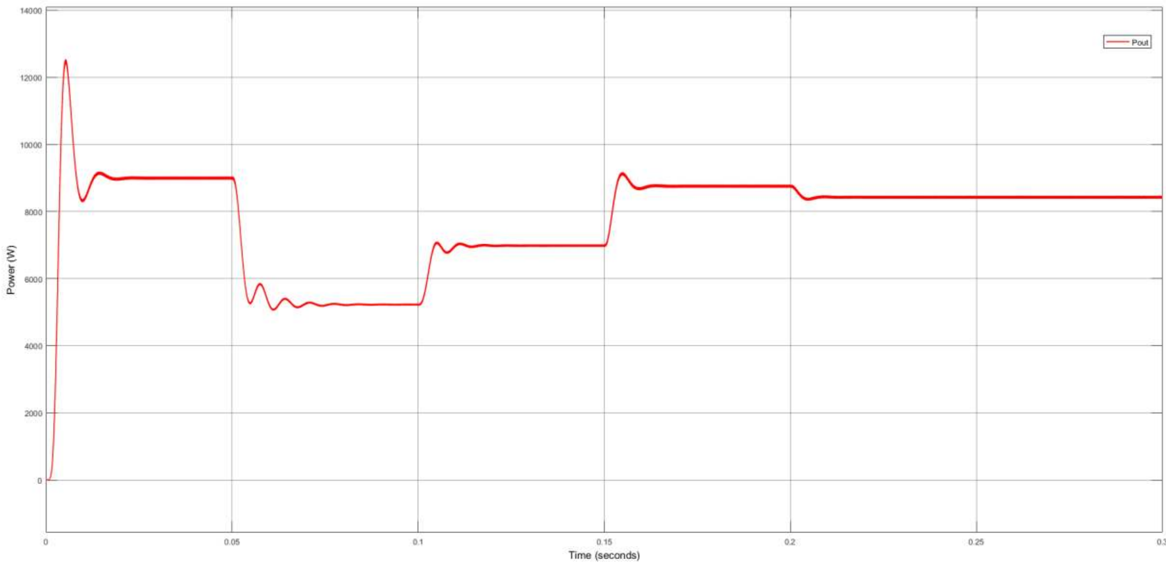

Figure 4.29. Converter output power graph for P&O and PSO Hybrid MPPT method under changing irradiation conditions

The graph given in Figure 4.30 is the PV array output voltage and reference voltage graphs. MPP has been successfully followed. Green colour represents the PV array voltage, red colour represents the reference voltage generated in the MPPT algorithm.

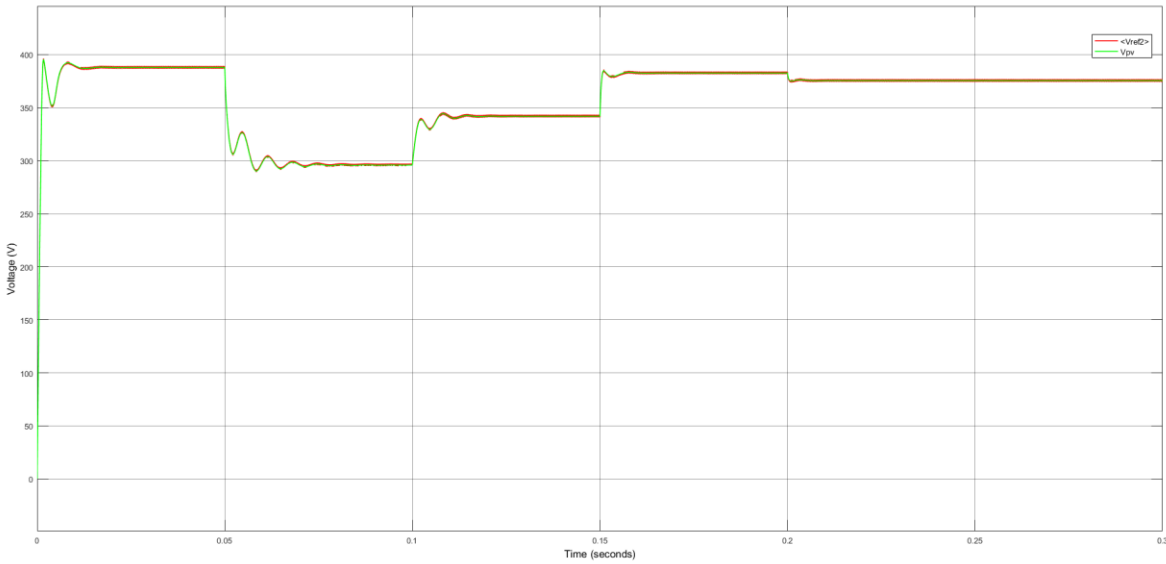

Figure 4.30. PV array output voltage and reference voltage graphs for P&O and PSO Hybrid MPPT method under changing irradiation conditions

Figure 4.31 shows a close-up view of the PV array output voltage and reference voltage graphs at varying irradiation stages.

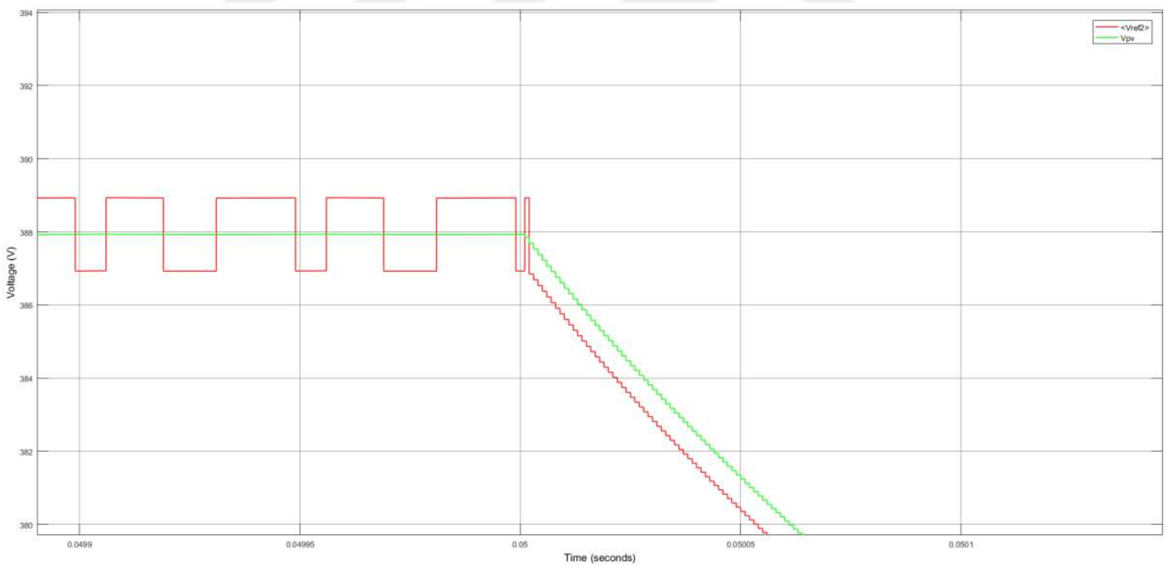

Figure 4.31. PV array output voltage and reference voltage graphs for P&O and PSO Hybrid MPPT method in changing irradiation stage

4.5. Summary of Simulation Results and Proposed Method

In this section of the thesis, the simulation cases created are analysed. For all simulations created, except for the algorithm codes in the MATLAB/Simulink Function block, all remaining circuit elements and values are the same. A signal generator is used for all simulation cases and 1000 W/m2, 800 W/m^2, 600 W/m^2, 500 W/m^2 and 900 W/m^2 irradiation values are given, respectively. Then, all simulation cases and the PV system including the proposed MPPT method are tested. The method proposed in this study is Perturb & Observe and Particle Swarm Optimization Hybrid Algorithm. The reference voltage generation graph is examined in detail compared to other simulation graphs. The reference voltage tracking speed is better than other algorithms. It is seen that the reference voltage fluctuation is less than other methods. It is observed that a graph closer to the reference voltage in terms of voltage value is formed. In most close-up views, the voltage pulses seen in other algorithms are less or not seen at all. Simulation results show that the proposed Perturb & Observe and Particle Swarm Optimization Hybrid MPPT algorithm is a more efficient algorithm than the algorithms used in other simulation cases.

The following graphs show the reference voltage plots for all running simulation cases. Purple represents the Perturb & Observe MPPT method. Blue represents the Perturb & Observe and Kalman Filter Hybrid MPPT method. Red represents the proposed Perturb & Observe and Particle Swarm Optimization Hybrid MPPT algorithm. Green represents the PV array voltage.

Figure 4.32 shows the reference voltages produced by different algorithms in a case where the irradiance value increases. When the graph is examined, the proposed P&O and PSO Hybrid MPPT algorithm produce a closer reference voltage than the P&O MPPT algorithm. Compared to the P&O and KF Hybrid MPPT algorithm, the pulse signal appearance is less or absent in the reference voltage graph of the proposed method.

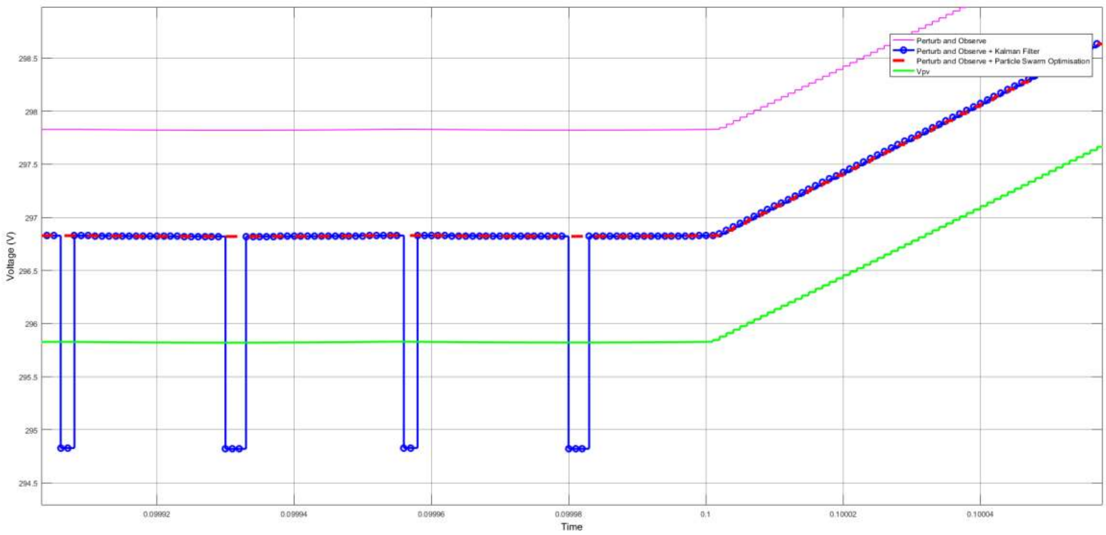

Figure 4.32. The reference voltages produced by different algorithms in a case where the irradiance value increases

Figure 4.33 shows the reference voltages produced by different algorithms in a situation where the irradiance value decreases.

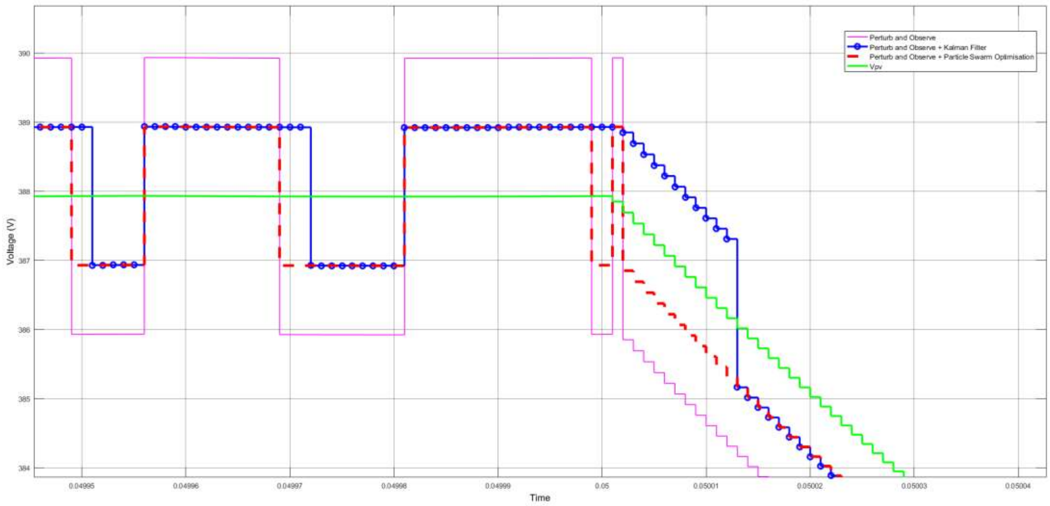

Figure 4.33. The reference voltages produced by different algorithms in a situation where the irradiance value decreases.

Figure 4.34 shows the reference voltages produced by different algorithms in a different situation where the irradiance value decreases. As seen in this graph, the P&O and PSO Hybrid MPPT algorithm provided tracking earlier than the P&O and KF hybrid MPPT algorithm.

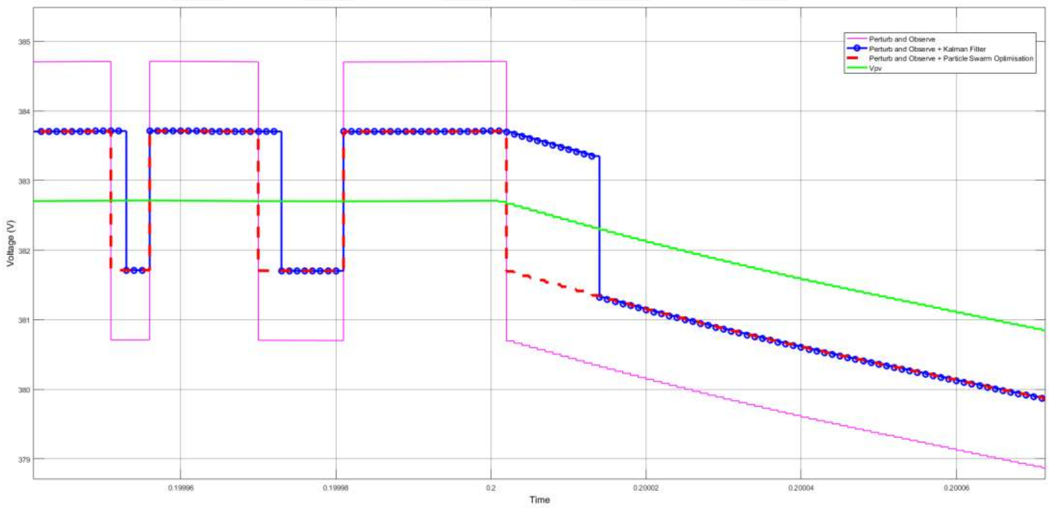

Figure 4.34. The reference voltages produced by different algorithms in a different situation where the irradiance value decreases.

Figure 4.35 shows the reference voltages produced by different algorithms in a stable situation where the irradiance value is constant. As can be seen from this graph, when the irradiation is constant, the P&O and PSO Hybrid MPPT algorithm produces a more stable and accurate reference signal than other algorithms.

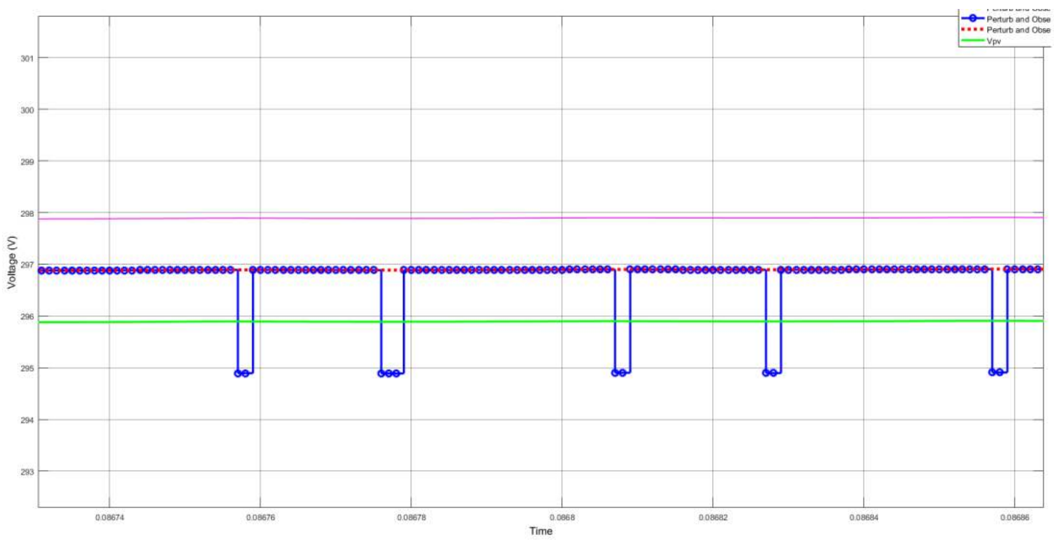

Figure 4.35. The reference voltages produced by different algorithms in a stable situation where the irradiance value is constant

In summary, the simulation results were compared and evaluated in terms of accuracy and tracking speed. Table 4.1 includes these evaluations.

Table 4.1. Comparison of MPPT methods based on simulation results

MPPT Algorithm	**Accuracy**	**Speed**
Perturb & Observe MPPT	Medium	High
Perturb & Observe and Kalman Filter Hybrid MPPT	Medium	Medium
Proposed Perturb & Observe and Particle Swarm Optimization Hybrid MPPT	High	High

Since no reference voltage is produced in the PV system where the MPPT method is not used, the MPP point cannot be followed. Since the MPP is not followed, the efficiency is low.

In the PV system where the Perturb & Observe MPPT algorithm was used, the reference voltage was followed by MMP at a moderate level compared to other methods.

In the simulation of the PV system where the Perturb & Observe and Kalman Filter Hybrid MPPT algorithm is used, the reference signal tracking is at a medium level. It has been observed that its performance at times of irradiation change is also at a medium level compared to the others.

In the PV system simulation where the Perturb & Observe and Particle Swarm Optimization Hybrid MPPT algorithm is used, a higher accuracy MPP tracking is observed compared to the others. It is understood that a fast tracking is done at the moments of irradiance value change.

5. CONCLUSIONS

In this thesis, a new hybrid MPPT algorithm based on Perturb and Observe and Particle Swarm Optimization algorithms has been developed. In this design developed using MATLAB/Simulink simulation program, the good aspects of both algorithms have been brought together. Partial shading conditions are an important phenomenon that significantly reduces the efficiency of PV systems and can damage PV panels and systems. In order to overcome this problem, there are many MPPT methods in the literature that work under partial shading conditions. A solution to these problems has been sought with this study.

In general, in this thesis study, various MPPT methods used under partial shading conditions in the literature have been investigated in detail. The features of these methods have been explained, their working methods have been discussed and their comparisons with each other have been examined. Detailed information about PV systems has been given and their situations have been examined. As a design, a PV system with a power of 11.76 kW has been created in MATLAB/Simulink simulation program. In this system, PV array, DC-to-DC boost converter, MPPT algorithm block and DC-to-DC boost converter control circuit have been used as structures. In the proposed hybrid MPPT algorithm, a reference voltage is produced as the output parameter. This reference voltage is used in the control circuit that will operate the DC-to-DC boost converter. The proposed hybrid MPPT algorithm has been tested by running it with three other simulation scenarios, namely PV system without MPPT algorithm, PV system with Perturb and Observe algorithm and PV system using Perturb and Observe and Kalman Filter Hybrid MPPT algorithm. The proposed method and other three simulation studies have been tested in MATLAB/Simulink simulation program using 1000 W/m^2, 500 W/m^2, 600 W/m^2, 900 W/m^2 and 800 W/m^2 radiation values, respectively. The obtained results are shown with graphics and comparisons are made. According to the simulation results, since no reference voltage is produced in the simulation study without MPPT algorithm, no maximum power point tracking has been performed. It has been observed that this system operates extremely inefficiently and experiences power loss. It has been determined that the simulation with Perturb and Observe MPPT algorithm tracks the maximum power point at a moderate level compared to other simulations. Although the tracking speed of this method is high, its efficiency is at a moderate level compared to others. In the system where Perturb and Observe and Kalman Filter Hybrid MPPT algorithm is used, the reference voltage generation accuracy is seen to be at a moderate level compared to others. Efficiency is seen to be at a high level. In the system where the proposed Perturb and Observe and Particle Swarm Optimization Hybrid MPPT algorithm is used, the power point tracking is at a high level compared to other simulations. The maximum power point tracking speed and efficiency are found to be at a high level compared to others. In summary, it has been observed that the proposed method produces a more accurate reference voltage under partial shading conditions.

In the future, better MPPT methods can be developed using fewer circuit elements. With the development of artificial intelligence, smart MPPT algorithms that give more accurate results can emerge. With the developments in the field of power electronics, DC-to-DC converters with less power loss can be produced. With all these developments, a transition to a cleaner world can be made. As a result, with these studies, it was aimed to contribute to the field of solar energy and support a clean world.

REFERENCES

Abdelkader, H., Belatrache, D., Boulal, K., Colak, I. and Kayisli, K., 2020. Social Acceptance of Renewable Energy dedicated to Electric Production. 9th International Conference on Renewable Energy Research and Applications, Glasgow, UK.

Abdel-Rahim, O. and Haoyu, W., 2020. A New High Gain DC-DC Converter with Model-Predictive-Control Based MPPT Technique for Photovoltaic Systems. CPSS Trans. Power Elect. Appl. 5(2):191-200.

Abdelsalam, A. K., Massoud, A. M., Ahmed, S. and Enjeti, P. N., 2011. High Performance Adaptive Perturb and Observe MPPT Technique for Photovoltaic-Based Microgrids. IEEE Trans. Power Electron, 26(4):1010-1021.

Abdel-Salam, M., El-Mohandes, M.-T. and Goda, M., 2018. An Improved Perturb-and-Observe Based MPPT Method for PV Systems under Varying Irradiation Levels. Sol. Energy, 171(1):547-561.

Adak, S., Cangi, H. and Yılmaz, A. S., 2019. Mathematical Modeling and Simulation of the Photovoltaic System's Output Power depends on Temperature and Irradiance. International Journal of Engineering Research and Development, 11(1): 316-327.

Aghatehrani, R. and Kavasseri, R., 2013. Sensitivity-Analysis-Based Sliding Mode Control for Voltage Regulation in Microgrids. IEEE Trans Sustain Energy, 4(1):50-57.

Ahmed, E. M. and Shoyama, M., 2011. Stability Study of Variable Step Size Incremental Conductance/Impedance MPPT for PV Systems. 8th Int. Conf. Power Electron. (ECCE Asia), Jeju, South Korea.

Ali, A., Almutairi, K., Padmanaban, S., Tirth, V., Algarni, S., Irshad, K., Islam, S., Zahir, Md. H., Shafiullah, Md. and Malik, M. Z., 2020. Investigation of MPPT Techniques under Uniform and Non-Uniform Solar Irradiation Condition-A Retrospection. Special Section on Evolving Technologies in Energy Storage Systems for Energy Systems Applications, IEEE Access, 8(1):127368-127392.

Almutairi, A., Abo-Khalil, A. G., Sayed, K. and Albagami, N., 2020. MPPT for a PV Grid-Connected System to Improve Efficiency under Partial Shading Conditions. Sustainability, 12(24):1-18.

Alqaisi, Z. and Mahmoud, Y., 2019. Comprehensive Study of Partially Shaded PV Modules with Overlapping Diodes. IEEE Access, 7(1):172665-172675.

Altinkök, S., Karadeniz, S. and Altinkök, A., 2022. Photovoltaic System Design and Analysis at Faculty Scale. Journal of Naval Sciences and Engineering, 18(1):91-120.

Arhan, I. and Bilgin, M. Z., 2022. Yenilenebilir Sistemlerde Maksimum Güç Noktası Takibi ve Enerji Yönetimiyle Enerji Verimliliği. OKU Journal of the Institute of Science and Technology, 5(1):75-91.

Ashfaq, A. and Ianakiev, A., 2018. Features of Fully Integrated Renewable Energy Atlas for Pakistan; Wind, Solar and Cooling. Renew. Sustain. Energy, 97(1):14-27.

Awan, M. M. A., 2022. A Technical Review of MPPT Algorithms for Solar Photovoltaic System: SWOT Analysis of MPPT Algorithms. Sir Syed University Research Journal of Engineering & Technology, 12(1):98-106.

Aygül, K., Demirdelen, T. and Tümay, M., 2019. Modeling and Performance Analysis Of Grid Tied Photovoltaic Panel/Battery System Feeding Linear Loads On Complete/Partial Shading Conditions. Çukurova University Journal of the Faculty of Engineering and Architecture, 34(2):97-111.

Badak, U. and Yıldız, A. B., 2020. Fotovoltaik Güneş Paneli Sistemlerinde Maksimum Güç Noktası İzleyicisinin Verime Etkisi. Iğdır Üniversitesi Fen Bilimleri Enstitüsü Dergisi, 10(4):2496-2507.

Basha, C. H. H. and Rani, C., 2020. Performance Analysis of MPPT Techniques for Dynamic Irradiation Condition of Solar PV. Int. J. Fuzzy Syst. Taiwan Fuzzy Systems Association 2020, 22(8):2577-2598.

Behura, A. K., Kumar, A., Rajak, D. K., Pruncu, C. I. and Lamberti, L., 2021. Towards Better Performances for a Novel Rooftop Solar PV System. Solar Energy, 216(1):518-529.

Bhatnagar, P. and Nema, R. K., 2013. Maximum Power Point Tracking Control Techniques: State-of-the-Art in Photovoltaic Applications. Renewable and Sustainable Energy Reviews, 23(7):224-241.

Bi, Z., J. Ma, Man, K. L., Smith, J. S., Y. Yue and Wen, Y. H., 2019. Global MPPT Method for Photovoltaic Systems Operating Under Partial Shading Conditions Using the 0.8 Voc Model. 2019 IEEE International Conference on Environment and Electrical Engineering and 2019 IEEE Industrial and Commercial Power Systems Europe, Genoa, Italy.

Bi, Z., Ma, J., Wang, K., Man, K. L., Smith, J. S. and Yue, Y., 2020. Identification of Partial Shading Conditions for Photovoltaic Strings. Ieee Access, 8(1):75491-75502.

Bidram, A., Davoudi, A. and Balog. R. S., 2012. Control and Circuit Techniques to Mitigate Partial Shading Effects in Photovoltaic Arrays. IEEE J. Photovolt., 2(4):532-546.

Bingöl, O. and Özkaya, B., 2019. A Comprehensive Overview of Soft Computing Based MPPT Techniques for Partial Shading Conditions in PV Systems. Journal of Engineering Sciences and Design, 7(4):926-939.

Bishop, J. W., 1988. Computer Simulation of the Effects of Electrical Mismatches in Photovoltaic Cell Interconnection Circuits, Solar Cells, 25(1):73-89.

Bleijs, J. A. M. and Gow, J.A., 2001. Fast Maximum Power Point Control of Current-Fed DC-DC Converter for Photovoltaic Arrays. Electron Lett., 37(1):5-6.

Bollipo, R. B., Mikkili, S. and Bonthagorla, P. K., 2021. Hybrid, Optimal, Intelligent and Classical PV MPPT Techniques: A Review. CSEE Journal of Power and Energy Systems, 7(1):9-33.

Boonmee, C. and Kumsuwan, Y., 2013. Modified Maximum Power Point Tracking Based-on Ripple Correlation Control Application for Single Phase VSI Grid-Connected PV Systems. 10th Int. Conf. Electr. Eng./Electron., Comput., Telecommun. Inf. Technol., Krabi, Thailand.

Brecl, K., Bokalic, M. and Topic, M., 2021. Annual Energy Losses Due to Partial Shading in PV Modules with Cut Wafer-Based Si Solar Cells. Renewable Energy, 168(1):195-203.

Çabuk, A. S., 2022. Comparison of Innovative and Traditional Method for Optimizing the Efficiency of Photovoltaic Panels. International Journal of Energy Applications and Technologies, 9(2):45-49.

Chandra, S. S. and Gaur, P., 2018. Maximum Power Point Tracking Approaches for Wind-Solar Hybrid Renewable Energy System A Review. In Advances in Energy and Power Systems, Springer, Singapore, 3-12 p.

Chatterjee, A. and Mohanty, K. B., 2018. Current Control Strategies for Single Phase Grid Integrated Inverters for Photovoltaic Applications-A Review. Renew. Sustain. Energy Rev., 92(1):554-569.

Chekired, F., Larbes, C. and Mellit, A., 2012. Comparative Study between Two Intelligent MPPT-Controllers Implemented on FPGA: Application for Photovoltaic Systems. International. J. Sustainable Energy, 33(3):483-499.

Chepp, E. D., Gasparin, F. P. and Krenzinger, A., 2021. Accuracy Investigation in the Modeling of Partially Shaded Photovoltaic Systems. Solar Energy, 223(1063/1):182-192.

Correa-Betanzo, C., Calleja, H. and DeLeón-Aldaco, S., 2018. Module Temperature Models Assessment of Photovoltaic Seasonal Energy Yield. Sustain. Energy Technol. Assessments, 27(1):9-16.

Dadjé, A., Djongyang, N., Kana, J. D. and Tchinda, R., 2016. Maximum Power Point Tracking Methods for Photovoltaic Systems Operating under Partially Shaded or Rapidly Variable Insolation Conditions: A Review Paper. International Journal of Sustainable Engineering, 9(4):224-239.

Dash, S. K., Nema, S., Nema, R. K. and Verma, D., 2015. A Comprehensive Assessment of Maximum Power Point Tracking Techniques under Uniform and Non-Uniform Irradiance and Its Impact on Photovoltaic Systems: A Review. J. Renew. Sustain. Energy, 7(6):63-113.

De Carvalho, J.T., Andres, O.S. and Alberto, S.L., 2016. One Cycle Control Based Maximum Power Point Tracker Applied in Photovoltaic Systems. IEEE Latin Am. Trans. 14(2):602-609.

De Souza, A. C., Borges, D. T. D. S., Santos, I. N. and Macedo, J. R., 2018. Evaluation of Linear Current Control Methods in Single-Phase Grid-Tie Inverters. IEEE Latin Amer. Trans., 16(5):1424-1431.

Desai, H. P. and Patel, H. K., 2007. Maximum Power Point Algorithm in PV Generation: An Overview. Power Electronics and Drive Systems PEDS 7th International Conference, Bangkok, Thailand.

Dhivya P. and Kumar K. R., 2017. MPPT Based Control of SEPIC Converter Using Firefly Algorithm for Solar PV System under Partial Shaded Conditions. 2017 International Conference on Innovations in Green Energy and Healthcare Technologies (IGEHT), Coimbatore, India.

Dube, A., Rizwan, M. and Jamil, M., 2016. Analysis of Single Phase Grid Connected PV System to Identify Efficient System Configuration. Innovative Applications of Computational Intelligence on Power, Energy and Controls with their Impact on Humanity (CIPECH-16), 173-177.

Dulaimi, N. H. A., 2017. Design of an Off-Grid Solar PV System for a Rural Shelter. Graduation Thesis. German Jordanian University, Jordan, 44 p.

Eiselt, H.A. and Sandblom, C. L., 2007. Linear Programming and Its Applications. Springer, Germany, 390 p.

Eke, R. and Demircan, C., 2015. Shading Effect on the Energy Rating of Two Identical PV Systems on a Building Façade, Sol. Energy, 122(1):48-57.

El Hassouni, B., Ourahou, M., Ayrir, W., Haddi, A. and Amrani, A. G., 2018. A Study of Efficient MPPT Techniques for Photovoltaic System Using Boost Converter. Int. J. Emerg. Electr. Power Syst., 19(2).

Elavarasan, R. M., Gm. Shafiullah, GM., Padmanaban, S., Kumar, N. M., Annam, A., Vetrichelvan, A. M., Mihet-Popa, L. and Holm-Nielsen, J. B., 2020. A Comprehensive Review on Renewable Energy Development, Challenges, and Policies of Leading Indian States with an International Perspective. IEEE Access, 8(1):74432-74457.

El-Dein, M. S., Kazerani, M. and Salama, M., 2012. An Optimal Total Cross-Tied Interconnection for Reducing Mismatch Losses in Photovoltaic Arrays. IEEE Trans. Sustain. Energy, 4(1): 99-107.

El-Dein, M. Z. S., Kazerani, M. and Salama, M. M. A., 2013. Optimal Photovoltaic Array Reconfiguration to Reduce Partial Shading Losses. IEEE Trans. Sustain. Energy, 4(1):145-153.

El-Helw, H. M., Al-Hasheem, M. and Marei, M. I., 2016. Control Strategies for the DAB Based PV Interface System. Plos One, 11(8).

El-Helw, H. M., Magdy, A. and Marei, M. I., 2017. A Hybrid Maximum Power Point Tracking Technique for Partially Shaded Photovoltaic Arrays. IEEE Access, 5(1):11900-11908.

Elobaid, L. M., Abdelsalam, A. K. and Zakzouk, E.E., 2012. Artificial Neural Network Based Maximum Power Point Tracking Technique for PV Systems. 38th Annual Conference IEEE Ind. Electron. Soc. (IECON), Montreal, Canada.

EMBER, 2024. Global Electricity Review 2024. Clean Energy Policy and Data, 15-58 p.

Emikönel, S. and Bilhan, A. K., 2022. Analysis of Turkey's Solar Energy Potential in Different Regions. OKU Journal of the Institute of Science and Technology, 5(Special Issue):170-184.

Erdem, Z., 2017. A Review of MPPT Algorithms for Partial Shading Conditions. Acta Physica Polonica, 132(3):1128-1133.

Esram, T. and Chapman, P. L., 2007. Comparison of Photovoltaic Array Maximum Power Point Tracking Techniques. Ieee Trans. Energ. Convers. 22(2):439-449.

Fesharaki, V. J., Sheikholeslam, F. and Motlagh, M. R. J., 2017. Maximum Power Point Tracking with Constraint Feedback Linearization Controller and Modified Incremental Conductance Algorithm. Trans. Inst. Meas. Control, 40(7):2322-2331.

Filho, E. A. S., Fernandes, C. A. F. and Branco, P. J. D. C., 2021. A Complete Framework for the Simulation of Photovoltaic Arrays under Mismatch Conditions. Solar Energy, 213(1):13-26.

Fortunato, M., Giustiniani, A., Petrone, G., Spagnuolo, G. and Vitelli, M., 2008. Maximum Power Point Tracking in A One-Cycle-Controlled Single-Stage Photovoltaic Inverter. IEEE Trans. Ind. Electron., 55(7):2684-2693.

Francis, W. K., Beevi, S. S. and Mathew, J., 2014. MATLAB/Simulink PV Module Model of P&O and DC LINK CDC MPPT Algorithms with Labview Real Time Monitoring and Control Over P&O Technique. Int. J. Adv. Res. Electr. Electron. Instrum. Eng., 3(5):92-101.

Gao, C., and Chen, H., 2023. Electricity from Renewable Energy Resources: Sustainable Energy Transition and Emissions for Developed Economies. Utilities Policy, 82(1):10153.

Garrigos, A., Blanes, J. M, Carrasco, J. A. and Ejea, J. B., 2007. Real Time Estimation of Photovoltaic Modules Characteristics Its Application to Maximum Power Point Operation. Renewable Energy, 32(6):1059-1076.

Ghute, M., Korde, M., Kamble, K., Khade, S. and Niranjane, V., 2021. Power Generation Using Renewable Energy Sources. 2021 Fifth International Conference on I-SMAC (IoT in Social, Mobile, Analytics and Cloud) (I-SMAC), Palladam, India.

Gotz, D., Hahn, D., Gottschalg, R., Dabler, D., Schindler, S. and Hanifi, H., 2019. Evaluation of Shading Tolerance of PV Modules with Different Module Designs for Mobile Applications by Simulation, Indoor and Outdoor Measurements. 36th Eur. Photovolt. Sol. Energy Conf. Exhib., Marseille, France.

Güler, N. and Biricik, S., 2020. Fotovoltaik Sistemler için Üç Fazlı Evirici Tasarımı ve Kontrolü. Düzce Üniversitesi Bilim ve Teknoloji Dergisi, 9(1):453-466.

Halicioglu, F. and Ketenci, N., 2018. Output, Renewable and non-Renewable Energy Production, and International Trade: Evidence from EU-15 Countries. Energy, 159(1):995-1002.

Hangun, B., Eyecioglu, O. and Beken, M., 2022. Investigating the Energy Production Trends of Countries and Its Relationship between Economic Developments. 11th IEEE International Conference on Renewable Energy Research and Applications, Istanbul, Turkey.

Hao, D., Qi, L., Tairab, A. M., Ahmed, A., Azam, A., Luo, D., Pan, Y., Zhang, Z. and Yan, J., 2022. Solar Energy Harvesting Technologies for PV Self-Powered Applications: A Comprehensive Review. Renewable Energy, 188(1):678-697.

Hashim, I. J., 2021. A New Renewable Energy Index. 2021 6th International Conference on Renewable Energy: Generation and Applications (ICREGA), Al Ain, United Arab Emirates.

Ho, B. M. T., Chung, H. S. H. and Lo, W. L., 2004. Use of System Oscillation to Locate the MPP of PV Panels. IEEE Power Electron Lett., 2(1):1-5.

Hohm, D. P. and Ropp, M. E., 2003. Comparative Study of Maximum Power Point Tracking Algorithms. Prog Photovoltaics Res App., 11(1):47-62.

Horoufiany, M., Ghandehari, R., 2017. Optimal Fixed Reconfiguration Scheme for PV Arrays Power Enhancement under Mutual Shading Condition. Iet Renew. Power Gener., 11(11):1456-1463.

Hossain, M. Z., Rahim, N. A. and Selvaraj, J. A., 2018. Recent Progressand Development on Power DC-DC Converter Topology, Control, Designand Applications: A Review. Renew. Sustain. Energy Rev., 81(1):205-230.

Hsiao, Y.-T. and Chen, C.-H., 2002. Maximum Power Tracking for Photovoltaic Power System. IAS Annual Meeting Industry Applications Conference, Pittsburgh, USA.

Hsu, C-H., Shyr, W-J. and Kun-Huang Kuo, K-H., 2010. Optimizing Multiple Interference Cancellations of Linear Phase Array Based on Particle Swarm Optimization. Journal of Information Hiding and Multimedia Signal Processing, Ubiquitous International, 1(4):292-300.

Hua, Y., Oliphant, M. and Hu, E. J., 2016. Development of Renewable Energy in Australia and China: Acomparison of Policies and Status. Renewable Energy, Elsevier, 85(1):1044-1051.

Husak, M., Martinek, P., Janicek, V., Novak, J., Boura, A. and Foit., J., 2020. Piezoelectric Microgenerator. The 13th International Conference on Advanced Semiconductor 31 Devices and Microsystems (ASDAM2020), Smolenice, Slovakia.

Il-Song, K, Myung-Bok, K. and Myung-Joong, Y., 2006. New Maximum Power Point Tracker Using Sliding-Mode Observer for Estimation of Solar Array Current in the Grid-Connected Photovoltaic System. IEEE Trans Ind Electron, 53(4):1027-1035.

Irmak, E. and Güler, N., 2020. A Model Predictive Control-based Hybrid MPPT Method for Boost Converters. Int. J. Electron., 107(1):1-16.

Ishaque, K., Salam, Z., Amjad, M. and Mekhilef, S., 2012. An Improved Particle Swarm Optimization (PSO)-Based MPPT for PV With Reduced Steady-State Oscillation. IEEE Transactions on Power Electronics, 27(8):3627-3638.

Jahn, U. and Nasse, W., 2004. Operational Performance of Grid-Connected PV Systems on Buildings in Germany. Prog. Photovoltaic, 12(6):441-448.

Jain, S. and Agarwal, V., 2004. A New Algorithm for Rapid Tracking of Approximate Maximum Power Point in Photovoltaic Systems. IEEE Power Electron. Lett., 2(1):16-19.

Jain, S. and Agarwal, V., 2007. New Current Control Based MPPT Technique for Single Stage Grid Connected PV Systems. Energy Convers. Manage., 48(2):625-644.

Jamil, M., Saeed, H., Qaisar, S. and Felemban, E. A., 2013. Maximum Power Point Tracking of a Solar System Using State Space Averaging for Wireless Sensor Network. IEEE Int. Conf. Smart Instrum., Meas. Appl. (ICSIMA), Kuala Lumpur, Malasia.

Jasim, A. A. and Shepetov, Y., 2017. Novel Classification for Tracking Techniques Maximum Power Point in Solar Photovoltaic Systems. British Journal of Applied Science and Technology, 21(6):1-13.

Ji, Y. H., Jung, D. Y., Won, C. Y., Lee, B. K. and Kim, J. W., 2009. Maximum Power Point Tracking Method for PV Array under Partially Shaded Condition. IEEE Energy Convers. Congr. Expo, 307-312.

Jiang, L. L., Nayanasiri, D. R., Maskell, D. L. and Vilathgamuwa, D. M., 2015. A Hybrid Maximum Power Point Tracking for Partially Shaded Photovoltaic Systems in the Tropics. Renewable Energy, 76(1):53-65.

John, H.M. and Kurtis, K. F., 2004. Numerical Method Using MATLAB. Prentice-Hall Inc., USA, 680 p.

Joisher, M., Singh, D., Taheri, S., Espinoza-Trejo, D. R., Pouresmaeil, E. and Taheri, H., 2020. A Hybrid Evolutionary-Based MPPT for Photovoltaic Systems under Partial Shading Conditions. IEEE Access, 8(1):38481-38492.

Joshi, P. and Arora, S., 2017. Maximum Power Point Tracking Methodologies for Solar PV Systems: A Review. Renew. Sustain. Energy Rev., 70(1):1154-1177.

Joshi, P. B. and Vaishnav, S. R., 2021. A Simulation of Different Characteristics of Solar PV Grid Connected System. 2021 International Conference on Control, Automation, Power and Signal Processing (CAPS), Jabalpur, India.

Kakoli, S., 2014. Planning and Installing Photovoltaic Systems: A Guide for Installers, Architects and Engineers. Routledge, London, 536 p.

Karami, N., Moubayed, N. and Outbib, R., 2017. General Review and Classification of Different MPPT Techniques. Renew. Sustain. Energy Rev., 68(1):1-18, 62(1):350-371.

Karanfil, A., 2021. The Effect of Using Bypass Diode in Series Connected Photovoltaic (PV) Panels on System Power in Partial Shading Condition. DEÜ FMD, 23(68):621-630.

Keles, C., Alagoz, B. B., Akcin, M., Kaygusuz, A. and Karabiber, A., 2013. A Photovoltaic System Model for MATLAB/Simulink Simulations. 4th International Conference on Power Engineering, Energy and Electrical Drives, Istanbul, Turkey.

Khalili, S. and Breyer, C., 2022. Review on 100% Renewable Energy System Analyses: A Bibliometric Perspective. IEEE Access, 10(1):125792-125834.

Khatib, T., Elmenreich, W. and Mohamed, A., 2017. Simplified I-V Characteristic Tester for Photovoltaic Modules using a DC-DC Boost Converter, Sustainability, 9(4):657.

Kılıç, M. Y. and Adali, S., 2022. Supply the Energy Need of Work Offices Using Solar Cells. Düzce Üniversitesi Bilim ve Teknoloji Dergisi, 10(1):716-728.

Kılıç, U. and Kekezoğlu, B., 2021. A Review of Solar Photovoltaic Incentives and Policy: Selected Countries and Turkey. Ain Shams Engineering Journal, 13(5):101669.

Kim, S. Y., Park, S., Jang, S. J., Kim, G. H., Seo, H. R. and Yu, K., 2009. An Effective POS MPPT Control Method for PV Power Generation System. Proc. 12th Int. Conf. Electr. Mach. Syst. ICEMS, Tokyo, Japan.

Kitano, T., Matsui, M. and Xu, D., 2001. Power Sensor-less MPPT Control Scheme Itilizing power Balance at DC Link-system Design to Ensure Stability and Response. 27th annual conference of the IEEE Industrial Electronics Society IECON-01, Denver, USA.

Klasen, N., Lux, F., Weber, J., Roessler, T. and Kraft, A., 2022. A Comprehensive Study of Module Layouts for Silicon Solar Cells under Partial Shading. IEEE Journal of Photovoltaics, 12(2).

Koad, R. B. A., Zobaa, A. F. and Adel El-Shahat, A., 2017. Novel MPPT Algorithm Based on Particle Swarm Optimization for Photovoltaic Systems. IEEE Transactıons on Sustainable Energy, 8(2).

Kollimala S. K. and Mishra M. K., 2013. Adaptive Perturb & Observe MPPT Algorithm for Photovoltaic System. 2013 IEEE Power and Energy Conference at Illinois (PECI), Illinois, USA.

Kollimalla, S. K. and Mishra, M. K., 2014. Variable Perturbation Size Adaptive P&O MPPT Algorithm for Sudden Changes in Irradiance. IEEE Trans. Sustain. Energy, 5(3):718-728.

Kota, V. R. and Bhukya, M. N., 2016. A Simple and Efficient MPPT Scheme for PV Module Using 2-Dimensional Lookup Table. 2016 IEEE Power and Energy Conference at Illinois (PECI), Urbana, USA.

Labidi, Z.R., Horst, S. and Abdelkader, M., 2019. A Systematic Controller Design for a Photovoltaic Generator with Boost Converter Using Integral State Feedback Control. Eng. Technol. Appl. Sci. Res., 9(2):4030-4036.

Lasheen, M., Rahman, A. K. A., Abdel-Salam, M. and Ookawara, S., 2017. Adaptive Reference Voltage-Based MPPT Technique for PV Applications. IET Renew. Power Gener., 11(5):715-722.

Leedy, A. W. and Garcia, K. E., 2013. Approximation of P-V Characteristic Curves for Use in Maximum Power Point Tracking Algorithms, 45th Southeastern Symp. Syst. Theory, Madrid, Spain.

Levron, Y. and Shmilovitz, D., 2013. Maximum Power Point Tracking Employing Sliding Mode Control. IEEE Trans. Circuits Syst. I, Reg. Papers, 60(3):724-732.

Li, X., Wen, H. and Zhao, C., 2015. Improved Beta Parameter Based MPPT Method in Photovoltaic System. 9th Int. Conf. Power Electron. ECCE Asia (ICPE-ECCE Asia), Seoul, Korea.

Ma, T., Yang, H. and Lu, L., 2014. Solar Photovoltaic System Modeling and Performance Prediction. Renewable and Sustainable Energy Reviews, 36(1):304-315.

Maoa, M., Cui, L., Zhang, Q., Guo, K., Zhou, L. and Huang, H., 2020. Classification and Summarization of Solar Photovoltaic MPPT techniques: A Review Based on Traditional and Intelligent Control Strategies. Energy Reports, 6(2020):1312-1327.

Masoum, M. A. S. and Dehbonei, H., 1998. Optimal Power Point Tracking of Photovoltaic System under All Operating Conditions. 17th Congress of the World Energy Council, Houston, USA.

Matsui, M., Kitano, T., Xu, D. and Yang, Z., 1999. A New Maximum Photovoltaic Power Tracking Control Scheme Based on Power Equilibrium at DC_{link}. IEEE Industry Applications Conference, Conference Record of the Thirty-Fourth IAS Annual Meeting, Phoenix, USA.

Mesquita, D. D. B., Silva, J. L. D. S., Moreira, H. S., Kitayama, M. and Villalva, M. G., 2019. A Review and Analysis of Technologies Applied in PV Modules. 2019 IEEE PES Innovative Smart Grid Technologies Conference, Gramado, Brasil.

Miao, Z., Jie, W. and Hui, Z., 2004. The Application of Slide Technology in PV Maximum Power Point Tracking System. Fifth World Congress on Intelligent Control and Automation WCICA, Hangzhou, China.

Mohanty, P., Bhuvaneswari, G., Balasubramanian, R. and Dhaliwal, N. K., 2014. MATLAB Based Modeling to Study the Performance of Different MPPT Techniques Used for Solar PV System under Various Operating Conditions. Renewable and Sustainable Energy Reviews, 38(1):581-593.

Moring, S. and Pols, A., 2012. Maximum Power Point Tracking: Algorithm and Software Development. Bachelor Thesis, Delft Univ. Technol., Delft, The Netherlands, 72 p.

Ngan, M. S. and Tan, C. W., 2011. Multiple Peaks Tracking Algorithm Using Particle Swarm Optimization Incorporated with Artficial Neural Network. Int. J. Elect., Computer, Energetic, Electron. Commun. Eng., 5(1):1320-1326.

Obaid, Z. A., Cipcigan, L. M. and Muhssin, M. T., 2017. Power System Oscillations and Control: Classifications and PSSs' Design Methods: A Review. Renew. Sustain. Energy Rev., 79(1):839-849.

Omar, F. A., Pamuk, N. and Kulaksız, A. A., 2023. A Critical Evaluation of Maximum Power Point Tracking Techniques for PV Systems Working under Partial Shading Conditions. Turkish Journal of Engineering, 7(1):73-81.

Ons, Z., Aymen, J., Craciunescu, A. and Popescu, M. O., 2015. Comparison of Hill Climbing and Artificial Neural Network Maximum Power Point Tracking Techniques for Photovoltaic Modules. 2nd Int. Conf. Math. Comput. Sci. Ind. (MCSI), Washington, USA.

Pan, C.-T., Chen, J.-Y., Chu, C.-P. and Huang, Y.-S., 1999. A Fast Maximum Power Point Tracker for Photovoltaic Power Systems. 25th Annual Conference of the IEEE Industrial Electronics Society IECON, San Jose, USA.

Park, H. and Song, J., 2009. A dP/dV Feedback-Controlled MPPT Method for Photovoltaic Power System using II-SEPIC. J. Power Electron., 9(4):604-611.

Patcharaprakiti, N., Premrudeepreechacharn, S. and Sriuthaisiriwong, Y., 2005. Maximum Power Point Tracking Using Adaptive Fuzzy Logic Control for Grid-Connected Photovoltaic System. Renewable Energy, 30(11):1771-1788.

Patel, H. and Agarwal, V., 2008. MATLAB-Based Modeling to Study the Effects of Partial Shading on PV Array Characteristics, IEEE Transactions on Energy Conversion, 23(1):302-310.

Pawar, A. S., Kolte, M. T. and Mehta, H., 2022. Review of PV MPPT Based Battery Charging Techniques Under Partial Shading Conditions. 2022 Second International Conference on Power, Control and Computing Technologies (ICPC2T), Raipur, India.

Petrone, G., Spagnuolo, G. and Vitelli, M., 2011. A Multivariable Perturb and Observe Maximum Power Point Tracking Technique Applied to a Single Stage Photovoltaic Inverter. IEEE Trans. Ind. Electron., 58(1):76-84.

Podder, A. K., Roy, N. K. and Pota, H. R., 2019. MPPT Methods for Solar PV Systems: A Critical Review Based on Tracking Nature. IET Renew. Power Gener., 13(10):1615-1632.

Pradeep, K. P. J., Reddy, K. S. P., Mouli, C. C. and Raju, K. N., 2015. Design and Implementation of Maximum Power Point Tracking in Photovoltaic Systems. Int. J. Eng. Sci. Invent., 4(3):37-43.

Pradhan R. and Subudhi, B., 2012. A Steepest-Descent Based Maximum Power Point Tracking Technique for a Photovoltaic Power System. 2nd Int. Conf. Power, Control Embedded Syst., Allahabad, India.

Prasad, K. K., Myneni, H. and Kumar, G. S., 2019. Power Quality Improvement and PV Power Injection by DSTATCOM with Variable DC Link Voltage Control from RSC-MLC. IEEE Trans. Sustain. Energy, 10(2):876-885.

Qazi, A., Hussain, F., Rahim, N., Hardaker, G., Alghazzawi, D., Shaban, K. and Haruna, K., 2019. Towards Sustainable Energy: A Systematic Review of Renewable Energy Sources, Technologies, and Public Opinions, IEEE Access, 7(1):63837-63851.

Raedani, R. and Hanif, M., 2014. Design, Testing and Comparison of P&O, IC and VSSIR MPPT Techniques. Int. Conf. Renew. Energy Res. Appl. (ICRERA), Milwakuee, USA.

Raheem, A., Abbasi, S. A., Memon, A., Samo, S. R., Taufiq-Yap, Y. H., Danquah, M. K. and Harun, R., 2016. Renewable Energy Deployment to Combat Energy Crisis in Pakistan. Energy, Sustain. Soc., 6(1):16.

Rajesh, R. and Mabel, M. C., 2015. A Comprehensive Review of Photovoltaic Systems. Renewable and Sustainable Energy Reviews, 51(1):231-248.

Ram, J. P., Babu, T. S. and Rajasekar, N., 2017. A Comprehensive Review on Solar PV Maximum Power Point Tracking Techniques. Renew. Sustain. Energy Rev., 67(1):826-847.

Rao, G. V., Kumar, S. Ch. S., Sivaprasad, A. V., Sukthana, S. A. and Bharathi, A., 2021. A Novel Design and Development of Self Maintained Solar Panel. 10th International Conference on Advances in Computing and Communications (ICACC), Kochi, India.

Reisi, A. R., Moradi, Moradi H. and Jamasb, S., 2013. Classification and Comparison of Maximum Power Point Tracking Techniques for Photovoltaic System: A Review. Renewable Sust. Energy, 19(1):433-443.

Renewable Capacity Statistics 2021, 2021. Abu Dhabi (Uae), Eau: International Renewable Energy Agency Irena. https://Irena.Org/Publications/2021/March/Renewable-Capacity-Statistics-2021 [Last access date: 20.08.2024].

Republic of Turkey Ministry of Energy and Natural Resources, General Directorate of Renewable Energy (YEGM), 2024. Solar Energy Potential Atlas. https://gepa.enerji.gov.tr [Last access date: 20.08.2024].

Ribeiro, H., Silva, F., Pinto, S. and Borges, B., 2009. Single Stage Inverter for PV Applications with One Cycle Sampling Technique in the MPPT Algorithm. 35th Annu. Conf. IEEE Ind. Electron., Porto, Portugal.

Rodriguez, C. and Amaratunga, G. A. J., 2007. Analytic Solution to the Photovoltaic Maximum Power Point Problem. IEEE Trans. Circuits Syst. I, Reg. Papers, 54(9):2054-2060.

Sadeq, G. G., Sanusi, A. N. Z. and Abdullah, F., 2021. Solar Power Assessment for Photovoltaic Installation in Malaysia University Campus. 2021 Third International Sustainability and Resilience Conference: Climate Change, Sakheer, Bahrain.

Sadiq, M., Ali, S. W., Terriche,Y., Mutarraf, M. U., Hassan, M. A., Hamid, K., Ali, Z., Sze, J. Y., Su, C.-L. and Guerrero, J. M., 2021. Future Greener Seaports: A Review of New Infrastructure, Challenges, and Energy Efficiency Measures. IEEE Access, 9(1):75568-75587.

Salas, V., Olías, E., Barrado, A. and Lázaro, A., 2006. Review of the Maximum Power Point Tracking Algorithms for Stand-Alone Photovoltaic Systems. Sol. Energy Mater. Sol. Cells, 90(11):1555-1578.

Sarıoğlu, G. and Eke, R., 2012. Parameter Analysis of a Multi Crystalline Silicon (mc-Si) Photovoltaic Module under Partially Shaded Insolation. SDU Journal of Science (E-Journal), 7(2):123-140.

Schuss, C., Kotikumpu, T., Eichberger, B. and Rahkonen, T., 2014. Impact of Dynamic Environmental Conditions on the Output Behaviour of Photovoltaics. 20th Int. Symp. and 18th Int. Workshop ADC Model. Testing Res. Electrical Electron. Meas. Econ. Upturn, Benevento, Italy.

Shabaan, S., El-Sebah, M. I. A. and Bekhit, P., 2018. Maximum Power Pointtracking for Photovoltaic Solar Pump Based on Anfis Tuning System. J. Electr. Syst. Inf. Technol., 5(1):11-22.

Singh, B., Nishant, K. and Bijaya, K. P., 2020. Steepest Descent Laplacian Regression Based Neural Network Approach for Optimal Operation of Grid Supportive Solar PV Generation. Express Briefs, IEEE Transactions on Circuits and Systems II, Express Briefs, 1(1):99.

Singh, D. And Singh, H., 2019. Technical Survey and Review on MPPT Techniques to Attain Maximum Power of Photovoltaic System. 5th IEEE International Conference on Signal Processing, Computing and Control (ISPCC 2k19), JUIT, Solan, India.

Solodovnik, E. V., Liu, S. and Dougal, R. A., 2004. Power Controller Design for Maximum Power Tracking in Solar Installations. IEEE Trans Power Electron, 19(5):1295-1304.

Sreeraj, S., Chatterjee, K. and Bandyopadhyay, S., 2013. One-Cycle Controlled Single-Stage Single-Phase Voltage-Sensorless Grid-Connected PV System'' IEEE Trans. Ind. Electron., 60(3):1216-1224.

Statista. The Statistics Portal for Market Data. https://www.statista.com [Last access date: 20.08.2024].

Sundareswaran, K., Kumar, V. V. and Palani, S., 2015. Application of A Combined Particle Swarm Optimization and Perturb and Observe Method for MPPT in PV Systems under Partial Shading Conditions. Renewable Energy, 75(1):308-317.

Tan, C. W., Green, T. C. and Hernandez-Aramburo, C. A., 2005. An Improved Maximum Power Point Tracking Algorithm with Current Mode Control for Photovoltaic Applications. Int. Conf. on Power Electronics and Drives Systems, Kuala Lumpur, Malaysia.

Tan, C. Y., Rahim, N. A. and Selvaraj, J., 2015. Employing Dual Scaling Mode for Adaptive Hill Climbing Method on Buck Converter. IET Renew. Power Gener., 9(8):1010-1018.

Teulings, W., Marpinard, J. C., Capel, A. and O'Sullivan, D., 1993. A New Maximum Power Point Tracking System. 24th Annual IEEE Conference on Power Electronics Specialists PESC, Seattle, USA.

Tey, K. S. and Mekhilef, S., 2014. Modified Incremental Conductance MPPT Algorithm to Mitigate Inaccurate Responses Under Fast-Changing Solar Irradiation Level. Sol Energy, 101(1):333-342.

Torkian, F. and Ghandehari, F. R., 2022. Power Recovery of the PV Arrays under Partial Shading by a Power Electronic Compensator. Solar Energy, 237(1):284-292.

Tozlu, O. F. and Calik, H., 2021. A Review and Classification of Most Used MPPT Algorithms for Photovoltaic Systems. Hittite Journal of Science and Engineering, 2021, 8(3):207-220.

Trzmiel, G., Głuchy, D. and Kurz, D., 2020. The Impact of Shading on the Exploitation of Photovoltaic Installations. Renewable Energy, 153(1):480-498.

Tsang, K. M. and Chan, W. L., 2015. Maximum Power Point Tracking for PV Systems under Partial Shading Conditions Using Current Sweeping. Energy Convers. Manage., 93(1):249-258.

Vasant, L. G. and Pawar, V. R., 2017. Optimization of Solar-Wind Energy System Power for Battery Charging using MPPT. International Conference on Energy, Communication, Data Analytics and Soft Computing (ICECDS-2017), Chennai, India.

Vázquez, N., Azaf, Y., Cervantes, I., Vázquez, E. and Hernández, C., 2015. Maximum Power Point Tracking Based on Sliding Mode Control. Int. J. Photoenergy, 2015(1):1-8.

Verma, D., Nema, S. Shandilya, A. M. and Dash, S. K., 2016. Maximum Power Point Tracking (MPPT) Techniques: Recapitulation in Solar Photovoltaic Systems. Renewable and Sustainable Energy Reviews, 54(1):1018-1034.

Vicente, E. M., Moreno, R.L. and Ribeiro, E. R., 2015. MPPT Technique Based on Current and Temperature Measurements, Int. J. Photoenergy, 2015(6):1-9.

Victoria, M., Haegel, N., Peters, I. M., Sinton, R., Jager-Waldau, A., Del Canizo, C., Breyer, C., Stocks, M., Blakers, A., Kaizuka, I., Komoto, K. and Smets, A., 2021. Solar Photovoltaics is ready to Power a Sustainable Future, Joule, 5(5):1041-1056.

Wang, J., Chung, S., Kontar, R., AlShelahi, A Byon, E. and Saigal, R., 2021. Look-Ahead Decision Making For Renewable Energy: A Dynamic ‘‘Predict And Store’’ Approach. Applied Energy, 296(C).

Wang, P., Zhu, H., Shen, W., Choo, F. H., Loh, P. C., Tan, K. K., 2010. A Novel Approach of Maximizing Energy Harvesting in Photovoltaic Systems Based on Bisection Search Theorem. Twenty-Fifth Annual IEEE Conference and Exposition (APEC) on Applied Power Electronics, Piscataway, USA.

Wasynczuk, O., 1983. Dynamic Behavior of a Class of Photovoltaic Power Systems. IEEE Trans Power Appar Syst., PAS-102(9):3031-3037.

Wei, T., Liu, D. and Zhang, C., 2017. An Improved Particle Swarm Optimization (PSO)-Based MPPT Strategy for PV System. MATEC Web of Conferences, ICMITE 2017, 139(52).

Xiao, W. and Dunford, W. G., 2004. A Modified Adaptive Hill Climbing MPPT Method for Photovoltaic Power Systems. IEEE 35th Annu. Power Electron. Specialists Conf., Aachen, Germany.

Xiao, W., Dunford, W. G., Palmer, P. R. and Capel, A., 2007. Application of Centered Differentiation and Steepest Descent to Maximum Power Point Tracking. IEEE Trans. Ind. Electron., 54(5):2539-2549.

Xiong, G., Li, L., Mohamed, A. W., Yuan, X. and Zhang, J., 2021. A New Method for Parameter Extraction of Solar Photovoltaic Models Using Gaining-Sharing Knowledge Based Algorithm. Energy Reports, 7(7):3286-3301.

Yang, C. and Smedley, K. M., 2004. A Cost-Effective Single-Stage Inverter with Maximum Power Point Tracking. IEEE Trans Power Electron, 19(5):1289-1294.

Yavuz, C. and Botsalı, A. R., 2022. A Weather-Based Forecasting System for the Solar Power Plants in the Konya Region. Sigma J Eng Nat Sci, 40(1):144-149.

Yilmaz, U., Kircay, A. and Borekci, S., 2018. PV System Fuzzy Logic MPPT Method and PI Control as a Charge Controller. Renew. Sustain. Energy Rev., 81(1):994-1001.

Zhang, L., Hurley, W. G. and Wolfle, W., 2011. A New Approach to Achieve Maximum Power Point Tracking for PV System with a Variable Inductor. IEEE Trans Power Electron. 26(4):1031-1037.

Zhang, W., Zhou, G., Ni, H. and Sun., Y., 2019. A Modified Hybrid Maximum Power Point Tracking Method for Photovoltaic Arrays under Partially Shading Condition. IEEE Access, 7(1):160091-160100.

Zhu, W., Shang, L., Li, P. and Guo, H., 2018. Modified Hill Climbing MPPT Algorithm With Reduced Steady-State Oscillation and Improved Tracking Efficiency. The J. Eng., 2018(17):1878-1883.

CURRICULUM VITAE

Bayram Kaan UZUNDAĞ, He graduated from Adana IMKB Anatolian Teachers High School in 2013 in Adana, Türkiye. He graduated from Cukurova University, Faculty of Engineering, Department of Electrical and Electronics Engineering in 2018. He started his master's degree in the same department in 2021. He worked as a solar energy project engineer in various EPC companies in Turkey for about 2.5 years.

He has been working as a research assistant in Çukurova University, Faculty of Engineering, Department of Electrical and Electronics Engineering since March 2024. He is interested in power electronics, solar systems and renewable energy fields.